Adsorption characteristics at a solid-solution interface

Deuchar, J. A.

ADSORPTION CHARACTERISTICS AT A SOLID–SOLUTION INTERFACE

BY

J. A. DEUCHAR

THESIS SUBMITTED FOR THE DEGREE OF

MASTER OF SCIENCE

IN THE UNIVERSITY OF DURHAM

DERBY AND DISTRICT

COLLEGE OF

TECHNOLOGY

SEPTEMBER

1969

ACKNOWLEDGEMENTS

The author wishes to thank Dr.D.A.Ibbitson for the suggestion of this topic and for his continual guidance and encouragement during the course of this investigation.

I am indebted to Dr.G.Kohnstam,my Supervisor in Durham,for his valuable comments and for the interest he has shown in this work.

Grateful thanks are also due to Mr.M.S.J.Twisleton for all the research facilities made available to the author and without whose support this work would have not been possible.

Derby

September 1969

J.A.Deuchar

Abstract

The adsorption characteristics at an alumina-solution interface have been studied for solutions consisting of a series of p-substituted phenols (methyl-, chloro-, bromo-, tertiary-butyl-, and nitro-) dissolved in cyclohexane and tetrahydrofuran.

Characterisation of the alumina surface has been attempted by X-ray diffraction photography, electron microscopy, low-temperature nitrogen adsorption and dehydration experiments. The presence of pores in the alumina sample has been confirmed and a pore size distribution analysis carried out.

Consideration of the porosity and surface area values obtained by the use of gas adsorption and solution adsorption methods, has enabled the area of the alumina surface available to the adsorptives to be assessed. The molecular area requirements of the adsorptives on the alumina surface have been determined from the adsorption isotherms and indicate that the phenols are perpendicularly orientated to the adsorbent surface. From the nature of the alumina surface and the orientation of the adsorptives, a probable mechanism of adsorption has been suggested.

An assessment of the influence of the solvent on the adsorptive capacity of the alumina surface for the phenols has been

made by resolving the composite adsorption isotherms into the individual isotherms using experimentally determined monolayer values for the adsorptives from vapour and solution phase measurements.

In order to compare the adsorptive affinity of the alumina surface for the phenols, an index of adsorption K_A has been defined as "the number of moles of adsorptive present in the adsorbed phase at constant equilibrium mole fraction of the mobile phase". The values of K_A for the substituted phenols are seen to reflect the changes occurring in the electrical character of the hydroxyl group of the adsorptive due to the presence of thep-substituent, and are in accord with the relationship observed between hydrogen-bonding association in solution and p-substituent character.

CONTENTS

Experimental

INTRODUCTION

A. Adsorption at the Solid-Solution Interface

The importance of the study of adsorption characteristics at the solid-solution interface arises from the numerous practical uses which involve this type of interface. The purification of liquids such as drinking water and wines by solid adsorbents has been familiar for centuries, while more recently the growth of the chemical industry has enormously increased the range of substances to be purified in this manner. Other applications include the dyeing of fabrics, chromatography and chemical processes which require the use of a catalyst.

It is not surprising therefore, that in practice, adsorption at the solid-solution interface is more frequently encountered than adsorption at other types of interface. In the academic study of the adsorption process at the solid-solution interface, an important distinction from gas phase adsorption is immediately recognised, i.e. the adsorbed layer is complete at all equilibrium concentrations of bulk phase and contains a mixture of solute and solvent molecules.

The experimental study, to be described later in this thesis, is concerned with the adsorption of solids from solution. In order to understand the many factors responsible for isotherm characteristics, however, it is useful first of all to consider the experimental data obtained from adsorption from solutions consisting of completely miscible liquids.

1. Completely Miscible Liquids

The main types of isotherm experimentally realisable are shown in Fig.1,[1] (a) often representing adsorption data in dilute solution.

Whereas several attempts[2][3] have been made to derive a general equation for the isotherm, no simple equation has been put forward which can be applied universally.

(a) The Composite Isotherm [1]

The isotherm obtained experimentally when two or more components in the system are capable of being adsorbed by the solid adsorbent is termed the composite isotherm. An equation expressing the relationship between concentration change and the number of moles of each component adsorbed at equilibrium can be derived in the following manner.[4]

Consider a system of two components 1 and 2, the total number of moles being n_o. When placed in contact with m grams of solid adsorbent, let the mole fraction of component 1 decrease by Δx_1^1 This change in concentration is a result of the transfer of n_1^s moles of component 1 and n_2^s moles of component 2 from the solution to the surface of one gram of adsorbent.

At equilibrium, there remains in solution n_1^1 moles of component 1 and n_2^1 of component 2, giving mole fractions x_1^1 and x_2^1 respectively, initial mole fractions being represented by $(x_1^1)_o$ and $(x_2^1)_o$.

FIG I : TYPES OF ADSORPTION ISOTHERM

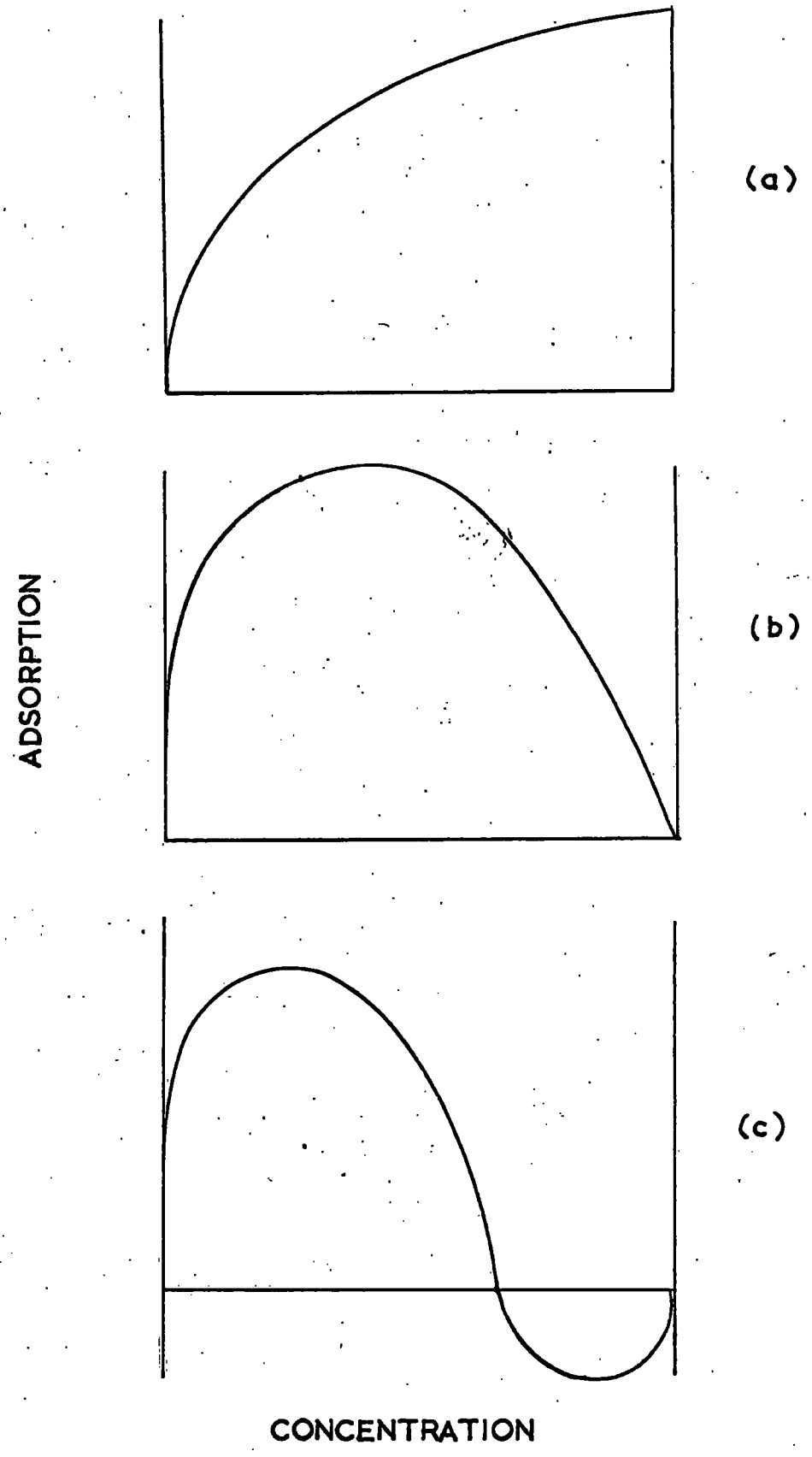

Then $n_o = n_1^l + n_2^l + n_1^s m + n_2^s m$

and $(x_1^l)_o = \dfrac{n_1^l + n_1^s m}{n_o}$, $x_1^l = \dfrac{n_1^l}{n_1^l + n_2^l}$

$$\Delta x_1^l = (x_1^l)_o - x_1^l = \frac{n_1^l + n_1^s m}{n_1^l + n_2^l + n_1^s m + n_2^s m} - \frac{n_1^l}{n_1^l + n_2^l}$$

$$= \frac{n_2^l n_1^s m - n_1^l n_2^s m}{(n_1^l + n_2^l)\, n_o}$$

$$\frac{n_o \Delta x_1^l}{m} = \frac{n_1^s n_2^l}{n_1^l + n_2^l} - \frac{n_1^l n_2^s}{n_1^l + n_2^l}$$

$$\frac{n_o \Delta x_1^l}{m} = n_1^s x_2^l - n_2^s x_1^l \qquad (1)$$

The composite isotherm is obtained by plotting $n_o \Delta x_1^l / m$ against x_1^l

(b) The Individual Isotherms

In order to resolve the composite isotherm into its two individual isotherms, a further expression involving n_1^s and n_2^s is necessary.

If it be assumed that the solid surface is completely covered by the adsorbed layer whatever the composition of the liquid phase and that this layer is unimolecular[5], then

$$n_1^s A_1 + n_2^s A_2 = A \qquad (2)$$

where A_1, A_2 are the partial molar areas occupied at the surface by the two components, 1 and 2 respectively, and A is the surface area of unit weight of solid.

This expression will only hold if the whole of the solid

surface is potentially accessible to each component. Thus it is true when considering non-porous solids but is not necessarily valid when molecules of appreciably different sizes are adsorbed onto a solid having narrow pores.

Kipling and Tester[6] suggested the alternative form of this expression:

$$\frac{n_1^s}{(n_1^s)m} + \frac{n_2^s}{(n_2^s)m} = 1 \qquad (3)$$

$(n_1^s)m$ and $(n_2^s)m$ being the numbers of moles of the individual components required to cover the surface area of unit weight of solid completely. These latter quantities can be determined by vapour phase adsorption of the individual components.

If adsorption at the solid-solution interface is multimolecular, then

$$\frac{n_1^s}{(n_1^s)m} + \frac{n_2^s}{(n_2^s)m} > 1 \qquad (4)$$

Day and Parfitt[7] have used equation (3) in interpreting adsorption on rutile from solutions of long chain alcohols (e.g. n-octanol) and hydrocarbons (e.g. n-heptane). They conclude that multilayer adsorption of the parallel-orientated hydrocarbon molecules occurs in the spaces between the perpendicularly-orientated adsorbed alcohol molecules to an extent dependent upon the length of the alcohol molecule. On this basis, the appropriate value of $(n_2^s)m$ is the number of moles of hydrocarbon which occupy the same volume

as that of a monolayer of alcohol molecules in a perpendicular orientation. Use of this value led to acceptable individual isotherms and substitution in equation (3) gave a value of 0·96 for the n-octanol-n-heptane system. This illustration emphasises the need to consider each system on its own merits in order to decide whether the assumption of monomolecular coverage of the adsorbent surface is justified.

(c) The "Perfect" Adsorbed Monolayer

Everett[8] proposed the use of a simple molecular model as a basis for an ideal system which would provide a reference state from which the behaviour of real systems could be studied. Deviations from this reference state could then be expressed in terms of activity coefficients enabling a comparison of real and ideal systems to be made.

Adsorption was considered to occur from a perfect solution consisting of two components 1 and 2 of different molar energies and entropies but of approximately similar molecular area onto a perfect adsorbing surface. This surface consisted of a number of exactly equivalent adsorption sites and adsorption was assumed to be monomolecular. The molecules when adsorbed occupied one adsorption site each and were assumed to have no interaction with each other. The liquid phase was described as an assembly of plane lattices stacked together with their planes parallel to the surface of the adsorbent.

Each plane, except the one adjacent to the adsorbent surface, was of the same composition with respect to components 1 and 2, the adsorbed phase being of different composition because of the selective adsorption of one or more components of the solution.

The free energy F of the system is defined as:-

$$F = U - T\,(S_{CONFIG.} + S_{THERM.}) \qquad (5)$$

where U is the energy of the system and $S_{CONFIG.}$, $S_{THERM.}$ are the configurational and thermal entropies respectively. Consideration of the total number of ways of arranging the molecules on the surface and in the solution enables the configurational entropy to be expressed in terms of the number of the moles in each phase. The total entropy is computed by addition of the molar thermal entropies of the molecules in both phases, assuming independence of the composition of both surface and solution. Similarly the energy of the system can be expressed in terms of the molar energies of the two kinds of molecules.

The adsorption equilibrium is described as

$$(1)^s + (2)^l \rightleftharpoons (1)^l + (2)^s \qquad (6)$$

where s and l superscripts represent the solid and liquid phase respectively.

On considering a perturbation of the system at equilibrium such that dn moles of component 1 are replaced on the surface by the same number of molecules of component 2 from the solution, then the corresponding change in free energy dF can be found from expression (5).

Introducing the condition of equilibrium,

$$\left(\frac{dF}{dn}\right)_{T,V} \equiv 0$$

Everett showed that:

$$\frac{x_1^s x_2^l}{x_1^l x_2^s} = K_1 \qquad (7)$$

where x_1^s, x_2^s; x_1^l, x_2^l are the mole fractions of components 1 and 2 on the solid and in solution, respectively, and K_1 replaces an exponential factor which contains terms relating to the changes of entropy and energy occurring on adsorption.

Rearrangement of equation (7) to

$$\frac{x_1^s}{(1-x_1^s)} = K_1 \frac{x_1^l}{x_2^l} \qquad (8)$$

reveals a close analogy to the Langmuir isotherm[9][10] for gas adsorption written in the form:

$$\theta/(1-\theta) = K_2 p \qquad (9)$$

where θ is the fraction of surface sites occupied, p the partial pressure of the gas and K_2 a constant.

Equation (9) can be shown to follow from equation (8) by identifying component 2 with the unoccupied sites on the adsorbent surface i.e. "holes", whose mole fraction in the gas phase is unity and which have zero energy and thermal entropy of adsorption.

Since $x_2^1 = (1-x_1^1)$ and $x_2^s = (1-x_1^s)$, equation (7) becomes

$$x_1^s = \frac{K_1 x_1^1}{1+(K_1-1)x_1^1} \qquad (10)$$

If the two components have the same molecular area, then at all equilibrium concentrations:

$$n_1^s + n_2^s = n^s \qquad (11)$$

where n^s is the total number of moles which can be accommodated in the adsorbed phase by unit weight of solid.

$$\text{Also } x_1^s = \frac{n_1^s}{n^s} \qquad (12)$$

Combining (10) and (12) gives

$$n_1^s = \frac{K_1 n^s x_1^1}{1+(K_1-1)x_1^1} \qquad (13)$$

$$\text{Similarly } n_2^s = \frac{n^s x_2^1}{K_1 - x_2^1(K_1-1)} \qquad (14)$$

Combining equations (1), (13) and (14) gives

$$(mx_1^1 x_2^1/n_o \Delta x_1^1) = \frac{1}{n^s}\left[x_1^1 + \frac{1}{(K-1)}\right] \qquad (15)$$

A plot of the left hand side of this equation against x_1^1 should give a linear graph of slope $\left(\frac{1}{n^s}\right)$ and of intercept $\frac{1}{n^s(K-1)}$, so allowing both n^s and K to be determined.

Experimental data for three simple systems when plotted according to equation (15) give reasonably straight lines as shown in Fig. 2 [11][12]

FIG 2

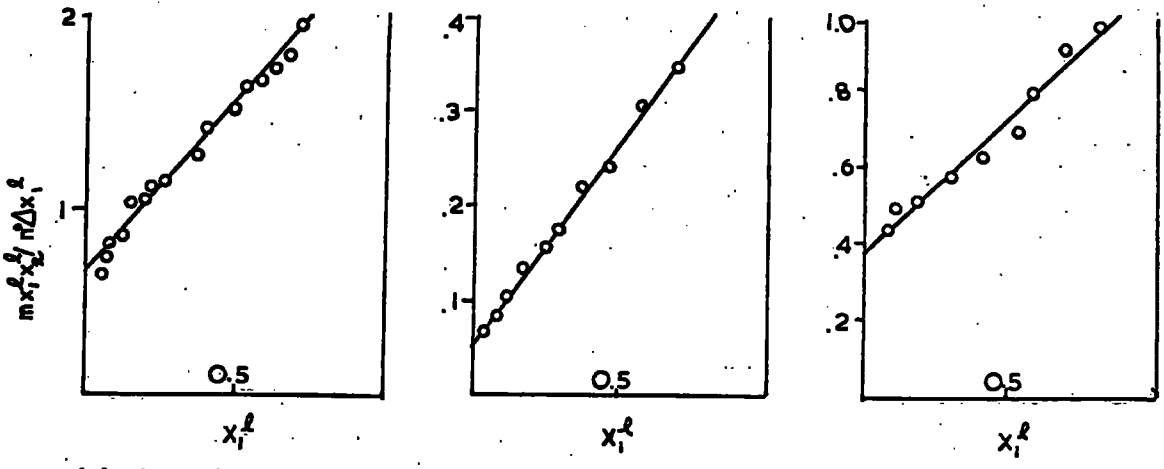

(a) Adsorption of Benzene and Cyclohexane on Spheron 6

(b) Adsorption of Benzene and Cyclohexane on Charcoal

(c) Adsorption of Benzene and Ethylene Dichloride on Boehmite

FIG 3

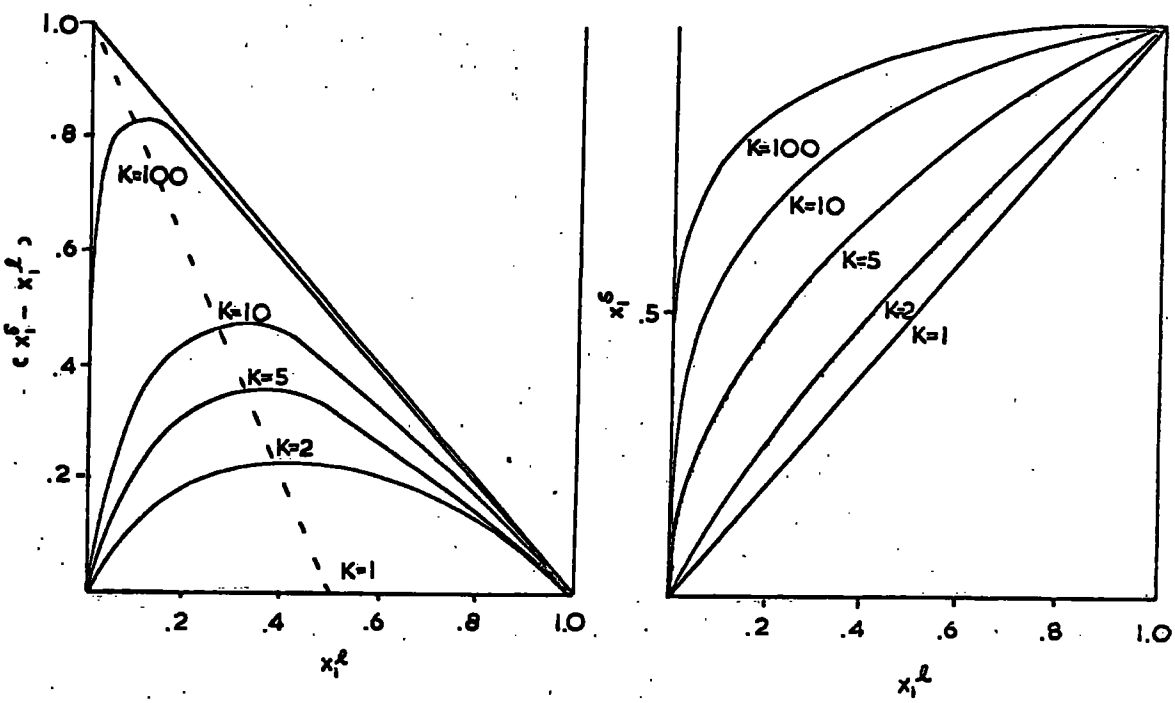

(a) Composite Isotherms For Different Values of K

(b) Individual Isotherms For Different Values of K

The surface areas of adsorbents calculated from these graphs using known values for the area requirements of the molecules adsorbed, show reasonable agreement with values determined from adsorption studies in the vapour phase.

Theoretical composite and individual isotherms for different values of K are shown in Fig. 3[8].

2. Solids in Solution

As a result of the extensive application of the process of adsorption of solids in solution, importance and interest attaches to:-

(a) the shape of the adsorption isotherm and the possibility of fitting it with an appropriate equation.

(b) the extent to which the solvent is adsorbed.

(c) the significance of the adsorption limit found in most isotherms.

(d) whether adsorption is confined to a single molecular layer or extends over several layers.

(e) the orientation of the adsorbed molecules.

(f) the existence of both physical and chemical adsorption.

(g) the effect of temperature

and it is proposed to consider each of these aspects in turn.

(a) The Adsorption Isotherm

Since the range of concentration over which adsorption of solids from solution can be studied, is limited by the solubility of the solid, it is often found that the isotherm of concentration change is almost identical with the individual isotherm.

From equation (1)

$$n_0 \Delta x_1^1/m = n_1^s x_2^1 - n_2^s x_1^1$$

If $x_1^1 \ll 1$ and $x_2^1 \sim 1$, then, even if n_2^s is large

$$n_0 \Delta x_1^1/m \sim n_1^s \qquad (16)$$

If the solid is strongly adsorbed, as is usually the case, then $K \gg 1$ and equation (13) becomes

$$n_1^s = \frac{K_1 n^s x_1^1}{1 + K_1 x_1^1} \qquad (17)$$

Combining (6) and (7) gives

$$n_0 \Delta x_1^1/m = K_1 n^s x_1^1 / (1 + K_1 x_1^1)$$

$$\frac{m x_1^1}{n_0 \Delta x_1^1} = \frac{1}{K n^s} + \frac{x_1^1}{n^s} \qquad (18)$$

which is a modification of the Everett equation for a perfect system, applied to a strongly adsorbing solid solute in dilute solution, and is of the Langmuir-type.

Plotting $\frac{mx_1^1}{n_o \Delta x_1^1}$ against x_1^1 should give a straight line of intercept $1/K.n^s$ and slope $1/n^s$, enabling n^s and K to be evaluated. It must be remembered, however, that the application of equation (18) is subject to the same assumptions and limitations as the original Everett treatment of the perfect adsorption system.

The isotherm equation (17) is a Langmuir-type equation and gives a curve of the form shown in Fig. 1(a).

Although the majority of experimental adsorption data in dilute solution fits the curve shown in Fig. 1(a), several other shapes of isotherms have been observed. These have been classified by Giles[13] according to the scheme shown in Fig.4. The main classification is based on the initial slope of the isotherm and the minor classification on the shape at higher concentrations.

The S curve is obtained if (i) the solvent is strongly adsorbed, (ii) there is strong inter-molecular attraction within the adsorbed layer, (iii) the adsorbate is mono-functional.

The L curve is found when there is no strong competition from the solvent for the sites on the surface. The H curve occurs when a high affinity exists between the adsorbate and the adsorbent and the C curve indicates constant partition of the adsorbate between the solution and the adsorbent.

FIG 4
CLASSIFICATION OF ISOTHERMS

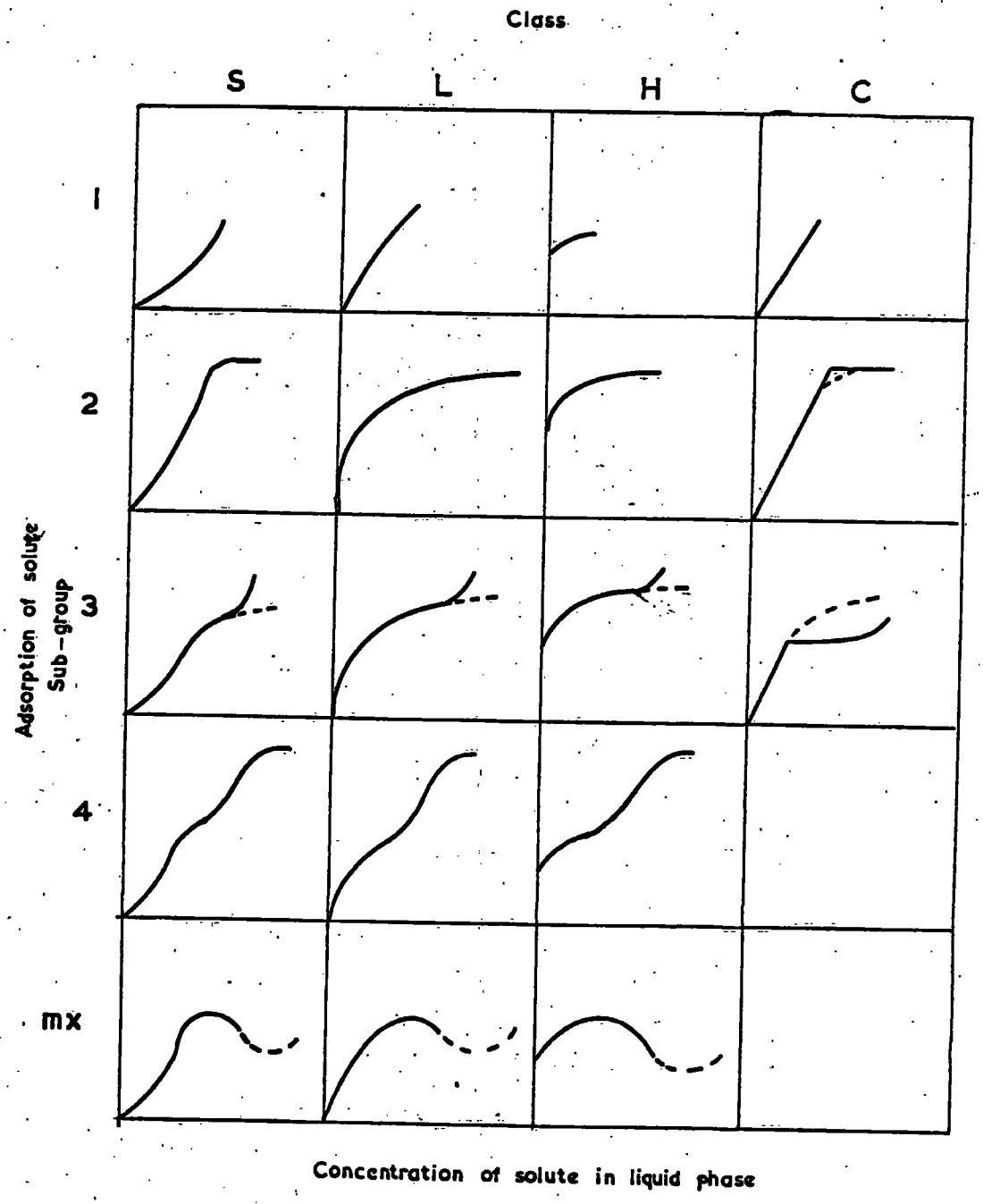

(b) Adsorption of the Solvent

In systems where the extent of the isotherm is limited by the solubility of the solid, the form of the composite isotherm is seen to almost coincide with that of the individual isotherm even if considerable adsorption of the solvent occurs. However, if the solid is appreciably soluble, divergencies between the two isotherms become more marked with increasing concentration and adsorption of the solvent becomes important in explaining isotherm characteristics. This is shown in Fig. 5 for the adsorption of malonic acid from aqueous solutions onto Graphon.[14]

The divergence can be attributed to two effects. One is the high value of x_1^1 making the approximation (16) no longer valid and the other is the relatively high value of n_2^s at high concentrations. The importance of the second effect can be seen by comparison of Figs. 5 and 6. For both systems, the adsorption of solvent is particularly high in relation to that of the solute. This can be explained by reference to the comparative sizes of the solute and solvent molecules.

(c) The Adsorption Limit

The isotherm in Fig. 6 approaches a limiting value of adsorption with increasing concentration. Resemblance of the isotherm to those obtained from studies in the vapour phase led to the assumptions that the plateau represents complete monolayer

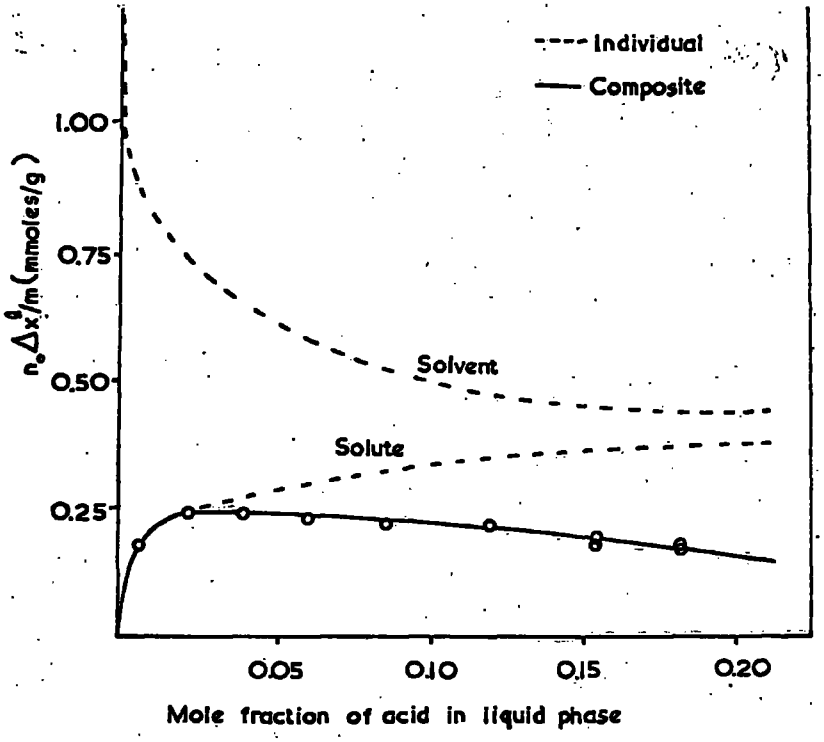

FIG 5

ADSORPTION OF MALONIC ACID FROM AQUEOUS SOLUTION BY GRAPHON

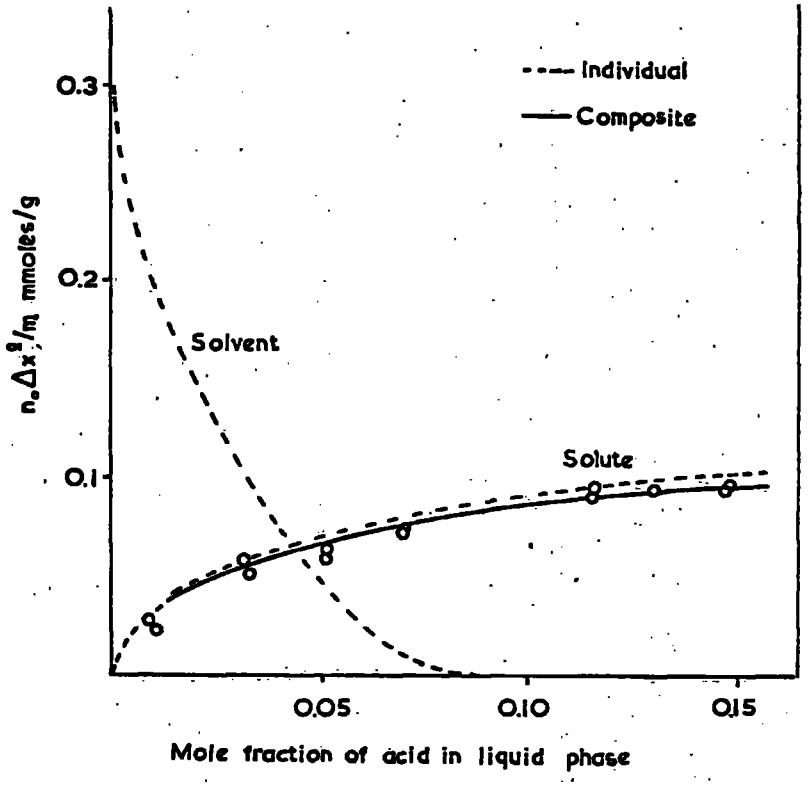

FIG 6

ADSORPTION OF LAURIC ACID FROM CARBON TETRACHLORIDE BY GRAPHON

coverage of the surface by the solute and that the isotherm should be fitted by a Langmuir-type equation. However, a Langmuir-type equation also fits those isotherms of the shape shown in Fig.7, which do not form a plateau before the solubility limit is reached.[14] For these systems, equation (17) gives such different values for the adsorption limit that all of them cannot correspond to complete monolayer coverage of the adsorbent surface. Thus, the applicability of a Langmuir-type equation to a system does not necessarily indicate monomolecular adsorption of the solute, nor are the derived constants (n^s) and (K) necessarily meaningful.

Independent methods used for the determination of surface areas of suitable adsorbents can provide information on the significance of the plateau found in certain systems. For the adsorption of stearic acid onto Graphon[14], the plateau is the same for four different solvents as shown in Fig. 8.

This plateau corresponds to an area of 114 Å^2 for each monomeric molecule of adsorbed stearic acid. This is the value calculated, assuming the molecules are in a complete monolayer packed with their major axis parallel to the surface. The arrangement is shown in Fig. 9.

It seems reasonable to assume therefore, that in this case, the limit of adsorption corresponds to the completion of a monolayer.

Certain isotherms show an extensive decline after attaining the adsorption limit. The decline could be attributed to the continuing adsorption of the solvent at high concentrations but

FIG 7

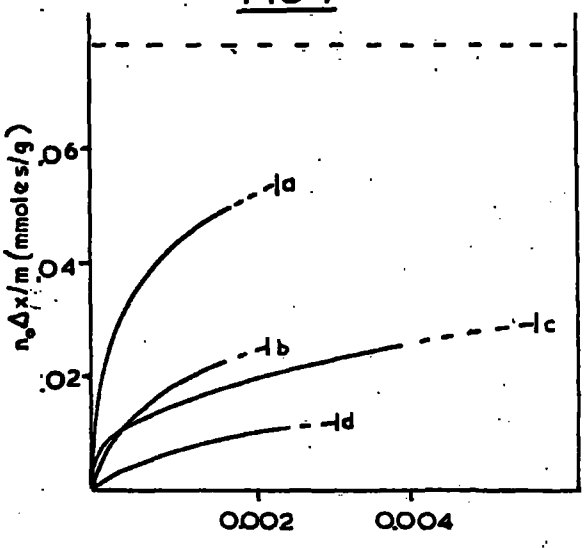

Mole fraction of dimeric acid in liquid phase

ADSORPTION OF STEARIC ACID ON SPHERON 6 FROM

(a) Cyclohexane
(b) Ethyl Alcohol
(c) Carbon Tetrachloride
(d) Benzene

FIG 8

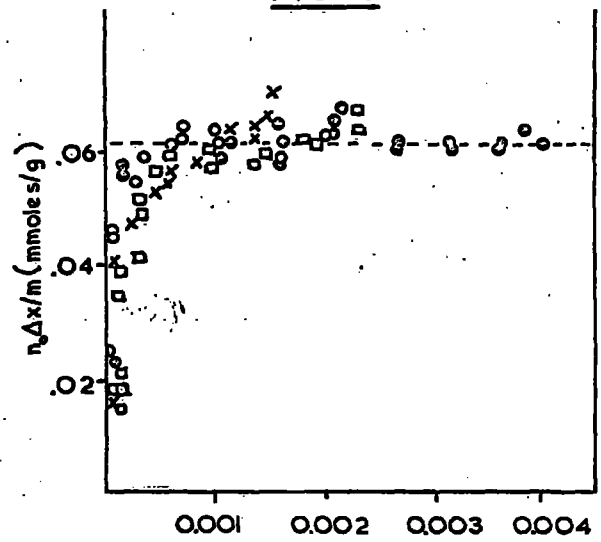

Mole fraction of dimeric acid in liquid phase

ADSORPTION OF STEARIC ACID ON GRAPHON FROM

o Cyclohexane
• Carbon Tetrachloride
x Ethyl Alcohol
□ Benzene

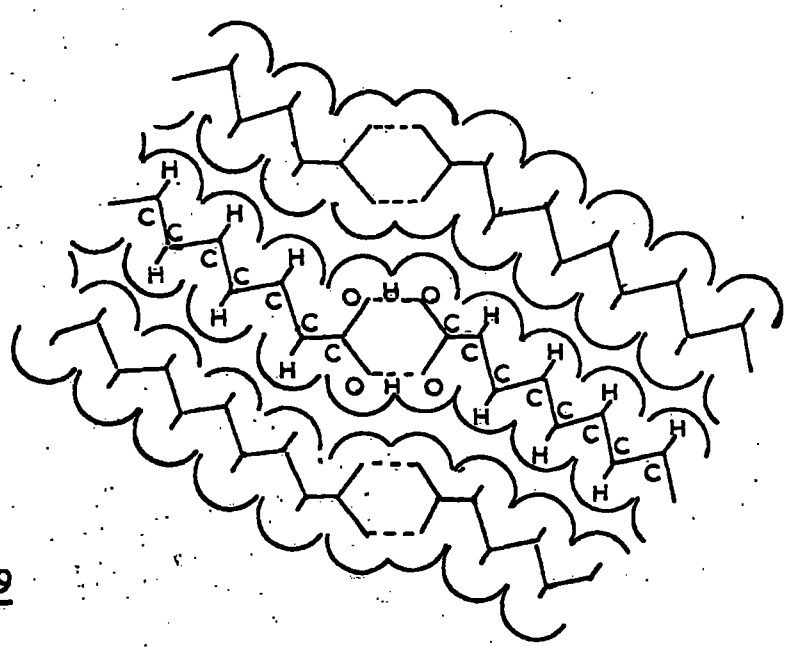

FIG 9

ARRANGEMENT OF STEARIC ACID MOLECULES IN A COMPLETE MONOLAYER ON GRAPHON

this cannot apply in systems where a complete monolayer of solute is formed at a low concentration which is appreciably below the solubility limit. In such systems, the approximation (16) is no longer justified as n_1^s is constant and n_2^s is zero; thus equation (1) becomes:-

$$n_o \Delta x_1^1 / m = n_1^s (1 - x_1^1) \qquad (19)$$

Therefore, after the adsorption limit has been reached, the composite isotherm must fall linearly with concentration and extrapolation of this linear section to $x_1^1 = 0$, gives a value of n_1^s corresponding to a complete monolayer.

A few isotherms are known for which a linear section occurring after a maximum is not indicative of monolayer coverage of the adsorbent surface because extrapolation to $x_1^1 = 1$ does not give a value of zero for $(n_o \Delta x_1^1 / m \quad)$. An example of such a system[15] is illustrated in Fig.10 and the implication is that adsorption of the solvent is also important and the adsorbed phase probably consists of a hydrate of malonic acid instead of the anhydrous acid.

(d) Multilayer Formation

Some reasons for supposing that in many cases adsorption is confined to a single molecular layer have been discussed above. However, some systems are known in which the composite isotherm possesses a plateau followed by a subsequent rise (Fig.11) close to the solubility limit.

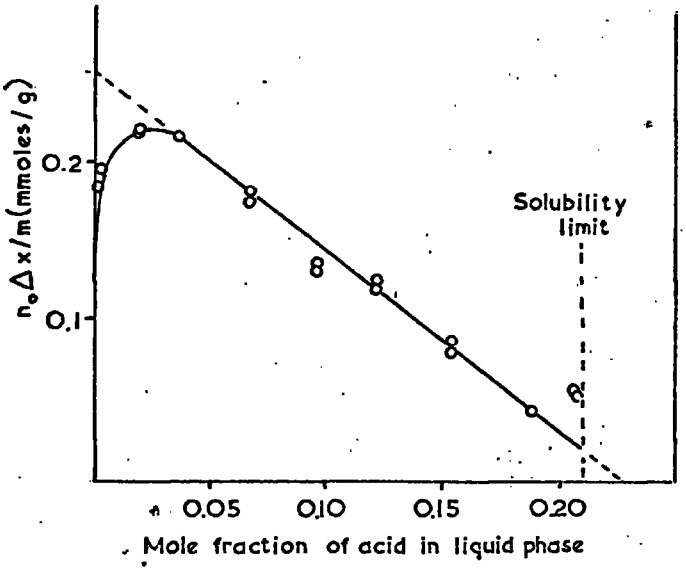

FIG 10

ADSORPTION ON SPHERON 6 FROM AQUEOUS SOLUTIONS OF MALONIC ACID

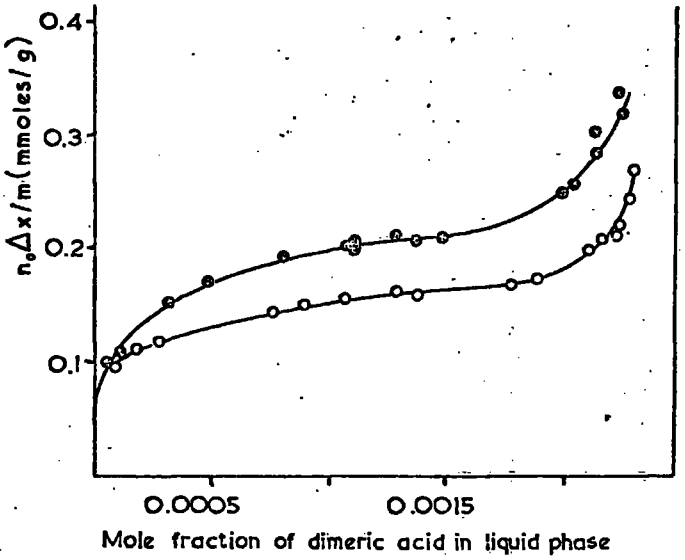

FIG 11

ADSORPTION OF STEARIC ACID FROM CYCLOHEXANE SOLUTION ON CARBON BLACK

- • Carbolac I (2400°C)
- o Monarch 74 (2000°C)

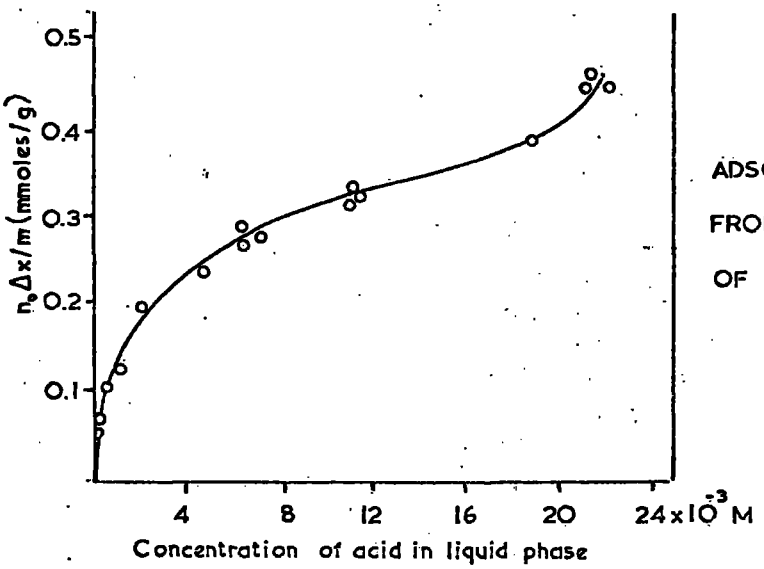

FIG 12

ADSORPTION ON GRAPHON FROM AQUEOUS SOLUTIONS OF BENZOIC ACID

The rise is thought to correspond to the solute crystallising out onto the adsorbent surface.[14]

In the adsorption of benzoic acid from water by Graphon,[16] the isotherm has the form shown in Fig.12.

The slight knee probably corresponds to a completed monolayer of benzoic acid while the subsequent rise suggests multilayer formation.

In general, the occurrence of multilayer adsorption can be deduced from a consideration of the equation for the composite isotherm. The highest value which ($n_o \Delta x_1^1/m$) can have assuming monolayer adsorption, corresponds to complete coverage of the surface by component 1 and no adsorption of component 2. Equation (1) then reduces to

$$\frac{n_o \Delta x_1^1}{m} = (n_1^s)_m . (1 - x_1^1) \qquad (20)$$

Thus if a value of ($n_o \Delta x_1^1/m$) exceeds that of $(n_1^s)m(1-x_1^1)$, multilayer adsorption will occur.[17]

Application of equation (20) requires a knowledge of the value for $(n_1^s)m$. This cannot usually be obtained from adsorption in the vapour phase and has to be calculated either from data for the crystal or from an assumed packing of the molecules drawn to scale on the basis of accepted bond lengths and bond angles. The latter involves a knowledge of the orientation of the adsorbed molecule and this may have to be assumed as there is no reliable method for its determination.

(e) Orientation of the Adsorbed Molecule

In order to resolve the composite isotherm into its individual components using equation (3), a value for complete monolayer coverage of the adsorbent surface by the solute i.e. $(n_1^s)_m$ is required. As discussed above, $(n_1^s)_m$ has to be calculated mathematically using an assumed orientation of the adsorbed molecules. To predict the probable orientation of the adsorbed molecule, it is necessary to consider both the nature of the adsorbate and the adsorbent surface.

(i) Carbon Surfaces

In the adsorption of stearic acid onto non-porous carbon adsorbents from organic solvents,[14] the experimental results indicate that the acid is adsorbed with the hydrocarbon chain parallel to the surface to form a close-packed monolayer. The orientation can be explained on the basis of the acid being largely dimerised in the solvent phase. On adsorption, the double hydrogen bonding of the carboxyl groups of the dimer is not broken if the molecules assume a parallel orientation to the surface whereas for a perpendicular orientation, the bonds have to be broken with resulting adsorption of the monomer. Thus a perpendicular orientation is only possible if the polarity of the adsorbent is sufficiently high to form a bond with the adsorbate which can compensate for the rupture of the hydrogen bonds in the dimeric molecule. When the carbon surface possesses oxygen complexes, a

close-packed monolayer is not formed even at the highest concentrations, implying adsorption of the solvent. If the solute is so strongly attached to the surface that it adopts a perpendicular orientation, then assuming that monomeric molecules are adsorbed by hydrogen bonding at specific sites (i.e. oxygen complexes) on the surface, the closeness of packing in the adsorbed phase will be determined by the spacing of these sites.

When phenol is adsorbed from organic solvents, it covers only a small proportion of the charcoal surface.[18] The extent of adsorption may be regarded as a measure of the surface occupied by polar (oxygen) groups. Alkyl substituents in the ortho position reduce the extent of adsorption indicating that phenol is attached to the surface via its hydroxyl group and thus is orientated perpendicularly to the surface. Phenol is readily adsorbed from water by Graphon,[13] a carbon which possesses no specific adsorption sites. It is likely in this system that interaction occurs between the π -electron system of the benzene ring and the carbon surface with the molecules being adsorbed from solutions of low concentrations with the benzene ring parallel to the surface. At higher concentrations, the form of the adsorption isotherm indicates that the molecules reorientate with their major axis perpendicular to the surface and with the hydroxyl group pointing towards the polar aqueous phase.

Molecules such as the paraffins which contain no functional groups can be expected to assume parallel orientation to the carbon surface. This has been shown experimentally in the adsorption on carbon blacks from carbon tetrachloride solution.[19]

(ii) Silica Surfaces

In the adsorption of monocarboxylic acids onto silica from non-polar solvents,[20] the isotherms expressed in terms of weight adsorbed per unit weight of solid were found to be identical for a range of acids, implying a parallel orientation for the adsorbed molecules.

The orientation assumed by alcohols on a silica surface[21] appears to be related to the length of the hydrocarbon chain. This is seen from the adsorption of various alcohols on three samples of silica having different degrees of hydration. The limiting adsorption values per unit area of surface are as follows:-

Sample of Silica	A	B	C
Water content %	7.9	4.2	2.8
Limiting adsorption (μ moles/m^2)			
CH_3OH	13.5	9.5	8.5
C_3H_7OH	5.0	4.8	4.4
$C_6H_{13}OH$	3.6	3.4	3.2
$C_8H_{17}OH$	2.6	2.6	2.6

From these values, it would appear that octanol is adsorbed parallel to the surface while the shorter chain alcohols probably tend to a

perpendicular orientation. The limiting adsorption values for the lower alcohols are seen to vary with the water content of the silica. As water content provides a guide to the surface concentrations of hydroxyl groups, it would appear that the lower members of the alcohols are adsorbed perpendicularly on specific sites. In conclusion, the adsorption of the shorter chain alcohols probably depends on the interaction of their hydroxyl groups with those of the silica surface, whereas the longer chain alcohols are adsorbed primarily because the hydrocarbon chain is held by the surface.

(iii) Alumina Surfaces

Adsorption of monocarboxylic acids from organic solvents onto alumina occurs with the major axis of the adsorbed molecule perpendicular to the surface.[22,23] The adsorbed molecules do not form a close-packed monolayer, implying adsorption onto specific sites such as oxygen atoms or ions. Thus the most effective use of the surface of the polar adsorbent is achieved by the hydrogen bonding of a large number of monomeric molecules in contrast to the van der Waals adsorption of a small number of dimeric molecules in the case of non-polar solids.[24]

The effect that specific site adsorption has on the packing arrangement of stearic acid on alumina is shown in Fig. 13.[22] The spacings of the lattice of the 'a' plane of γ-alumina monohydrate are such that specific site adsorption of stearic acid results in only about $\frac{1}{2}$ of the specific surface being covered.

When the nature of the crystal lattice is known, the 'coverage' can be calculated approximately and is found to agree well with experimental values. Thus De Boer considered that specific site adsorption of lauric acid from pentane solution could be used for the determination of the surface area of alumina. This method is discussed later in 'Characterisation of the Alumina Surface'.

Phenols when adsorbed from cyclohexane[25] are found to adopt a perpendicular orientation and cover the alumina surface with an almost complete monolayer. If water is used as the solvent, it competes with the phenol for the adsorption sites on the alumina surface and the isotherm is found to be convex to the concentration axis near the origin.[26] Fig. 14.

In the adsorption of aromatic hydrocarbons[19] from xylene onto alumina, the isotherm (Fig.15) is convex to the concentration axis at low concentrations and may not reach a limiting value. In the case of phenanthrene,[27] the limiting value corresponds to a coverage of a very small fraction of the surface. Giles argues that the molecules are probably adsorbed with the plane of the rings perpendicular to the surface, small clusters being formed on active sites. These latter may be aluminium atoms exposed on the outer surface as a result of mechanical damage.

FIG 13

ADSORPTION OF STEARIC ACID ON THE a PLANE OF γ-ALUMINA MONOHYDRATE

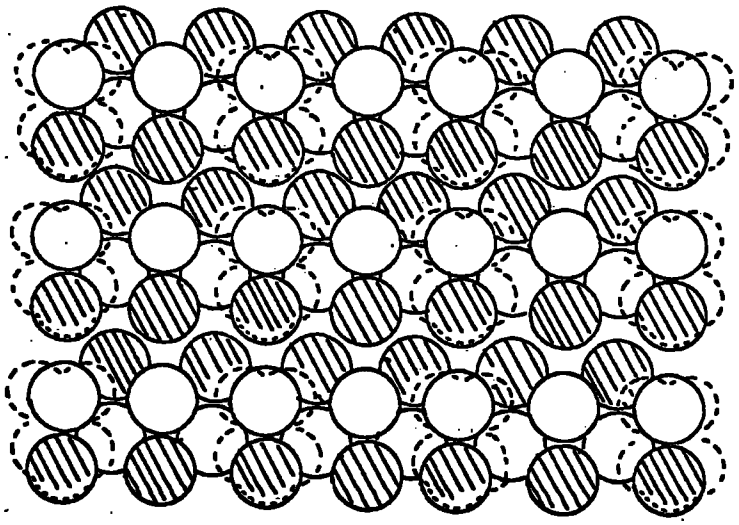

O Oxide ions ⊛ Hydroxide ions ---- Stearic acid

FIG 14

ADSORPTION ON ALUMINA FROM AQUEOUS SOLUTIONS OF PHENOL

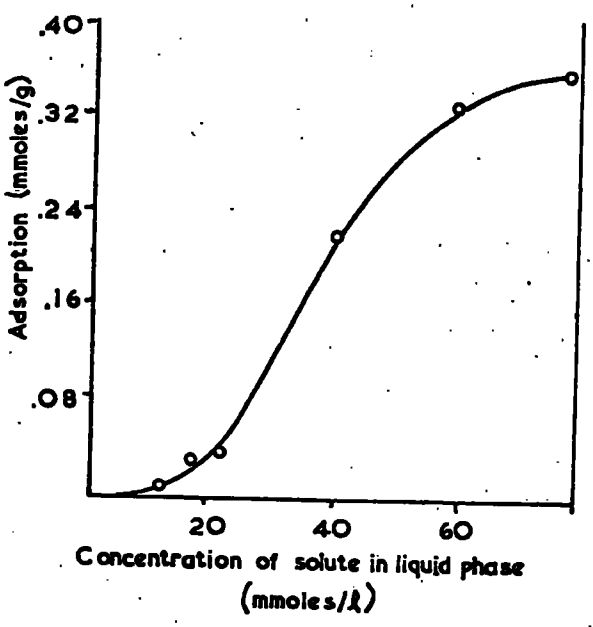

FIG 15

ADSORPTION OF PHENANTHRENE FROM XYLENE ON ALUMINA

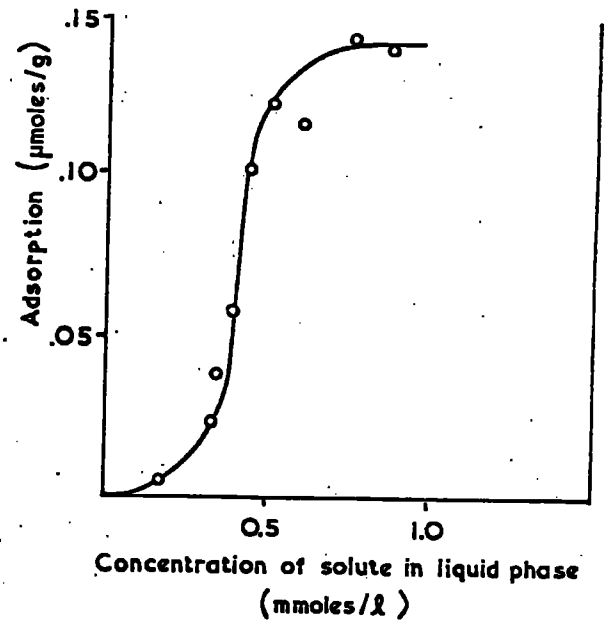

(f) Physical and Chemical Adsorption

Chemisorption is known to occur in a number of systems during adsorption at room temperature.[28][29][30] The most obvious case arises when the isotherm shows an independence of concentration except at the very lowest values[31] (Fig.16).

The level of adsorption is also found to be independent of the solvent used and of the chain length of the solute in a homologous series. In systems where physical adsorption occurs on top of a chemisorbed first layer, the isotherm originates at a point well above the origin but rises with increasing concentration.[32] The observed isotherm is thus the sum of two isotherms, one dependent and one independent of the concentration of the solution. (Fig.17.)

Desorption of the solute can occasionally provide further evidence as to whether chemisorption has occurred since a derivative formed by reaction between the adsorbate and adsorbent is sometimes recovered. Thus a soap is frequently desorbed after a fatty acid has been chemisorbed by a metallic oxide.[28] In general, chemisorption is a much slower process than physical adsorption and the time taken for a system to attain equilibrium may indicate the predominant adsorption mechanism.

(g) The Effect of Temperature

As adsorption is an exothermic process, increase in temperature should result in diminished adsorption at low equilibrium concentrations. At high concentrations, the isotherm may almost reach the same limiting adsorption value.[28] (Fig.18)

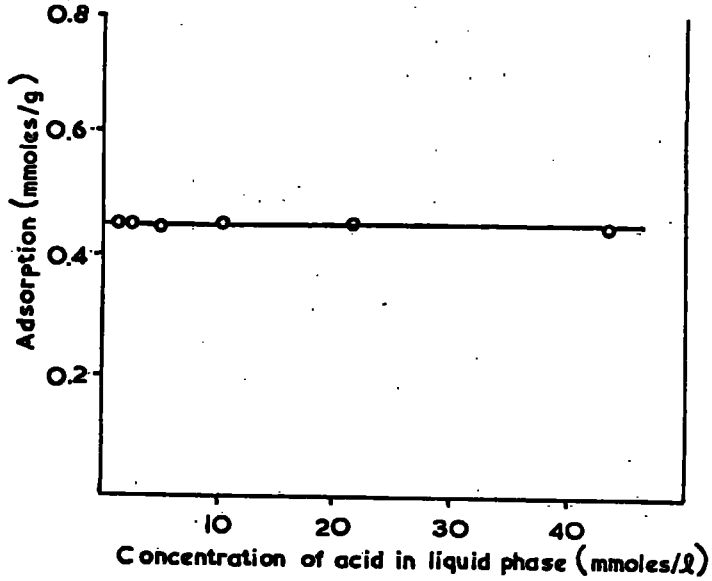

FIG 16

CHEMISORPTION OF PALMITIC ACID FROM BENZENE BY ADAMS PLATINUM CATALYST

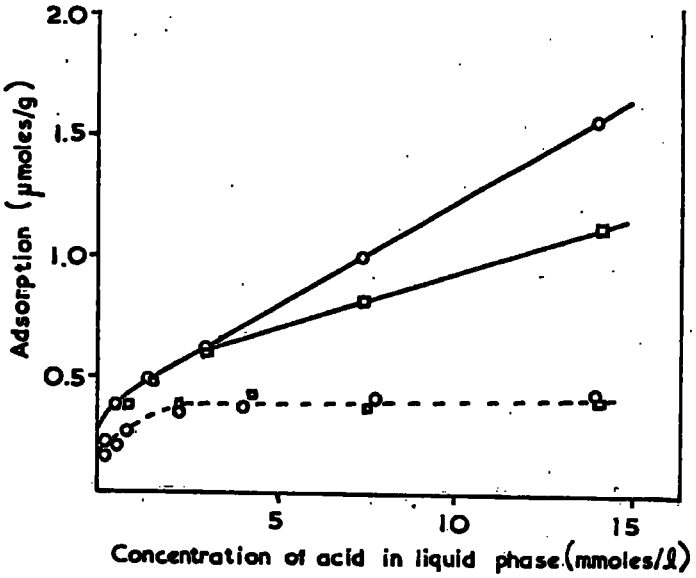

FIG 17

CHEMISORPTION AND PHYSICAL ADSORPTION OF CAPRIC □ AND STEARIC o ACIDS FROM BENZENE ON STEEL

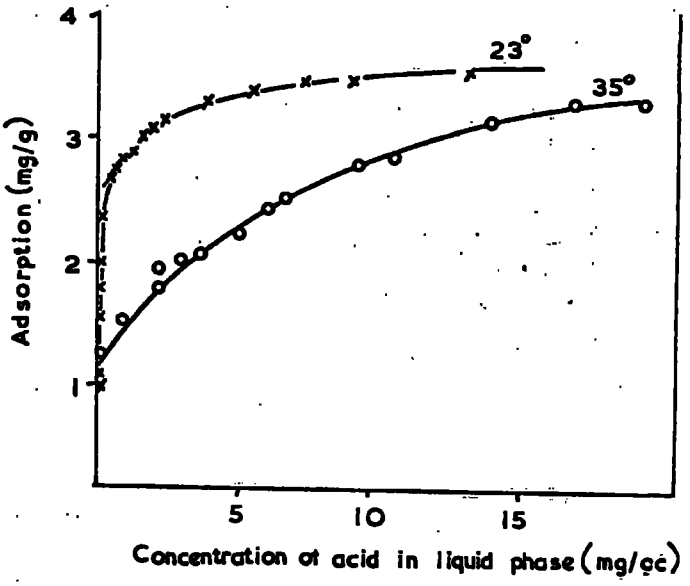

FIG 18

EFFECT OF TEMPERATURE ON ADSORPTION OF STEARIC ACID FROM BENZENE BY NICKEL

The observed change in the shape of the isotherm corresponds to a weakening of the attractive forces between the solute and the solid surface and the rise in solubility of the solute in the solvent. In certain cases, use of a relative concentration term (i.e. C/C_o where C is the equilibrium concentration and C_o the concentration of a saturated solution) as a measure of the activity or escaping tendency of the solute, enable isotherms obtained at two different temperatures to be superimposed. Thus the activity of the solute may well be a dominant factor when considering the effect of temperature on the adsorption process.(33)

(3) Factors Influencing Competitive Adsorption

As both components in a binary mixture are capable of being adsorbed, preferential adsorption(34) will be of common occurrence. Several factors are responsible for competitive adsorption at the solid-solution interface and the most important of these concern the interactions between each component in the liquid phase and the interactions of each with the solid surface. The nature of the adsorbent also requires consideration in the respect of porosity and surface heterogeneity as both are known to influence competitive adsorption.

(a) Interaction between Adsorbates and Adsorbent

The existence of competition in physical adsorption between the components of a solution depends most frequently on the difference in the strengths of interaction between adsorbent and the adsorbates. It seems likely that quite small differences in adsorptive forces may

be responsible for preferential adsorption which can readily be detected experimentally. In discussing the importance of the surface of the adsorbent in so far as selective adsorption is concerned, it must be realised that heterogeneity of the surface may have a dominant effect. Thus it is convenient to discuss the nature of the interaction between adsorbates and adsorbent by reference to two distinct types of adsorbent surface, i.e. non-polar carbon surfaces and polar metal oxide surfaces.

In general, carbon surfaces adsorb benzene in preference to alcohols,[35] Fig.19, a result which is to be expected in view of the non-polar nature of the surfaces. However, at very low concentrations the alcohol is seen to be preferentially adsorbed due to the presence of a small proportion of polar sites[36] on the surface. The nature of the interaction of the alcohol with the surface is probably hydrogen-bonding as this mechanism is certainly important in explaining the strong preferential adsorption of phenol from cyclohexane by charcoal.[19] In this latter adsorption system, substitution of tertiary butyl groups in the two ortho positions of the phenol considerably reduces the extent of adsorption. As these groups have a mainly steric effect and also indirectly weaken the hydrogen bond, it is inferred that the hydroxyl group is the centre of adsorption and that hydrogen bonding is probably the nature of the interaction between the phenol and the surface.

The effect of complete removal of oxygen complexes from a carbon surface is shown by comparing adsorption from alcohol-benzene

mixtures by a carbon black, Spheron 6 and by Graphon (Spheron 6 which has been heated to 2,700°C to remove oxygen complexes).[37] Graphon shows complete preferential adsorption of benzene, whereas Spheron 6 shows preferential adsorption of alcohols over a considerable range of concentration.[38] It has been similarly shown that the degree of preferential adsorption of octadecanol from benzene increases with the oxygen content of carbon black. When the carbon black has been heated to remove all traces of surface oxygen,[39] the competition for the adsorption sites is then virtually between a paraffin chain and an aromatic molecule and experiments using mixtures of cyclohexane and benzene have shown the aromatic material to be preferentially adsorbed by the carbon black.[38]

Similarly, methyl acetate is only preferentially adsorbed to benzene at very low concentrations[35] Fig.20. This is indicative of the strong interaction between the ester group and the polar sites on the charcoal surface. When these sites are saturated, adsorption is governed by the π -electron interaction between the aromatic solid and the aromatic benzene molecules which is stronger than that between the solid and the aliphatic ester. In the preferential adsorption of ethylene dichloride from benzene solution by charcoal,[40] the isotherm reverses midway through the concentration range reflecting the heterogeneity of the charcoal surface. The interaction, in this case, is probably due to inductive forces produced as a result of the more polar sites having a polarising influence on the chlorine atoms.

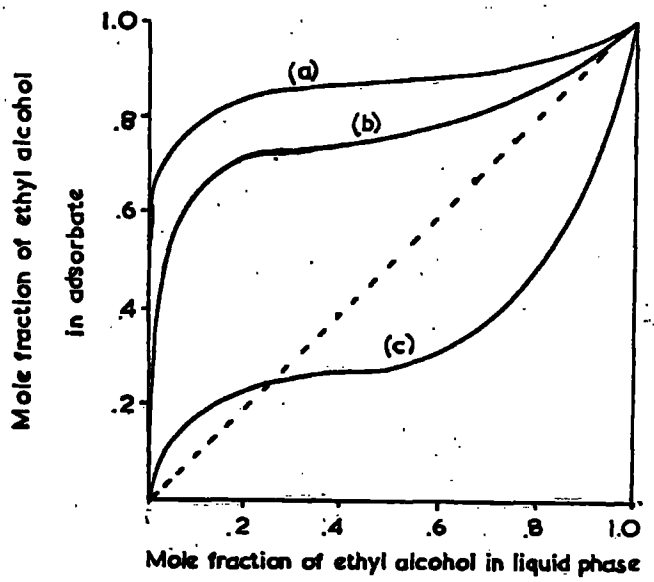

FIG 19

ADSORPTION OF ETHYL ALCOHOL FROM MIXTURES WITH BENZENE ON

(a) Silica gel
(b) γ-Alumina
(c) Charcoal

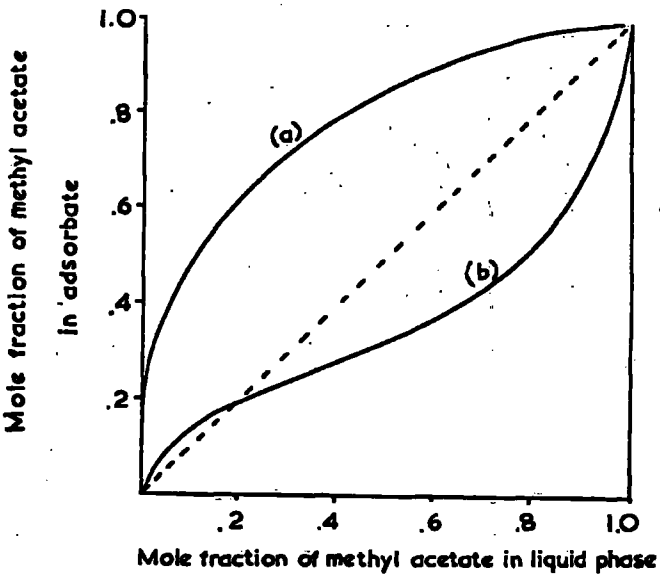

FIG 20

ADSORPTION OF METHYL ACETATE FROM MIXTURES WITH BENZENE ON

(a) Silica gel or boehmite
(b) Charcoal

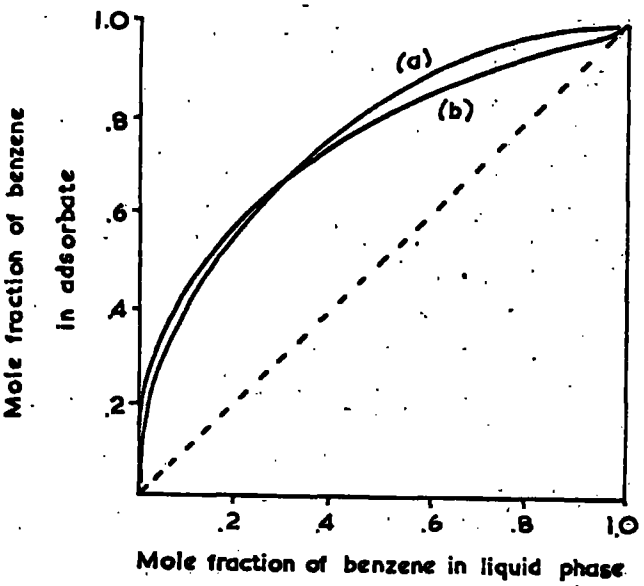

FIG 21

ADSORPTION OF BENZENE FROM MIXTURES WITH CYCLOHEXANE ON

(a) Spheron 6
(b) Boehmite

Substances with substituents in the aromatic ring (e.g. mesitylene, o- and p-xylene, t-butylbenzene and isopropylbenzene) are adsorbed much less strongly then benzene at low concentrations.[19] The substituent groups have the effect of increasing the distance between the plane of the aromatic ring and the solid surface (if the plane is parallel to the surface) or between the plane of adjacent rings (if the plane is perpendicular to the surface). In either case, a reduction in adsorption would occur.

In the absence of specific polar groups, the π -electrons of aromatic systems ensure that aromatic compounds are adsorbed preferentially to corresponding aliphatic compounds by polar solids or any others capable of specific interactions with π -electron systems. This is illustrated by the preferential adsorption of benzene from mixtures with cyclohexane by Spheron 6[35] and is shown in Fig. 21.

Metal oxide surfaces are found to adsorb alcohols in preference to benzene (Fig.19)[41][42][43] over the whole of the concentration range, thus reflecting the polar nature of these surfaces. The interaction between the lower alcohols and the surface is most probably hydrogen bonding. Similarly methyl acetate is preferentially adsorbed to benzene by silica and alumina[35] surfaces (Fig.20) and this can be attributed to specific interaction of the polar centre of the ester molecule with the polar groups which cover the solid surface. Oxide gels adsorb ethylene dichloride from mixtures preferentially[40] with benzene and this can be attributed to polarisation of the chlorine atoms, in which respect it is probably

significant that alumina, with a greater ionic character than silica, shows a stronger preference for ethylene dichloride. Evidence that hydrogen bonding is important in the study of adsorption on metal oxide surfaces is shown by the relative affinities of silica gel for a series of nitro- and nitroso- derivatives of diphenylamine and N-ethylamine dissolved in simple solvents. The affinity of these compounds for the surface is found to depend on the strength of the hydrogen bond which can be formed between adsorbent and adsorbate.(44)

The preferential adsorption of one component over the whole of the concentration range in the above examples infers that the surfaces of metal oxides are essentially homogeneous in contrast to the marked heterogeneity of carbon surfaces. This is because heterogeneity in oxide surfaces generally arises from the presence of both oxide and hydroxide groups and as these are both highly polar, their different discriminations between pairs of adsorbates is not always easy to detect. It is thought to be important in the adsorption of fatty acids by silica gel(45) as the occurrence of hydrogen-bonding is postulated as:

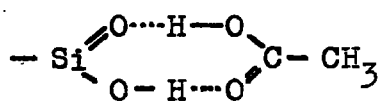

which is analogous to the formation of a dimeric molecule of fatty acid. The double hydrogen bond could not be formed on a surface consisting of oxide groups only. A similar effect is important in determining the spacing between stearic acid molecules adsorbed from solution in organic solvents on various kinds of alumina.(22)

In conclusion, if the interaction between adsorbate and adsorbent is responsible for the preferential adsorption of one component from a binary mixture, then the shape of the composite isotherm is seen to be influenced by the nature of the adsorbent surface. Thus U-shaped isotherms are to be expected when considering a homogeneous surface which can adsorb one component of a binary mixture more strongly than the other. This is generally observed with oxide adsorbents. S-shaped isotherms would be expected if two types of chemical groups were present on the adsorbent surface, each having different affinities for the two components of the liquid. This type of isotherm is very frequently found in adsorption by charcoals and other carbons.[6][41]

The two types of isotherm are shown in Fig. 1b, c.

(b) Porosity of the Adsorbent

The existence of pores in an adsorbent can result in preferential adsorption of the smaller component irrespective of the competition arising from other factors. Pores range in size from less than 20Å (micro) up to 200Å (intermediate) and beyond.[46] The general effect of porosity is shown by those types of adsorbent for which a series of related solids can be produced with varying degrees of porosity, e.g. chargoals by varying the degree of activation,[47] silica gels by varying the conditions of forming or calcining the gel.[48] In these cases, the increase in porosity is normally accompanied by an increase in specific surface area and thus by an

increase in the magnitude of the selective adsorption e.g. adsorption of fatty acids from water on a series of steam-activated carbon blacks[49] and on steam activated charcoals.[50]

Non-porous solids are known to undergo adsorption by an area-filling process while it is thought that adsorption by porous solids may involve a pore-filling process in which the volume of pores available to the adsorbate is the controlling factor.[51] For example, Kiselev and Shcherbakova[52] showed that the limiting values for adsorption (expressed in millimoles per gram) of the lower fatty acids from aqueous solution by a porous charcoal decreased with increasing chain length. However, the limiting molar volume adsorbed was almost the same for all the acids studied. This was assessed against the observation that for non-porous solids, the limiting molar adsorption of such compounds is independent of chain length.[53] It was concluded that a pore-filling process dominated the adsorption on the porous charcoal, the volume adsorbed (0.28cc per gram) representing the pore volume of the adsorbent. The conclusion, however, is not necessarily valid, because on less polar solids solutes may be adsorbed with chains parallel to the surface. When a complete monolayer is formed, the area covered is the same for all members of the series (but the number of moles adsorbed per gram varies) and the limiting volume of adsorbate remains approximately constant.

For some solids (e.g. a silica gel with wide pores), the volume of a monolayer would be much smaller than the total pore volume. For others (e.g. many activated charcoals with narrow pores), the

difference might be small as most of the surface area is located in pores too narrow to adsorb more than one molecular layer. Adsorption on the charcoal used by Kiselev[52][54] was probably confined to a monolayer because the amount of methanol adsorbed from the vapour phase just before the onset of capillary condensation was also 0.28cc. per gram expressed as a liquid volume. Kiselev found that the limiting adsorption of other solutes varied as follows: Congo Red (0.04cc/g), succinic acid (0.12), dimethyl ethyl carbinol (0.17), salicylic acid (0.19), methylene blue (0.20), benzoic acid (0.22), cyclohexanol (0.23) and phenol (0.26). In some cases, the low value could be attributed to incomplete penetration by a large molecule into all of the pore system. This is unlikely to be the case with all the solutes studied and other possibilities are that the adsorbed molecules are of such a shape as to leave extensive gaps in the monolayer even at closest packing and the existence of solvent molecules in the adsorbed layer even at limiting adsorption. The low value for Congo Red probably results from the inability of the semi-colloidal material to enter the pores of the charcoal.

The nature of the internal surface of the solid has been studied in comparison with the external surface. In the adsorption of fatty acids from water by a series of steam activated carbon blacks[49] although the surface area was increased more than three-fold, the shape of the adsorption isotherms was very little altered if these were plotted in terms of adsorption per unit area. In this instance, there would appear to be no significant difference between the two

surfaces. However, it has been suggested that the influence of two adjacent surfaces in narrow pores might result in stronger adsorption of the adsorbate than at a free surface. This appears to be the case in the adsorption of methylene blue by a charcoal having narrow pores,[55] as the isotherm rises more steeply from the origin than for a non-porous carbon black or for graphite. This effect is important in chromatography, especially in the elution process.

(c) Interactions in the Liquid State

The more important consequences of interactions in the liquid state are best illustrated by considering suitable systems.

On the homogeneous surface of Graphon, benzene is preferentially adsorbed from both methyl and n-butyl alcohol. This seems to be due in part to the nature of the interaction at the solid surface, as discussed earlier. However the marked difference in the degree of preferential adsorption between the two systems indicates that another factor is important.[38] The methanol molecule is so small that the polar hydroxyl group forms a large fraction of the whole. This group cannot interact strongly with the non polar carbon surface, but is capable of forming hydrogen bonds with the hydroxyl groups of other molecules in the liquid phase. Thus the methanol molecules have a tendency to remain in the liquid phase and the interactions between them tend to exclude the benzene molecules which, being more strongly held by the surface, readily become adsorbed on the carbon surface. This is supported by reference to the partial pressure curves of the two components (Fig. 22) which show the liquid system

to be close to phase separation at room temperature. The multilayer formation observed at the solid surface, therefore appears to be incipient phase separation.

In butyl alcohol, the hydroxyl group forms a smaller part of the molecule and the longer hydrocarbon chain makes for readier miscibility with benzene. Benzene is therefore more soluble in the liquid phase and undergoes reduced preferential adsorption. Further, the increasing number of methylene groups in the butyl alcohol molecule results in it being more strongly adsorbed than methanol at the solid surface, therefore competing more effectively with benzene.

If hydrogen bonding occurs between two components which are completely miscible in the liquid phase, it may have little effect on the competitive nature of adsorption. Thus, for a system with moderate hydrogen bonding in the liquid state (e.g. pyridine and ethyl alcohol), resolution of the composite isotherm into its individual components assuming monolayer formation gave isotherms which showed only a slight departure from those expected in the absence of hydrogen bonding. However, for the system pyridine-water where the first component is strongly adsorbed and the second only weakly adsorbed, the composite isotherm is convex to the concentration axis over part of the range (Fig.23) suggesting that the adsorbed phase possesses a deficiency of pyridine relative to what would be expected with a normal U-shaped isotherm.

This has been explained on the basis of preferential adsorption of pyridine to form an initial layer followed by further adsorption of

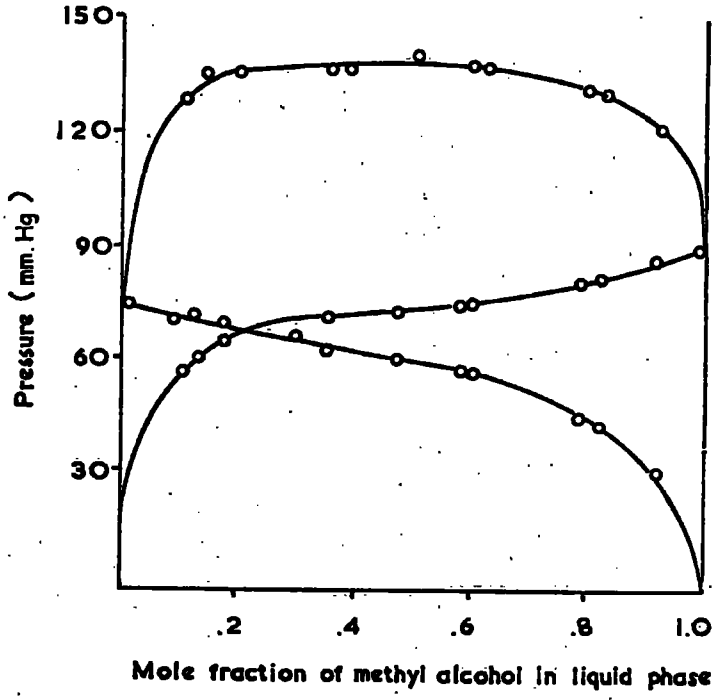

FIG 22

PARTIAL AND TOTAL PRESSURE CURVES FOR MIXTURES OF METHYL ALCOHOL AND BENZENE AT 20°C

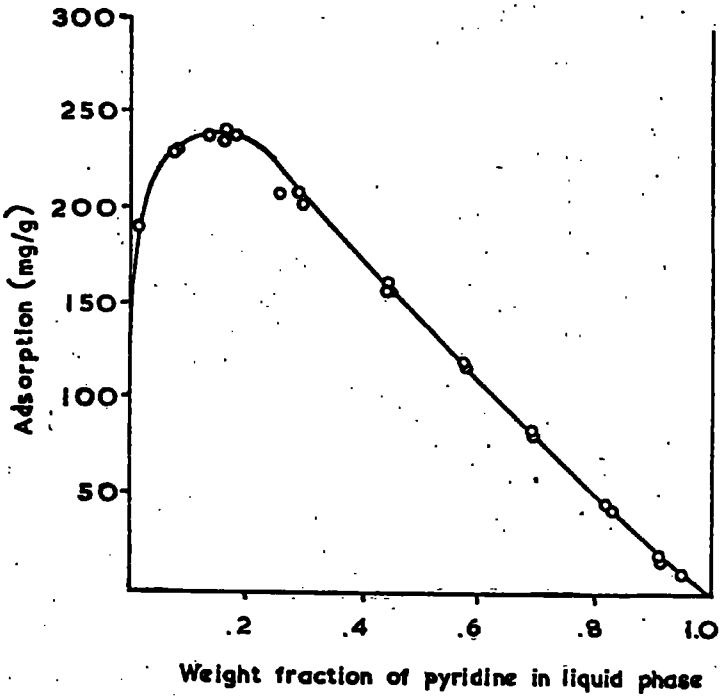

FIG 23

COMPOSITE ISOTHERM FOR ADSORPTION ON CHARCOAL FROM MIXTURES OF PYRIDINE AND WATER

water molecules due to their ability to hydrogen-bond to the pyridine molecules in the adsorbed layer.[11]

The effect of a moderate degree of interaction in the liquid phase has been studied by Jones and Mill[56] in respect of adsorption by silica gel from mixtures of nitromethane/carbon tetrachloride and ethanol/water. The apparent composite and individual isotherms for these systems are shown in Figs. 24 - 27. The vapour phase is regarded as the ideal phase of a binary mixture and the composition of both condensed phases (i.e. the liquid phase and the adsorbate) are plotted against the composition of the vapour. This is shown for the systems concerned in Figs. 28 and 29. The curves which would be realised if these systems were ideal are calculated by the use of Raoult's Law.

For the system nitromethane/carbon tetrachloride, Fig. 28 shows that deviation from Raoult's Law in the liquid phase is so great that an azeotropic mixture is formed at point A (i.e. $x_1^v = x_1^l$). The $(x_1^l - x_2^v)$ curve is seen to cross the Raoult's Law curve at point B and thus on either side of this point, the liquid phase contains an excess of one component or the other, with reference to the proportions present in the ideal solution. The greater concentration of CCl_4 at values of $x_1^v < B$ and of CH_3NO_2 at values of $x_1^v > B$ in the solution as compared to those values in the ideal solution is analogous to the type of apparent adsorption curve shown in Fig. 25 and could be referred to as an S-shaped adsorption curve.

ADSORPTION OF NITROMETHANE –CARBON TETRACHLORIDE ON SILICIC ACID GEL

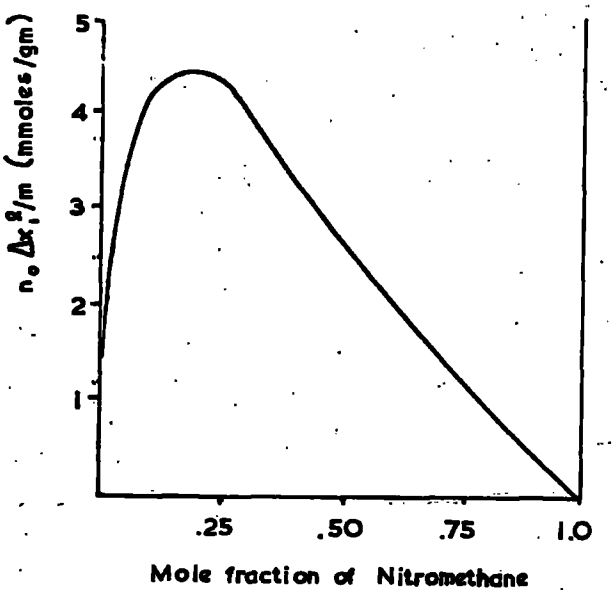

FIG 24 : COMPOSITE ISOTHERM

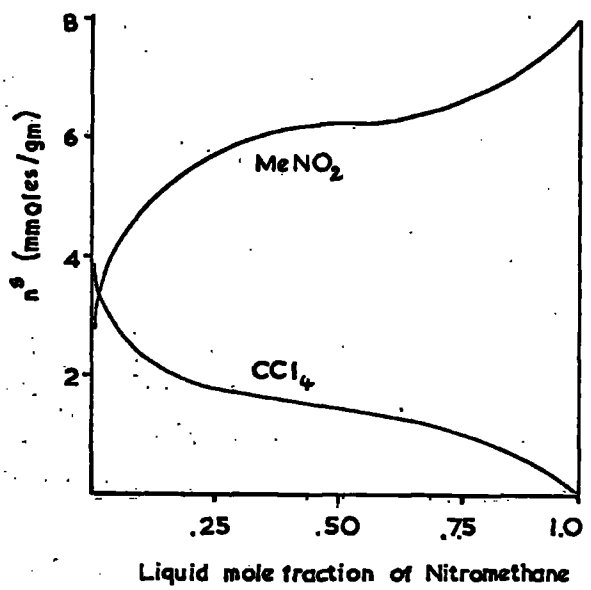

FIG 25 : INDIVIDUAL ISOTHERMS

ADSORPTION OF ETHYL ALCOHOL– WATER ON SILICIC ACID GEL

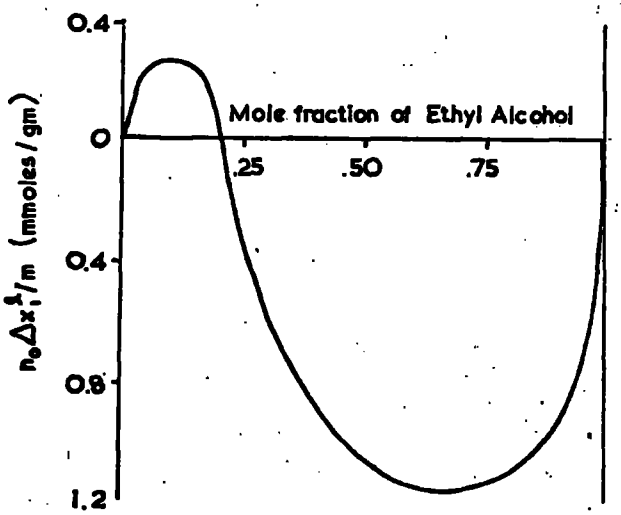

FIG 26 : COMPOSITE ISOTHERM

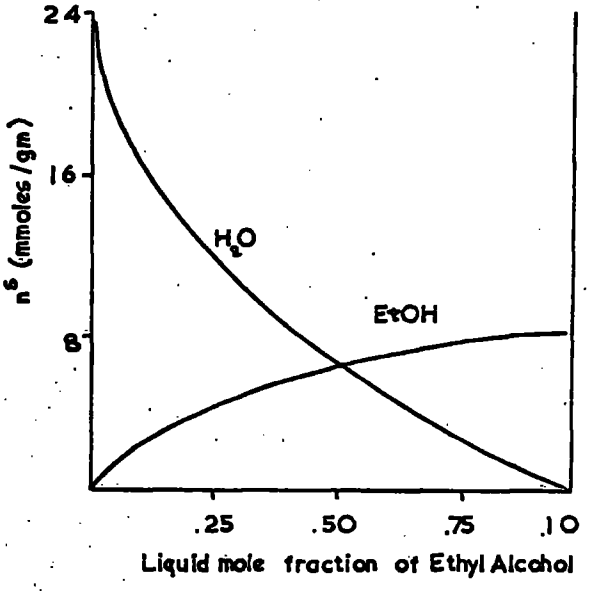

FIG 27 : INDIVIDUAL ISOTHERMS

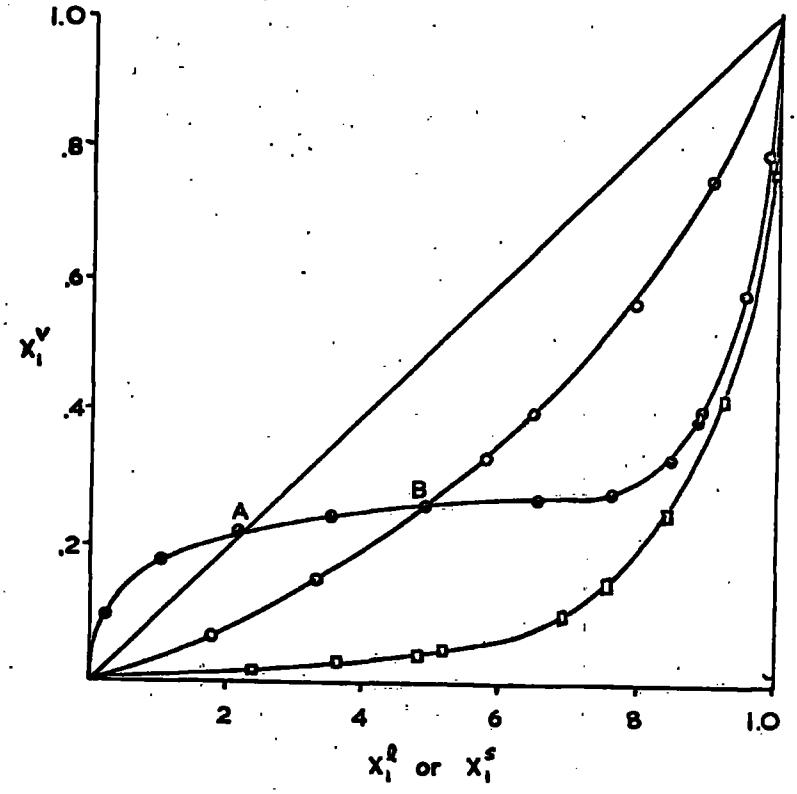

FIG 28

NITROMETHANE — CARBON TETRACHLORIDE

- ● $x_1^V - x_1^\ell$
- ○ $x_1^V - x_1^\ell$ (Raoult's Law)
- □ $x_1^V - x_1^s$

Component 1 : Nitromethane

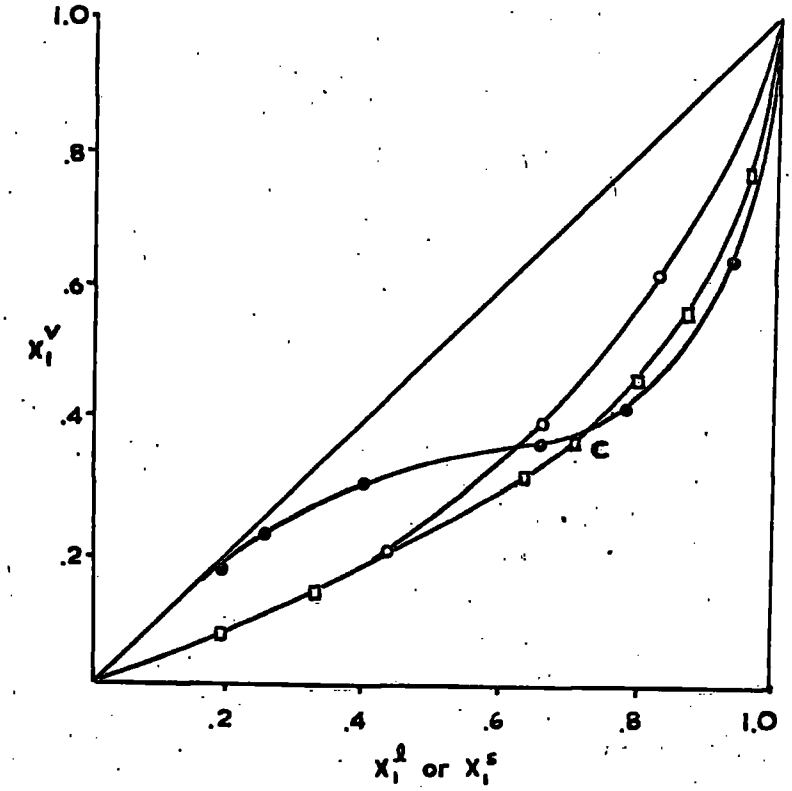

FIG 29

ETHYL ALCOHOL — WATER

- ● $x_1^V - x_1^\ell$
- ○ $x_1^V - x_1^\ell$ (Raoult's Law)
- □ $x_1^V - x_1^s$

Component 1 : Water

The mole fractions of the adsorbed phase in equilibrium with its vapour corresponds to a strong preferential adsorption of nitromethane over the whole concentration range, either from the vapour or from the liquid (ideal or actual). At values of $x_1^v > B$, the liquid phase now shows strong preferential adsorption of the mitromethane due to the positive deviation of this system from Raoult's Law and although the corresponding values of $x_1^{Ads.}$ are always greater than x_1^l, these two compositions are not greatly disparate in the region of $x_1^v = 0.3$ to $x_1^v = 1.0$. Thus the preferential adsorption of nitromethane from the mixed vapour phase is always sufficient to prevent that intersection of the $(x_1^l - x_1^v)$ and $(x_1^{Ads.} - x_1^v)$ curves which produces an S-shaped adsorption curve and in consequence a U-shaped curve is observed.

For the system ethanol/water, positive deviations from Raoult's Law in the liquid phase are also seen to be considerable. At low values of x_1^v, the x_1^l values show a considerable excess of ethanol, while at higher values, there is an excess of water in the equilibrium liquid phase above that calculated for an ideal solution, i.e. a strongly S-shaped adsorption curve. In the adsorbed phase, however, while there is always a preferential adsorption of water as compared to the equilibrium vapour phase, it is not sufficiently great to avoid the intersection of this curve by the $(x_1^v - x_1^l)$ curve (point C). It appears therefore, that either a greater preferential adsorption of water on the gel surface, or a smaller positive deviation from Raoult's Law in the liquid system, would have produced an apparent adsorption curve without a negative branch (i.e. a U-shaped curve).

Generally, S-shaped adsorption curves would be expected when a strong positive deviation from ideality in the liquid phase occurs in systems where the adsorbing surface is sufficiently similar in its attraction for both components.

The individual isotherms for both systems can now be plotted in terms of mole fractions in the equilibrium vapour phase. Figs. 30, 31. These curves should give a truer picture of the adsorption process since the vapour phase concentrations are representative of the true thermodynamic activities. Thus comparison of Figs. 26 and 30 for the system nitromethane/carbon tetrachloride shows that the points of inflexion present in the former figure have disappeared and combination of the two individual isotherms of Fig. 30 will give a U-shaped isotherm. The individual isotherms for adsorption from water/ethanol mixtures still show points of inflexion and this is possibly due to exceptional interaction between adsorbate and surface, e.g. chemisorption.(57)(58)

In conclusion then, when the effect due to deviation from ideality in the liquid phase has been allowed for by this method of plotting the individual isotherms, the competition for the surface and the interactions there can be seen in a much clearer perspective.

In the adsorption of solids from solution, the solubility of the solute is found to have a profound influence on competitive adsorption. Thus a complete monolayer may not be formed even at the highest available concentration if the solute is present in a good solvent which is also strongly adsorbed by the surface. In the absence of other effects, a given solute is more strongly adsorbed when relatively insoluble in a particular solvent. This is the

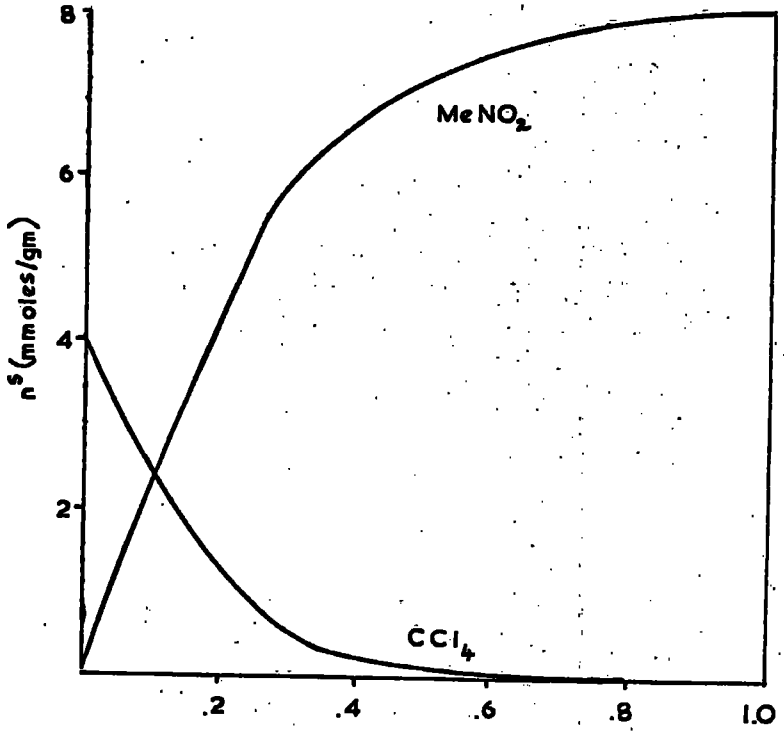

FIG 30

INDIVIDUAL ADSORPTION ISOTHERMS FOR $MeNO_2 - CCl_4$

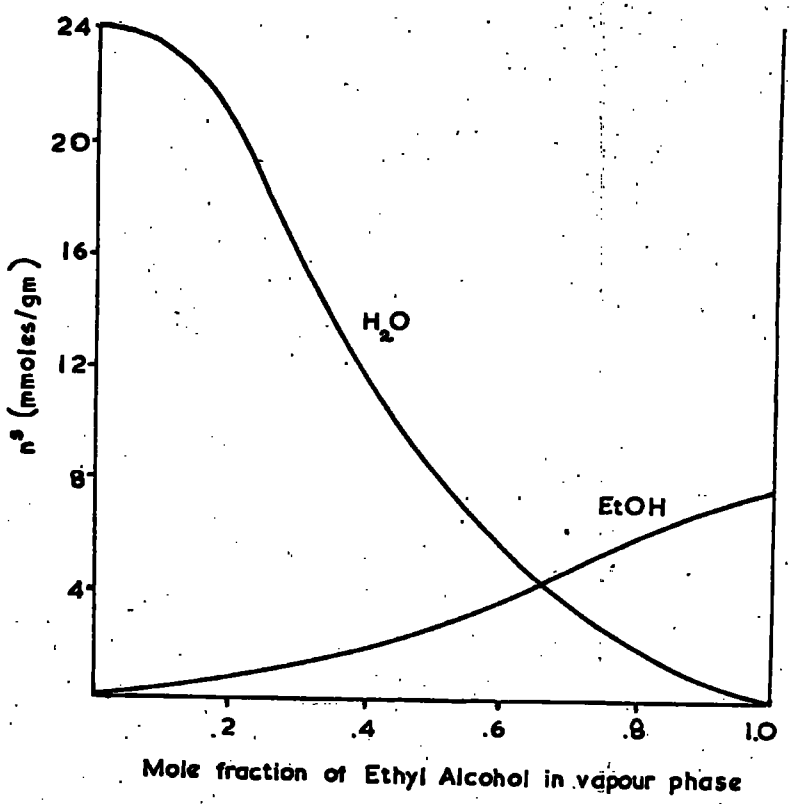

FIG 31

INDIVIDUAL ADSORPTION ISOTHERMS FOR $EtOH - H_2O$

Probable explanation of the results for adsorption by charcoal from aqueous solution of a large number of organic acids.[59] Increasing the solubility of the acid by introduction of further polar groups was found to decrease adsorption. The reduction was unlikely to be a result of the increased molecular size due to the addition of side groups, as it was observed at low as well as high concentrations. A similar reduction in adsorption of phenols from aqueous solution on charcoal occurs on increasing the number of (hydrophilic) hydroxyl groups in the molecule.[60] It is found that, on charcoal the more hydrophilic substances are more strongly adsorbed from hydrophobic than from hydrophilic solvents.[61]

B. Present Investigation

The present investigation constitutes a study of the adsorption characteristics at an alumina-solution interface, the solution phase consisting of a series of p-subsitututed phenols dissolved in cyclohexane and then tetrahydrofuran. Adsorption was carried out by the static method and the results expressed in the form of adsorption isotherms.

Characterisation of the alumina surface has been attempted using X-ray diffraction photography, electron microscopy, low-temperature nitrogen adsorption and dehydration experiments. An assessment of the porosity of the alumina sample has been made and a pore size distribution analysis carried out. Surface area values have been obtained by both gas adsorption and solution adsorption methods. Vapour phase adsorption of the solvents cyclohexane and tetrahydrofuran has been carried out in order to assess the molecular area requirements of these molecules on the alumina surface.

The results of the investigation have been used to:-

(1) elucidate the mechanism of adsorption of the p-substituted phenols at the alumina-solution interface and predict the orientation of the adsorbed molecules.

(2) assess the influence of the solvent on adsorptive capacity.

(3) correlate adsorptive affinity and structure of the adsorptive.

EXPERIMENTAL

A. Characterisation of the Adsorbent Surface

For an understanding of the mechanism of the adsorption process at the solid-liquid interface, a knowledge of the character of the adsorbent surface is essential. This involves a determination of the surface area by a reliable method and, in the case of porous solids, the value obtained must be assessed in relation to the extent of porosity of the adsorbent surface. For polar solids, a knowledge of the nature and distribution of specific adsorption sites on the surface is also of considerable importance.

1. Surface Area Determination by low temperature Nitrogen adsorption.

(a) Introduction

The most reliable and widely used method at present available for the determination of the surface area of solid adsorbents is the low temperature adsorption of nitrogen.

Brunaeur, Emmett and Teller[62][63] derived the following equation (21) for multimolecular adsorption on a non-porous surface.

$$\frac{p}{v(p_o - p)} = \frac{1}{v_m . c} + \frac{c - 1}{v_m . c} \cdot p/p_o \qquad (21)$$

where v = volume of gas adsorbed on the surface at equilibrium pressure p

v_m = the volume adsorbed corresponding to monolayer coverage of the surface by the gas per gram of adsorbent

P_o = the saturation vapour pressure

and c = a constant related to the heat of adsorption in the first layer.

It is assumed that the forces responsible for adsorption are the same as those involved in the process of liquefaction. The theory retains the concept of fixed, energetically uniform, adsorption sites as proposed by Langmuir, but allows for the formation of an adsorbed layer more than one molecule thick. The lateral interactions between molecules in the adsorbed phase are neglected and the molecules in all layers after the first are assumed to be subject to equal forces.

The shape of the isotherm obtained by plotting (v/v_m) against (p/p_o) varies according to the magnitude of 'c', as shown in Fig. 32.

Isotherms of these shapes are widely realised on the plotting of experimental data.

Equation (21) can be used to calculate the monolayer capacity v_m by plotting $p/v(p_o-p)$ against p/p_o when values for the intercept and slope of the linear plot are given by $1/v_m.c$ and $(c-1)/v_m.c$ respectively.

In practice, reliable v_m values are only obtained when the isotherm has a well defined 'knee' or plateau, implying a high value for the constant (c). In such a case, the isotherm is found to have a linear section and Brunauer and Emmett[64] concluded

FIG 32

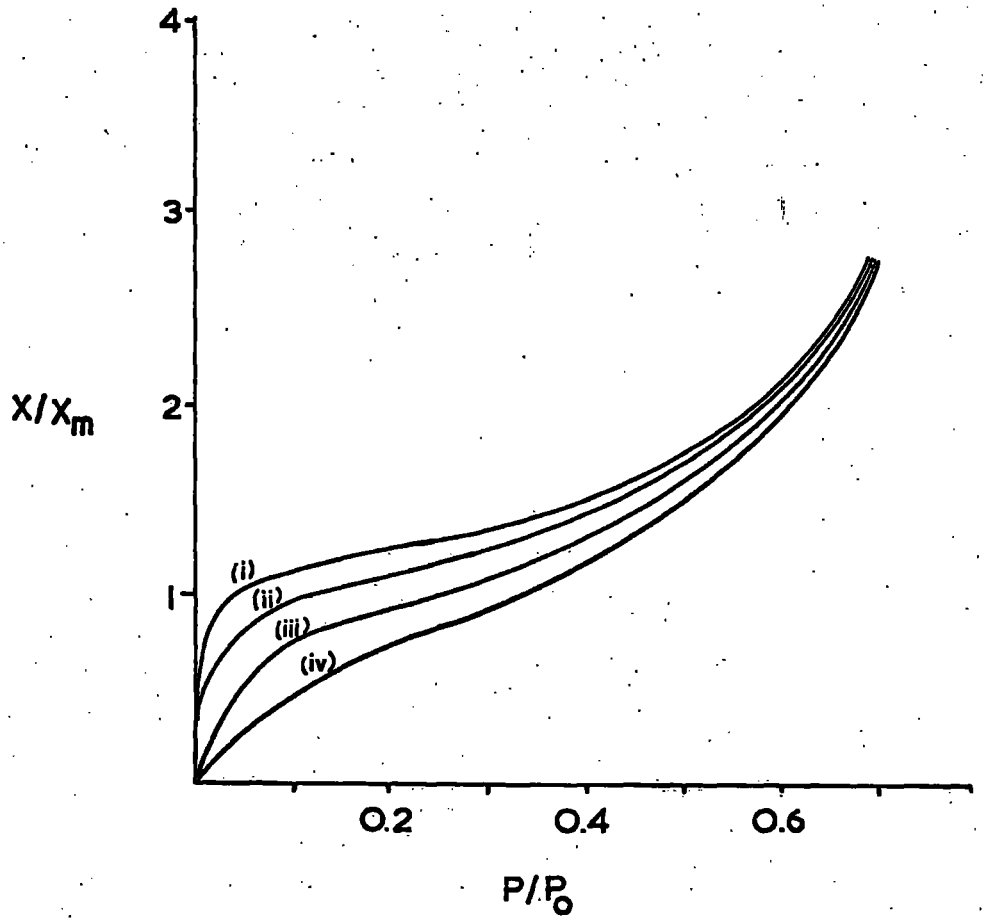

EFFECT OF MAGNITUDE OF 'c' ON TYPE II GAS ADSORPTION ISOTHERMS

(i) c = 1000 (ii) c = 100 (iii) c = 30 (iv) c = 10

that the beginning of this section (designated point B) corresponds to coverage of the adsorbent surface by a complete monolayer of adsorbed gas.

Having obtained the value of v_m from the experimental data, the area occupied by each molecule of the gas on the surface must be known before the surface area of the adsorbent can be determined. The average cross-sectional area of the adsorbed molecules is assumed to be the same as that obtained from the normal packing of the molecules in the liquified gas,[64] giving

$$A_m = f\left(\frac{M}{\rho N}\right)^{\frac{2}{3}} \times 10^{16} \quad \text{Å}^2 \qquad (22)$$

where A_m = the cross-sectional area of the molecule in the adsorbed phase in Å^2

M = the molecular weight of adsorbate

N = Avogradro's number

ρ = the density of the liquid gas in gms. per ml

f = a packing factor for the gas molecules on the surface.

For nitrogen, the packing of the molecules on the surface is assumed to be hexagonal with each molecule having twelve nearest neighbours, giving a value of 1.091 for the packing factor (f)

The specific surface area of the adsorbent is then obtained from:-

$$S = \frac{v_m}{22,400} .N.A_m \times 10^{-20} \ m^2 \qquad (23)$$

where v_m = volume in c.c. at N.T.P. corresponding to formation of a monolayer

and A_m = area per molecule in A^{o2}

(b) The Adsorption Experiment

The gas adsorption experiments were carried out in the apparatus shown on page 62 which is depicted schematically in Fig. 33. Nitrogen, from a gas cylinder, was purified by passing through alkaline pyrogallol (to remove oxygen) and then through a column of molecular sieves designed to remove water vapour. The apparatus was evacuated by means of a Towers mercury diffusion pump working in conjunction with a Speedivac oil vacuum pump.
A Macleod pressure gauge was incorporated in the system to check the 'hardness' of the vacuum obtained.

The apparatus was calibrated by first determining the gas storage volume by filling the appropriate section with water. The dosing and adsorption volumes were then determined by admitting a known volume of nitrogen at atmospheric pressure from the storage flask to the other parts of the evacuated apparatus in turn. By application of the gas laws, the two volumes are calculated from the observed changes in pressure. The correction to be applied to the dosing

volume, to take into account the varying height of the mercury meniscus (e) was found by determining the internal diameter of the barometer 'C'. The 'dead space' in the adsorption bulb 'D' due to the adsorbent was obtained from measurement of the density of the solid.

The experimental procedure used was as follows:-

One gram of alumina which had been dried for 48 hours at 120°C, was placed in the adsorption bulb 'D' and outgassed for several hours at room temperature. The storage flask 'A' was filled with nitrogen at atmospheric pressure and a known volume of the adsorption bulb immersed in liquid nitrogen. With taps (d), (f), (h) and (i) closed, a small volume of nitrogen, as indicated by the manometer 'C', was introduced into the dosing volume through tap (b). After recording the height of the mercury meniscus (e), the temperature and barometric pressure, tap (f) was opened and the system allowed to reach equilibrium. The equilibrium pressure, temperature and barometric pressure were then recorded and tap (f) closed. The procedure was repeated by admitting further volumes of nitrogen from the storage flask. By application of the gas laws, the volume of gas adsorbed at increasing equilibrium pressures was calulated.

For an assessment of the pore size distribution of the alumina (Section 3), the desorption isotherm is required and this can be conveniently determined after the adsorption experiment. With tap (f) closed, the equilibrium pressure of nitrogen in the doser

FIG 33

SCHEMATIC DIAGRAM OF THE GAS ADSORPTION APPARATUS

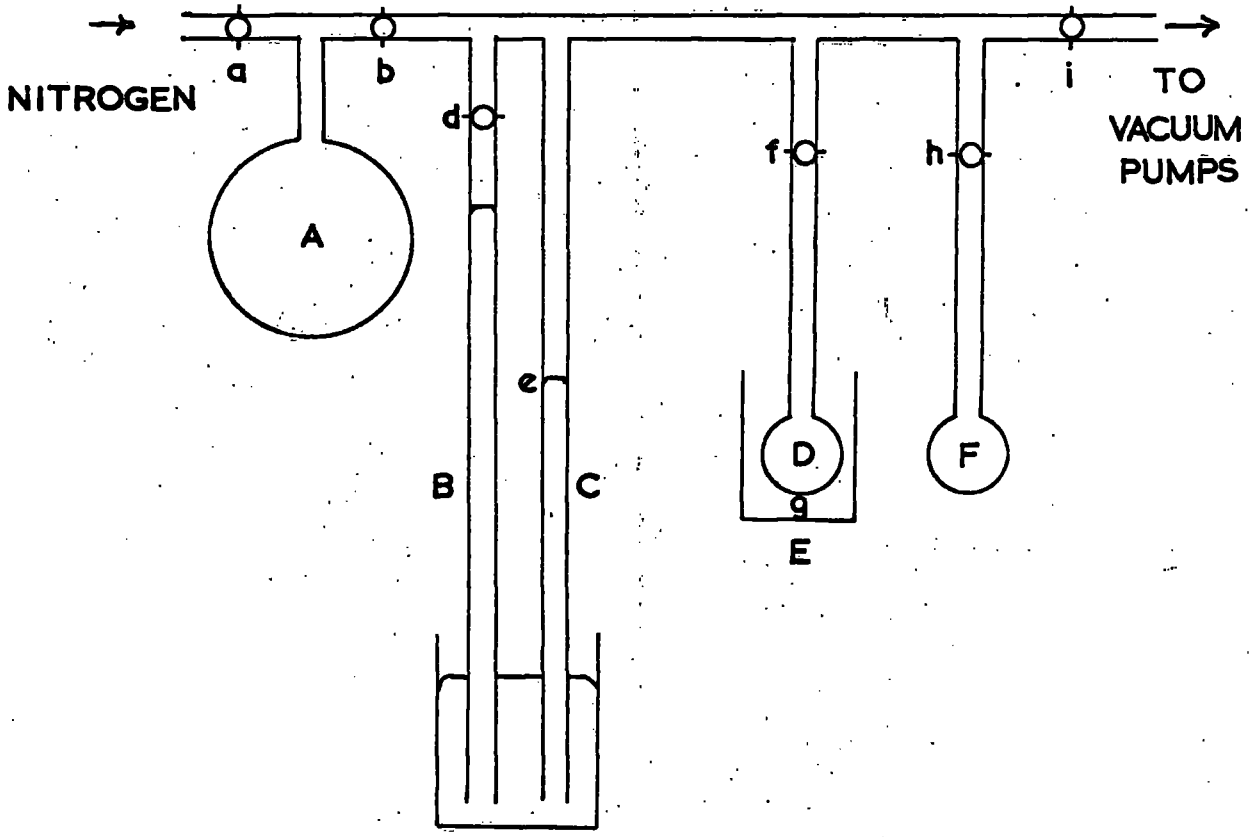

A storage flask containing nitrogen at atmospheric pressure
B a reference barometer
C the measuring barometer
D adsorption bulb containing the adsorbent
E thermos flask containing liquid nitrogen
F adsorption bulb for use in the adsorption of organic liquids as vapours

Volume between a and b = storage volume of gas
Volume represented by b,d,e,f,h,i = dosing volume
Volume between f and g = adsorption volume

volume resulting from the previous adsorption, was reduced by momentarily opening tap (i). The height of the mercury meniscus (e) temperature and barometric pressure were recorded and tap (f) opened. After allowing the system to reach equilibrium, the pressure, temperature and barometric pressure were again recorded. The procedure was repeated by successively reducing the pressure in the doser volume and the volume of gas adsorbed at decreasing relative pressures calculated.

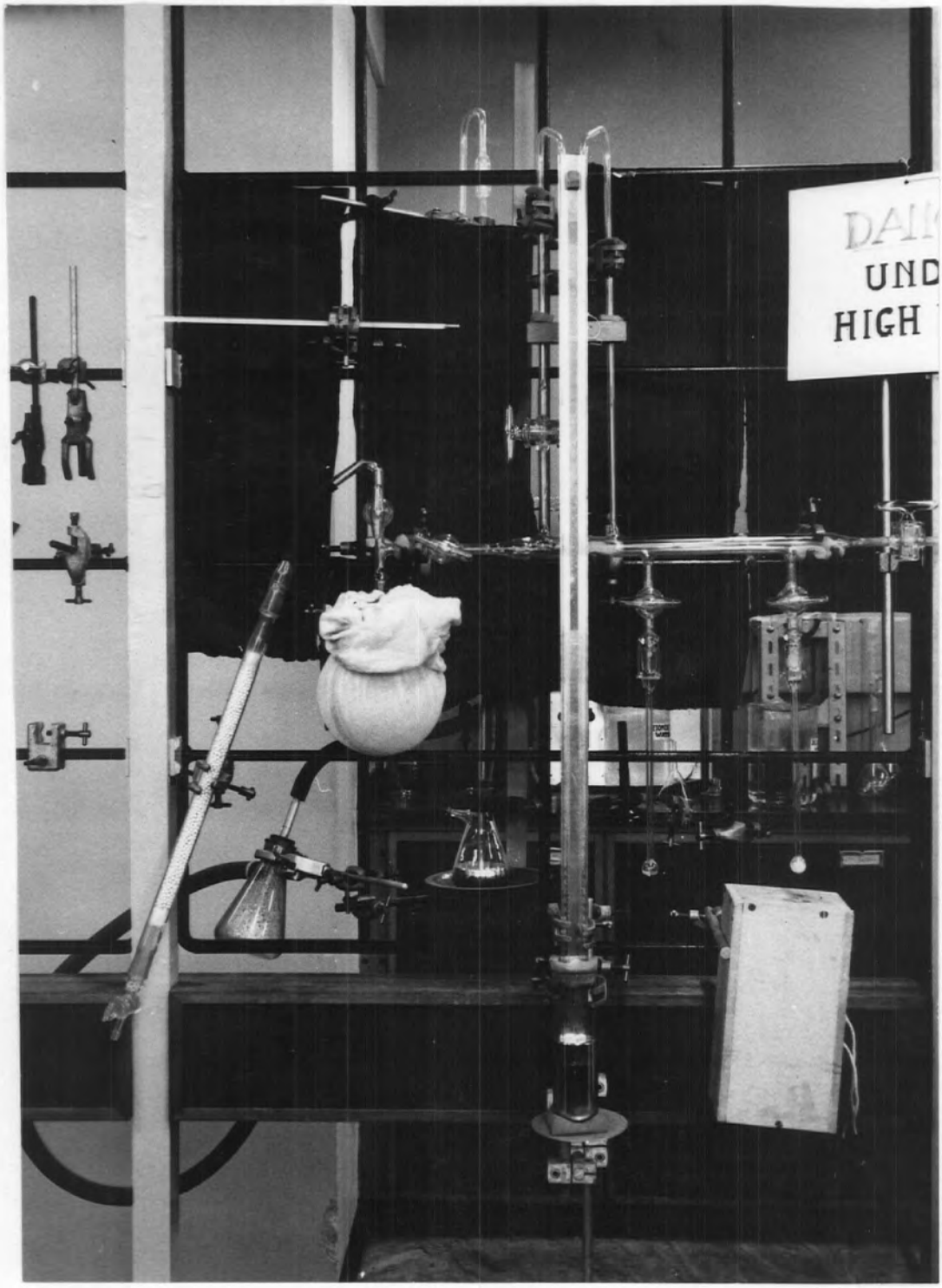
UND
HIGH

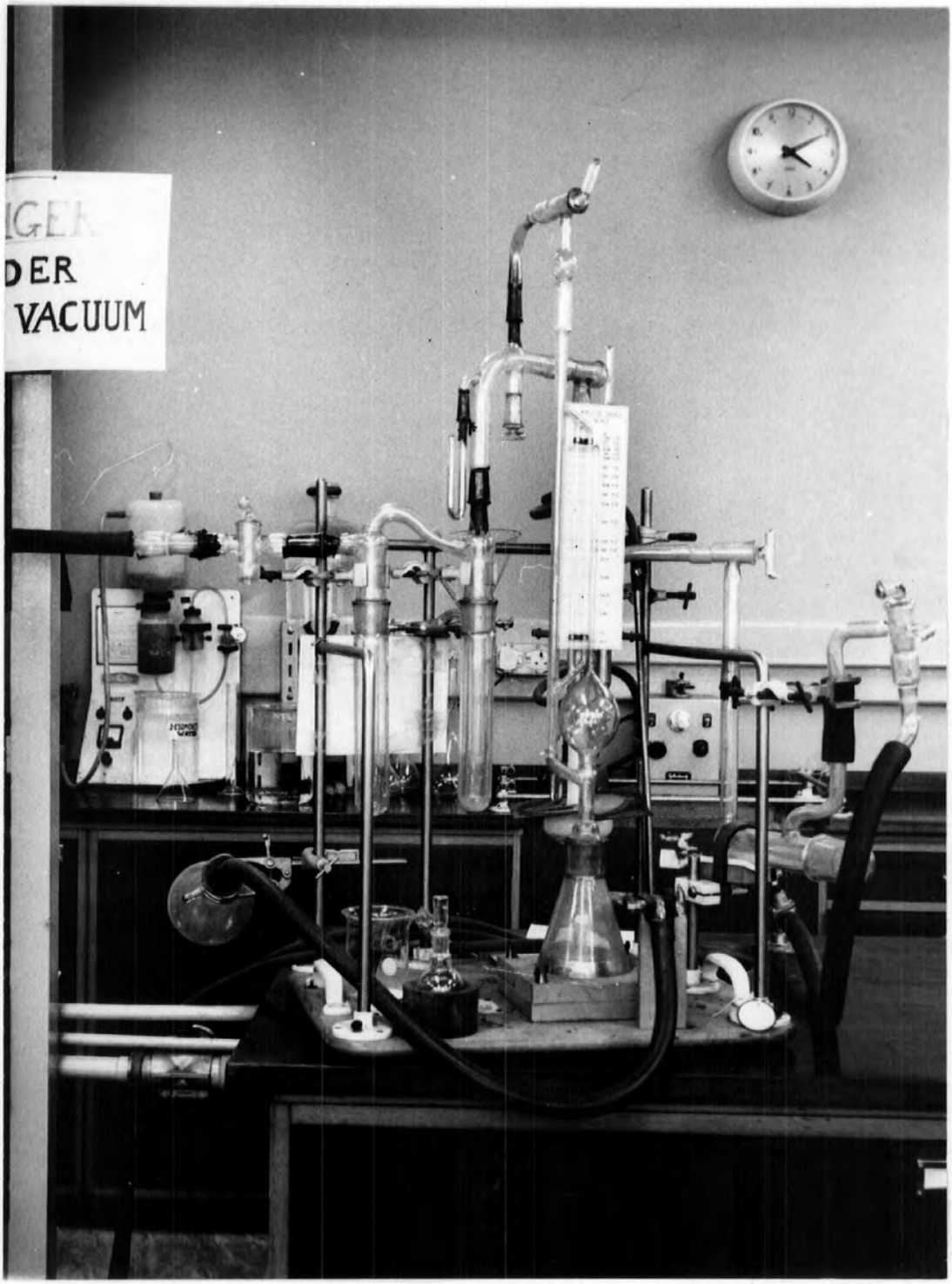
DER
VACUUM

(c) Calculation of Results

The volumes of the various parts of the gas adsorption apparatus are given in Table (1) and the experimental results recorded in Table (2). An example of the method of calculation of the volume of nitrogen adsorbed 'v' at an equilibrium pressure 'p', is given on P.65

Table (1)

Characteristics of the Gas Adsorption Apparatus

Volume of manometer tubing per cm. length	=	0.206 ml.
Storage volume	=	1,198.3 ml.
Volume of doser with mercury meniscus (e) at height 87.90 cm.	=	167.0 ml.
Volume of adsorption bulb D		
(i) 'dead space' occupied by alumina	=	0.3 ml.
(ii) at temperature of liquid nitrogen	=	5.2 ml.
(iii) at room temperature	=	9.5 ml.

Table (2)

Adsorption and Desorption of Nitrogen on Alumina

Doser Pressure(i) cm.	Equilibrium Pressure(ii) cm.	Mercury Meniscus(e) (i)	(ii)	Temperature °C (i)	(ii)	P/Po	Volume of gas at N.T.P. adsorbed (ml)
Adsorption							
13.19	1.49	36.15	24.50	24.5	23.7	.0196	21.59
19.47	11.49	42.35	34.87	23.7	24.1	.1571	32.48
26.71	21.27	49.52	44.12	24.1	24.0	.2799	39.89
36.48	30.38	59.20	53.12	24.0	23.6	.3997	48.90
47.63	39.41	70.25	62.10	23.6	24.2	.5186	62.90
58.01	46.87	80.55	69.47	24.2	24.3	.6167	83.85
67.53	55.17	89.95	77.65	24.3	25.7	.7259	108.12
73.77	66.82	96.10	89.20	25.7	25.9	.8792	119.31
Desorption							
57.79	60.78	80.22	83.17	25.9	25.8	.7997	115.02
44.09	49.19	66.60	71.65	25.8	25.1	.6472	108.33
33.63	42.53	56.22	65.07	25.1	25.0	.5596	92.53
17.41	35.35	40.12	58.00	25.0	24.9	.4651	59.51
0.57	16.43	23.47	39.82	24.9	24.0	.2162	36.09
1.34	7.08	24.85	30.55	24.0	24.1	.0932	28.68
0.78	3.46	24.30	26.97	24.1	24.1	.0455	24.96

Calculation of the Volume 'v' Adsorbed at an Equilibrium Pressure 'p' for the Nitrogen Adsorption and Desorption Experiment (Table 2)

Example

Doser Pressure	19.47 cm	Equilibrium Pressure	11.94 cm.
Position of mercury		Position of mercury	
Meniscus (e)	42.35 cm	Meniscus (e)	34.87 cm.
Temperature	23.7°C	Temperature	24.1°C

Using $nR = PV/T$

Moles of nitrogen in doser volume = $10.343/R$

Moles of nitrogen in adsorption bulb from previous adsorption = $0.148/R$

Total no. of moles of nitrogen prior to adsorption = $\underline{10.491/R}$

Total no. of moles of nitrogen after adsorption

$$= \frac{11.94\ (156.1)}{297.1\ R} + \frac{11.94(9.5)}{297.1\ R} + \frac{11.94(5.2)}{77.2\ R}$$

$$= \underline{7.459/R}$$

∴ Moles of nitrogen adsorbed = $\underline{3.032/R}$

Volume of nitrogen (at N.T.P.) adsorbed = 10.89 ml.

Volume of nitrogen previously adsorbed = 21.59 ml.

∴ Volume of nitrogen (at N.T.P.) adsorbed at an equilibrium pressure of 11.94 cm. = $\underline{32.48\ ml.}$

The combined adsorption and desorption isotherm obtained by plotting the volume of gas (at N.T.P.) adsorbed against the relative pressure is shown in Fig. 34.

Adsorption data up to a relative pressure of 0.4 are reproduced in Table (3) and plotted in the form of $p/v(p_o - p)$ against P/P_o in Fig. 35.

Table (3)

Adsorption of Nitrogen on Alumina

Relative Pressure P/P_o	Volume of gas (at N.T.P.) adsorbed v ml.	$\frac{p}{v(p_o-p)}$
0.0196	21.59	0.926
.0455	24.96	1.867
.0932	28.68	3.582
.1571	32.48	5.738
.2162	36.09	7.642
.2799	39.89	9.740
.3997	48.90	13.61

The slope of the plot shown in Fig. 35 is found to be 0.033 and the intercept has a value of 5.0×10^{-4}.

FIG 34

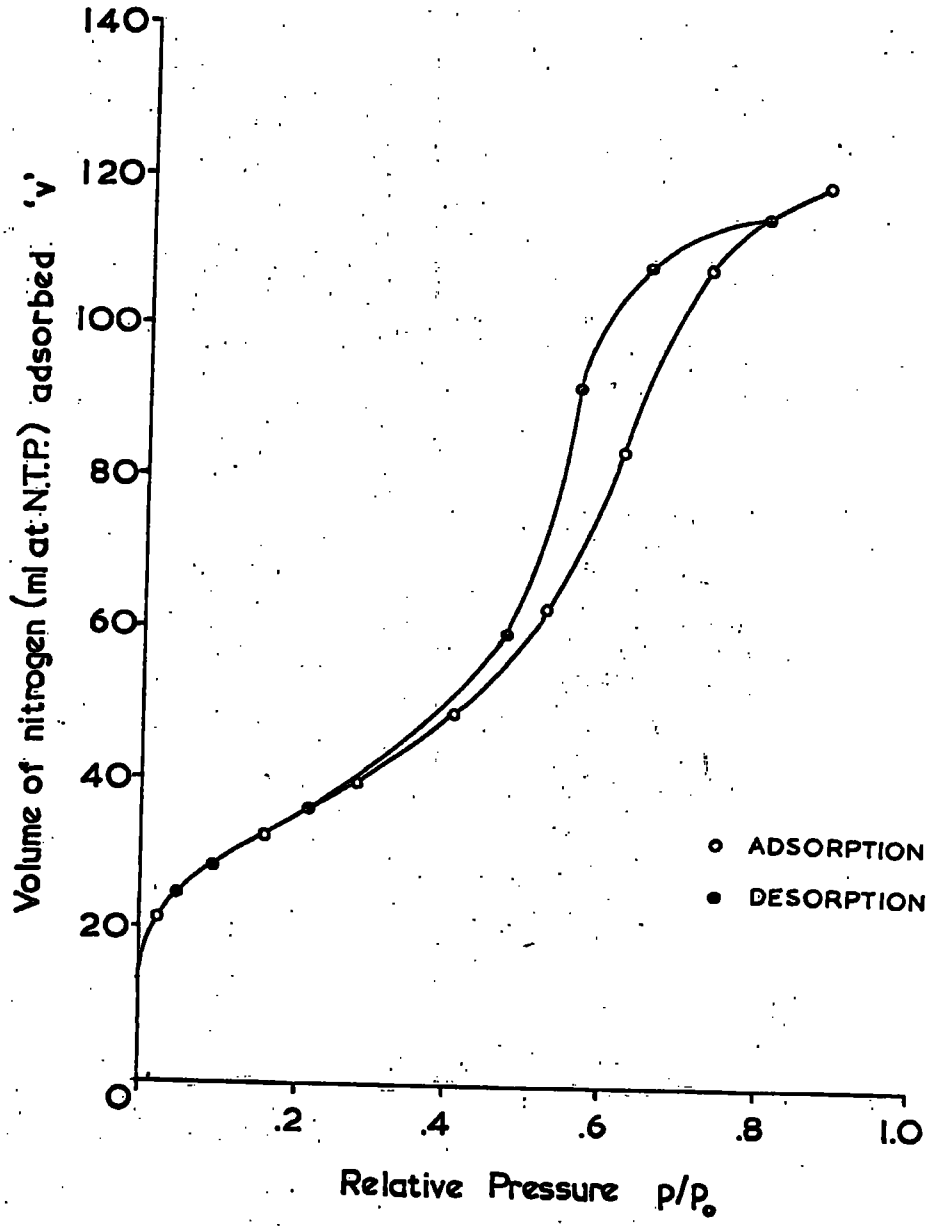

ADSORPTION AND DESORPTION OF NITROGEN ON ALUMINA

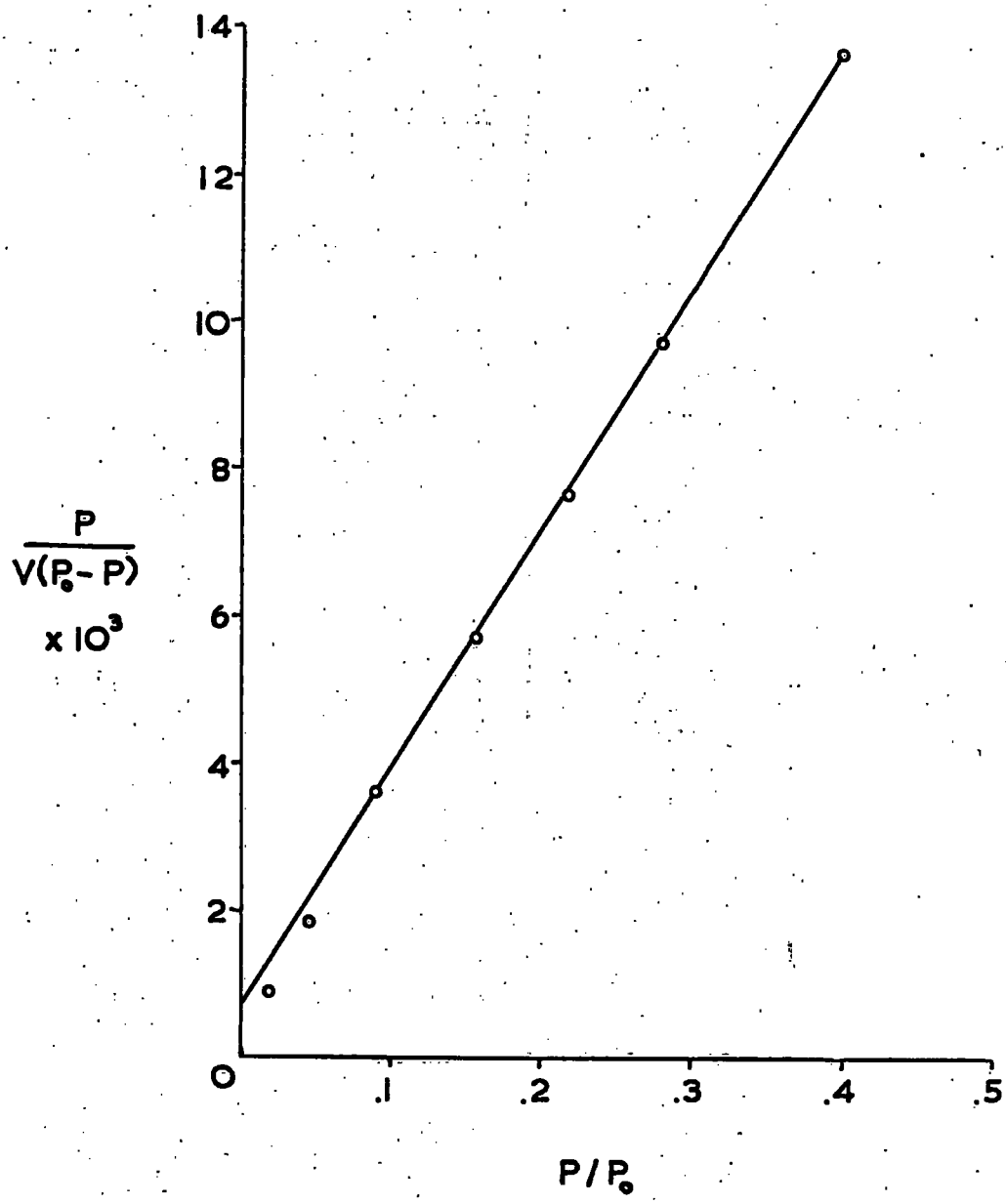

FIG 35

From equation (21)

$$\frac{c - 1}{v_m \cdot c} = 0.033 \qquad \frac{1}{v_m \cdot c} = 5.0 \times 10^{-4}$$

Eliminating 'c' gives $\underline{v_m = 30.0 \text{ ml.}}$

From equation (22), the area requirement per molecule of nitrogen, $\underline{A_m \text{ is } 16.25 \text{ Å}^2}$ (65)(66)(67)

From equation (23), the surface area of the alumina per gram, $\underline{S = 131.1 \text{ m}^2 \text{ g}^{-1}}$

2. Assessment of Porosity

(a) Introduction

It is found that if the gas adsorption process is restricted to one adsorbate (nitrogen) and carried out at a single temperature (boiling point of nitrogen), then it is a fortunate occurrence that for a wide variety of aluminas, the multimolecular adsorption isotherms prove to be identical provided no capillary condensation occurs and no narrow pores are put out of action during adsorption.(68)

If the density of the adsorbed layer is assumed to be the same as that of normal liquid nitrogen and the packing of the molecules in both cases is similar (hexagonal), the area requirement of a molecule in the monolayer is 16.2 Å^2. This gives a calculated

value for the thickness of the monolayer of 3.54 Å.

Hence, for multimolecular adsorption, the thickness of the adsorbed layer 't' is given by

$$t = \left(\frac{v_a}{v_m}\right)_l .3.54 = \left(\frac{v_a}{v_m}\right)_g . 3.54 \qquad (24)$$

where v_a = the volume adsorbed corresponding to the thickness t

v_m = the volume corresponding to the adsorbed monolayer and the subscripts 'l' and (g) refer to volumes of liquid and gas (cmls. at N.T.P.), respectively.

De Boer, Linsen and Osinga[69] have suggested that the adsorption data of Lippens, Linsen and De Boer[68] obtained by using several well selected samples of non-porous aluminas and aluminium hydroxides are suitable for the construction of an "experimental master curve", up to a relative equilibrium pressure of 0.75 (Fig. 36).

From this curve, values of 't' calculated using equation (24) can be tabulated as a function of relative equilibrium pressure P/Po (Table 4).

Equation (24) can be transformed to

$$t = 15.47 \left(\frac{v_a}{S}\right)_g \text{ Å} \qquad (25)$$

where v_a represents the volume of gas (cmls. at N.T.P.) adsorbed and S is the surface area in m^2g^{-1}

Thus a plot of v_a against t for non-porous solids should be linear, should pass through the origin and have a slope related to the

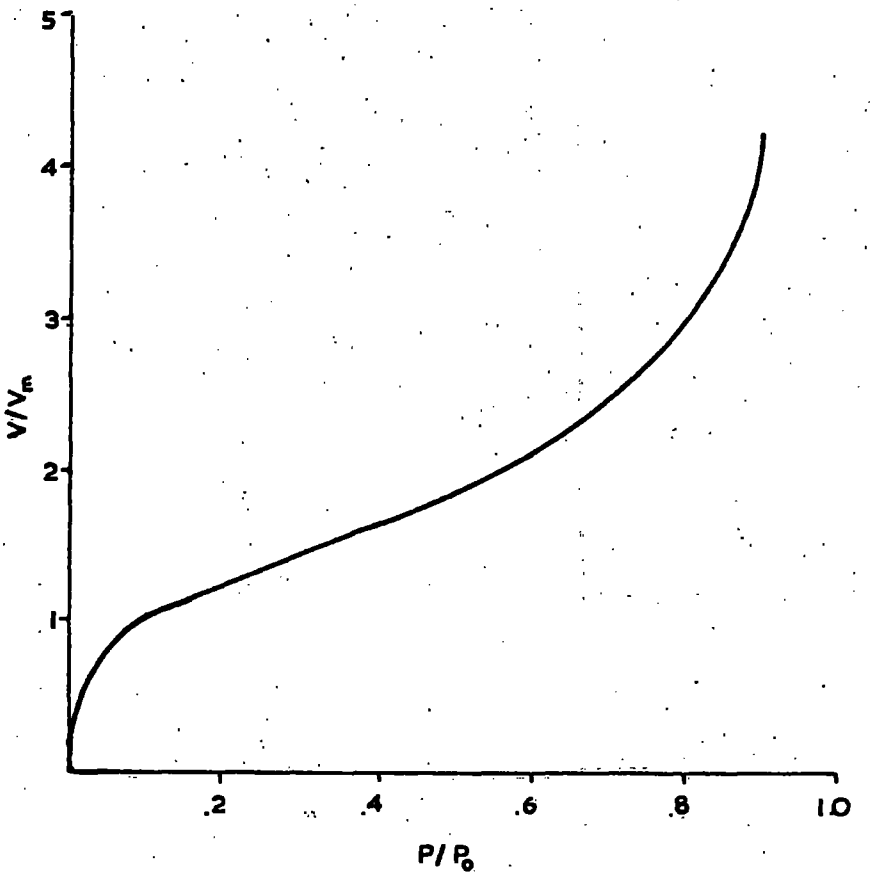

FIG 36

EXPERIMENTAL MASTER CURVE

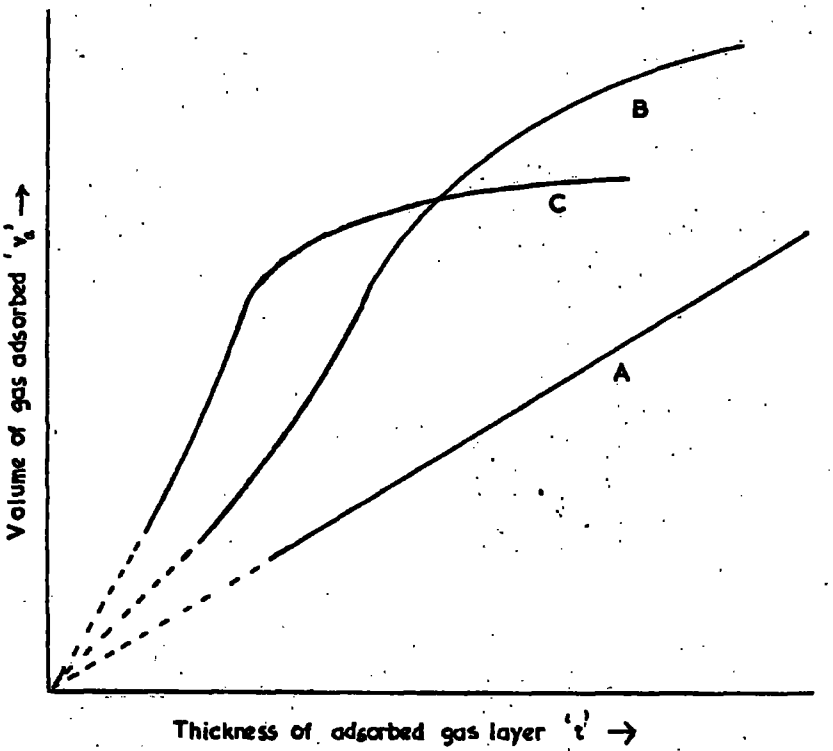

FIG 37

RELATION BETWEEN V_a AND t FOR NON POROUS(A) AND POROUS (B,C) ALUMINAS

Table 4

Experimental Thickness t of the Multimolecular layer, Adsorbed on Aluminium Hydroxides and Oxides

$P/_{Po}$	t	$P/_{Po}$	t
0.08	3.51	0.56	6.99
0.10	3.68	0.58	7.17
0.12	3.83	0.60	7.36
0.14	3.97	0.62	7.56
0.16	4.10	0.64	7.77
0.18	4.23	0.66	8.02
0.20	4.36	0.68	8.26
0.22	4.49	0.70	8.57
0.24	4.62	0.72	8.91
0.26	4.75	0.74	9.27
0.28	4.88	0.76	9.65
0.30	5.01	0.78	10.07
0.32	5.14	0.80	10.57
0.34	5.27	0.82	11.17
0.36	5.41	0.84	11.89
0.38	5.56	0.86	12.75
0.40	5.71	0.88	13.82
0.42	5.86	0.90	14.94
0.44	6.02	0.92	16.0 *
0.46	6.18	0.94	17.5 *
0.48	6.34	0.96	19.8 *
0.50	6.50	0.98	22.9 *
0.52	6.66		
0.54	6.82		

* Extrapolated values

surface area of the solid. No deviation from this linear plot should be observed unless the progress of multimolecular adsorption is hindered by capillary condensation or closing of pores. If at some value of 't', a positive deviation is observed then more nitrogen is being taken up than corresponds to multimolecular adsorption and the onset of capillary condensation is suggested. When the pores are full, the plot should become linear and almost parallel to the 't' axis, the slope indicating the outer surface area (Fig. 37).

In the case of curve 'c', capillary condensation occurs in narrow slit-shaped pores; the slope at high 't' values indicating the surface area of the wider pores and the outer surface.

It has been shown by Kelvin, using thermodynamic arguments, that if a liquid is present in a capillary tube of radius ' r_k ', the equilibrium vapour pressure 'p' over the meniscus will be less than the ordinary saturated vapour pressure ' p_o ', according to the equation:-

$$\log (p/p_o) = - \frac{2\gamma V \cos \theta}{r_k . R.T} \qquad (26)$$

For nitrogen:

γ = the surface tension of liquid nitrogen (8.2 dynes/cm^2)

V = the molar volume of the adsorbed and capillary condensed nitrogen (34.68 cm^3/mole)

T = the temperature of boiling liquid nitrogen (78^{o}K)

If the contact angle θ between the surface of the adsorbed liquid nitrogen and the wall of the capillary may be taken to be zero, the above equation reduces to

$$r_k = \frac{-4.05}{\log(p/p_o)} \qquad (27)$$

From the plot of v_a against t (Fig.37), the thickness corresponding to the onset of capillary condensation can be interpolated. Introducing the corresponding value of the relative pressure, P/P_o, into equation (27), permits calculation of the Kelvin radius, r_k. The pore diameter (d) can then be evaluated from the relationship between d and r_k, assuming a pore shape. According to De Boer, Steggerda and Zwietering,[70] slit-shaped pores commonly occur in many forms of activated alumina, and for this pore shape

$$d = r_k + 2t \qquad (28)$$

(b) Experimental Results

Values of v_a and P/Po obtained from the adsorption isotherm of Fig. 34 are recorded in Table (5). The plot of against t for the alumina under investigation, obtained by the use of De Boer's tabulated values of t and P/Po (Table 4) is shown in Fig. 38. The slope of the plot is similar to curve B of Fig. 37. If slit-shaped pores predominate in the alumina under investigation, then from Fig. 38 it can be seen that capillary condensation commences at $t = 5\text{Å}$ corresponding to a relative pressure of 0.3, in pores of width $d = 18\text{Å}$. Capillary condensation is complete at

Table (5)

Volume of Nitrogen adsorbed ' v_a ' on Alumina at various Relative Pressures 'P/P_o'

P/P_o	v_a	P/P_o	v_a
0.08	26.2	0.48	57.5
0.10	29.5	0.50	60.2
0.12	30.7	0.52	63.3
0.14	31.7	0.54	66.5
0.16	32.8	0.56	70.1
0.18	33.8	0.58	74.3
0.20	34.8	0.60	79.2
0.22	36.0	0.62	84.7
0.24	37.2	0.64	91.2
0.26	38.4	0.66	97.0
0.28	39.7	0.68	101.3
0.30	41.1	0.70	104.7
0.32	42.6	0.72	107.2
0.34	44.2	0.74	109.0
0.36	45.7	0.76	110.6
0.38	47.3	0.78	111.9
0.40	49.0	0.80	113.2
0.42	50.7	0.82	114.5
0.44	52.8	0.84	115.8
0.46	55.0	0.86	117.2

FIG 38

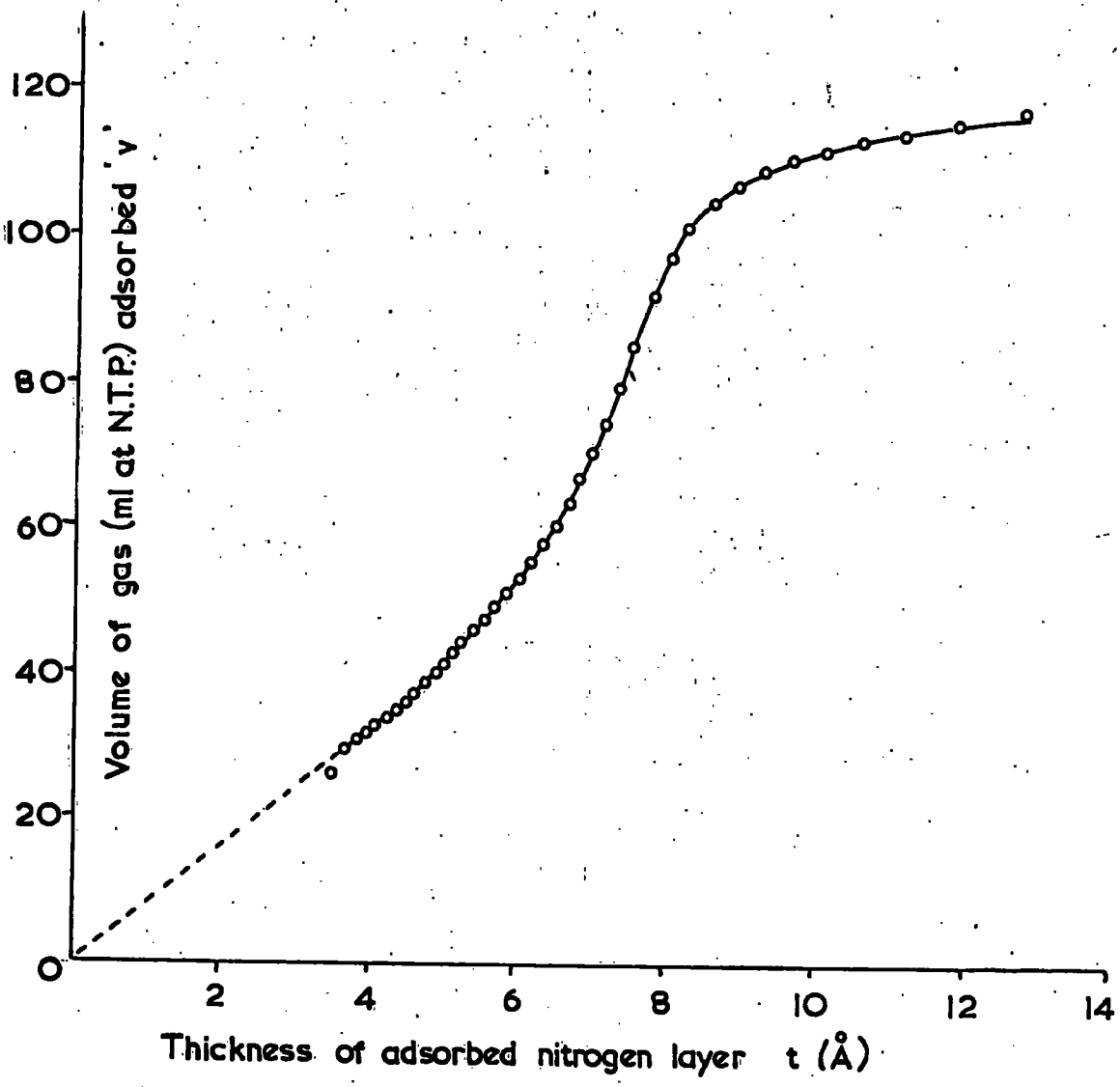

THE 't' CURVE

$t = 9.5A$ $(P/_{P_o} = 0.75)$ in pores of width $d = 51A$.

From the initial slope of the 't' curve (Fig. 38), the surface area is calculated to be 125.7 m^2g^{-1}, and this compares reasonably with the value of 131.1 m^2g^{-1} for the surface area of the alumina sample using the B.E.T. method. The second slope of the 't' curve corresponds to a surface area of 35.6 m^2g^{-1} and represents the outer surface area and wider pores of the alumina.

3. Pore Size Distribution

(a) Introduction

In the adsorption of a gas by a porous solid, it is found that the experimental desorption isotherm differs from the adsorption isotherm over a range of relative pressures such that the combined isotherm exhibits an hysterisis loop (Fig. 34). The occurrence of the hysterisis loop has been attributed to the manner in which the pores of the adsorbent fill and empty. During adsorption the gas is considered to condense as a cylindrical layer lining the walls of the pores thus forming an annular meniscus, while during desorption, evaporation is assumed to occur from a hemispherical meniscus.(71) The several types of hysterisis loops observed have been explained by assuming various shapes for the pores of the adsorbent.(72)

In assessing the pore size distribution of the adsorbent, it is convenient to analyse the desorption branch of the hysterisis loop of the isotherm.(68)
In this analysis, it is assumed that at a relative pressure $x = 1$ all pores (including a portion of intergranular space) are filled with liquid nitrogen. The desorption branch is divided into steps corresponding to equal relative pressure increments of $2\Delta x$ (Fig.39) At the beginning of the i th step, the relative pressure is $(x_i+\Delta x)$, the volume adsorbed (expressed in ml. liquid nitrogen) $X_{(x_i+\Delta x)}$, the surface area of the pores (or parts of pores) not

FIG 39

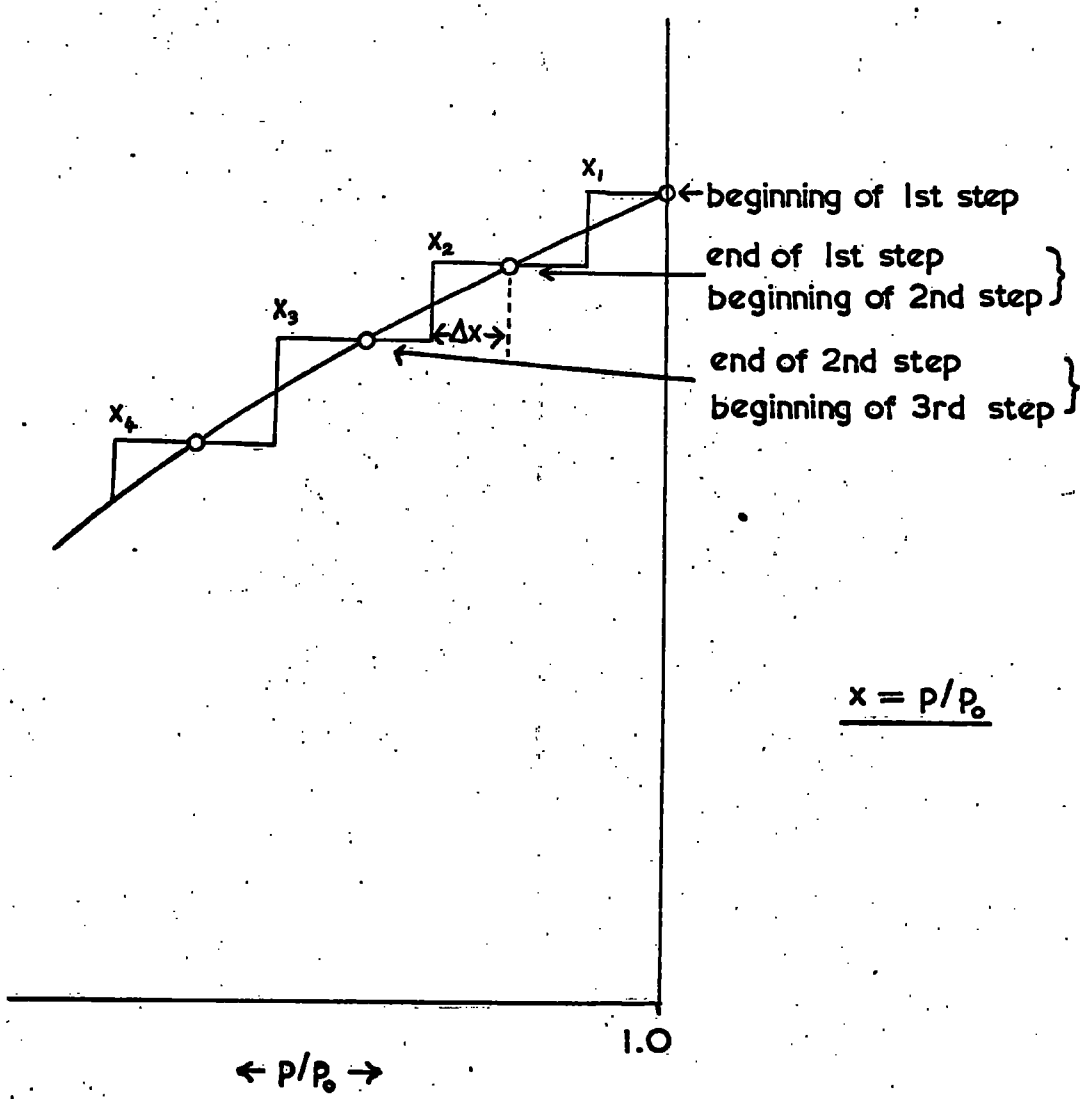

PORE SIZE DISTRIBUTION ANALYSIS

filled with liquid nitrogen $S_{(x_i+\Delta x)}$, and the thickness of the layers of nitrogen adsorbed on this surface $t_{(x_i+\Delta x)}$

If the relative pressure is lowered to $x_i-\Delta x$, those pores, having a Kelvin radius between $(r_k)_{(x_i+\Delta x)}$ and $(r_k)_{(x_i-\Delta x)}$ are emptied. If Δx is sufficiently small we may assign to this group of pores a mean Kelvin radius $(r_k)_{x_i}$ corresponding with the relative pressure x_i . The thickness of the adsorbed layer at this relative pressure x_i, is given by:-

$$d_{x_i} = (r_k)_{x_i} + 2t_{x_i} \qquad (29)$$

Representing the surface area of this group of pores by ΔS_{x_i} the volume ΔV_{x_i} is given by:-

$$\Delta V_{x_i} = \tfrac{1}{2}\Delta S_{x_i} d_{x_i} \qquad (30)$$

At the end of the i th step, the relative pressure is $(x_i-\Delta x)$, the adsorbed volume of nitrogen $X_{(x_i-\Delta x)}$, the surface area of the pores not completely filled with liquid nitrogen $S_{(x_i-\Delta x)}$ and the thickness of the adsorbed layer $t_{(x_i-\Delta x)}$

Thus during the i th step, the desorbed volume ΔX_i is given by:-

$$\Delta X_i = X_{(x_i+\Delta x)} - X_{(x_i-\Delta x)} \qquad (31)$$

This desorbed volume is formed by:-

(a) The volume originating from the capillary evaporation from the i th group of pores at the relative pressure x_i and the decrease of the thickness of the adsorbed layer of this group of pores by

lowering the relative pressure from x_i to $(x_i - \Delta x)$ ------ V_1

where $V_1 = \frac{1}{2}(d_{x_i} - 2t_{x_i - \Delta x}).\Delta S_{x_i}$ (32)

(b) The decrease of the thickness of the adsorbed layer in the pores which were already emptied at the relative pressure $x_i + \Delta x$, during the lowering of the pressure to $x_i - \Delta x$.

------ V_2

where $V_2 = (t_{x_i + \Delta x} - t_{x_i - \Delta x}).S_{(x_i + \Delta x)}$ (33)

Now $S_{(x_i + \Delta x)}$, obtained by summing up all contributions ΔS_x of the groups of pores having a width greater than $d_{(x_i + \Delta x)} = d_{(x_{i-1} - \Delta x)}$ is:-

$$S_{(x_i + \Delta x)} = \Sigma \Delta S_{x_{i-1}} \quad (34)$$

Hence, during the i th step,

Desorbed volume $\Delta X_i = V_1 + V_2$

$$= \frac{1}{2}\Delta S_{x_i}(d_{x_i} - 2t_{x_i - \Delta x}) + (t_{x_i + \Delta x} - t_{x_i - \Delta x})\Sigma \Delta S_{x_{i-1}} \quad (35)$$

Combination of (30) and (35) gives $\Delta V_{x_i} = \frac{1}{2}\Delta S_{x_i}.d_{x_i}$

$$= \frac{d_{x_i}\left\{ \Delta X_i - (t_{x_i + \Delta x} - t_{x_i - \Delta x}).\Sigma \Delta S_{x_{i-1}} \right\}}{d_{x_i} - 2t_{x_i - \Delta x}}$$

Then $\Delta V_{x_i} = (R_{x_i}.\Delta X_i) - (R'_{x_i}.\Sigma \Delta S_{x_{i-1}})$ (36)

where $R_{x_i} = \dfrac{d_{x_i}}{d_{x_i} - 2t_{x_i - \Delta x}}$

and $R'_{x_i} = R_{x_i}(t_{x_i + \Delta x} - t_{x_i - \Delta x})$

Summing up all contributions ΔV_{x_i} and ΔS_{x_i}, respectively, we obtain the cumulative quantities $V_{cum.}$ and $S_{cum.}$ representing the total volume and total surface area of the pores having a width greater than d_{xi}.

(b) Experimental Results

Results of the analysis of the desorption branch of the isotherm (Fig. 34) are recorded in Table (6), and the plot of cumulative surface area as a function of pore diameter is given in Fig. 40.

Table (6)

Pore Size Distribution Analysis

p/p_o	v_a (ml)	t (Å)	r_k (Å)	d (Å)	ΔX_i (ml)	ΔV_{x_i} ($x10^3$)	ΔS_{x_i} (m^2)	$\Sigma \Delta S_{x_i}$ (m^2)
0.90	122.0	14.94						
0.89		14.38	80.04	108.80	2.4	4.566	.8393	0.84
0.88	119.6	13.82						
0.87		13.29	66.94	93.52	1.8	3.708	.7930	1.63
0.86	117.8	12.75						
0.85		12.32	57.37	82.01	1.3	2.637	.6431	2.28
0.84	116.5	11.89						
0.83		11.53	50.06	73.12	1.0	1.993	.5451	2.82
0.82	115.5	11.17						
0.81		10.87	44.26	66.00	0.7	1.346	.4079	3.23
0.80	114.8	10.57						
0.79		10.32	39.55	60.19	1.3	2.782	.9243	4.15
0.78	113.5	10.07						
0.77		9.86	35.68	55.40	0.2	0.448	.1618	4.31
0.76	113.3	9.65						
0.75		9.46	32.43	51.35	0.7	1.440	.5607	4.88
0.74	112.6	9.27						
0.73		9.09	29.63	47.81	0.8	1.695	.7091	5.58
0.72	111.8	8.91						
0.71		8.74	27.24	44.72	0.7	1.450	.6485	6.23
0.70	111.1	8.57						

p/p_o	v_a (ml)	t (Å)	r_k (Å)	d (Å)	Δx_i (ml)	Δv_{x_i} ($\times 10^3$)	Δs_{x_i} (m^2)	$\Sigma \Delta s_{x_i}$ (m^2)
0.69		8.41	25.12	41.94	1.0	2.235	1.0658	7.30
0.68	110.1	8.26						
0.67		8.14	23.29	39.57	1.2	2.930	1.4813	8.78
0.66	108.9	8.02						
0.65		7.90	21.65	37.45	1.2	2.801	1.4955	10.28
0.64	107.7	7.77						
0.63		7.66	20.18	35.50	1.9	4.749	2.6755	12.95
0.62	105.8	7.56						
0.61		7.46	18.86	33.78	2.3	5.852	3.4648	16.42
0.60	103.5	7.36						
0.59		7.27	17.68	32.22	3.8	10.04	6.2315	22.65
0.58	99.7	7.17						
0.57		7.08	16.59	30.75	7.6	20.83	13.542	36.19
0.56	92.1	6.99						
0.55		6.90	15.60	29.40	15.0	42.18	28.691	64.88
0.54	77.1	6.82						
0.53		6.74	14.69	28.17	7.3	19.47	13.819	78.70
0.52	69.8	6.66						
0.51		6.58	13.85	27.01	4.1	9.810	7.2640	85.96
0.50	65.7	6.50						
0.49		6.42	13.07	25.91	4.0	9.435	7.2801	93.24
0.48	61.7	6.34						
0.47		6.26	12.35	24.87	2.7	5.344	4.2958	97.54

p/p_o	v_a (ml)	t (Å)	r_k (Å)	d (Å)	ΔX_i (ml)	ΔV_{x_i} ($\times 10^3$)	ΔS_{x_i} (m^2)	$\Sigma \Delta S_{x_i}$ (m^2)
0.46	59.0	6.18						
0.45		6.10	11.68	23.88	2.8	5.595	4.6859	102.2
0.44	56.2	6.02						
0.43		5.94	11.05	22.93	2.6	4.887	4.2644	106.5
0.42	53.6	5.86						
0.41		5.79	10.46	22.04	2.4	4.397	3.9900	110.5
0.40	51.2	5.71						
0.39		5.63	9.90	21.16	2.4	4.340	4.1021	114.6
0.38	48.7	5.56						
0.37		5.48	9.38	20.34	2.5	4.599	4.5221	119.1
0.36	46.4	5.41						
0.35		5.34	8.88	19.56	1.9	2.764	2.8262	121.9
0.34	44.3	5.27						
0.33		5.20	8.41	18.81	1.8	2.650	2.8177	124.7
0.32	42.5	5.14						
0.31		5.07	7.96	18.10	1.7	2.263	2.5006	127.2
0.30	40.8	5.01						
0.29		4.94	7.53	17.41	1.4	1.167	1.3406	128.6
0.28	39.4	4.88						
0.27		4.81	7.12	16.74	1.1	.073	.0872	128.7
0.26	38.3	4.75						
0.25		4.68	6.73	16.09	1.5	1.524	1.8943	130.6
0.24	37.2	4.62						
0.23		4.56	6.34	15.46	.9	-	-	-
0.22	36.3	4.49						

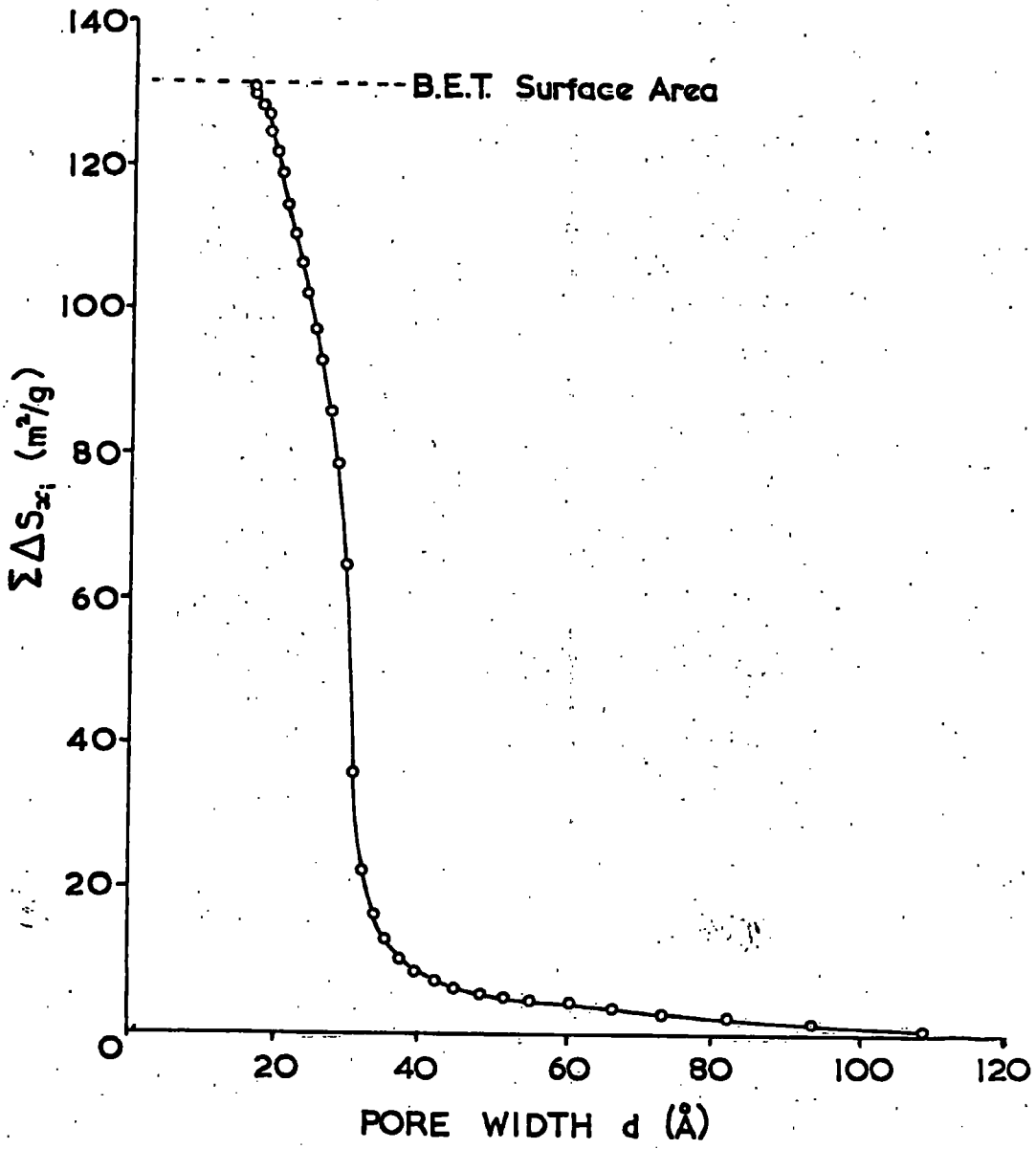

PORE SIZE DISTRIBUTION OF ALUMINA

FIG 40

(4) Specific Site Adsorption on the Alumina Surface

(a) Introduction

(i) Nature of the Alumina

Activated alumina is produced by the controlled heating of the hydrate which exists in four different modifications, i.e. hydrargillite, bayerite, diaspore and boehmite. Of these, hydrargillite, more commonly known as gibbsite, has received the most attention in the literature.

Stumpf et.al.[73] have reported the existence of seven nearly anhydrous forms of alumina intermediate between the hydrate and the final decomposition product, α-alumina obtained at 1000°C. Various investigators have designated these intermediate products as $\rho, \alpha, \varepsilon, \gamma, \varkappa, \varkappa', \eta, \delta, K, \theta$; the treatment for production being different by each worker.

Brown[74] heated gibbsite to various temperatures up to 1000°C. The sample was kept at each temperature for some hours and a X-ray powder diffraction pattern using copper filtered $K\alpha$ radiation obtained at each stage. From these it was assumed that the first stage involved decomposition of the trihydrate to either the monohydrate (i.e. boehmite) or to a nearly anhydrous form (designated as x). On raising the temperature, the decomposition of these two products was seen to follow independent routes but at 1000°C both gave α-alumina. In conclusion, Brown postulated two mechanisms for the decomposition of the trihydrate:-

(i) to x-alumina

(ii) to boehmite, subsequently to γ-alumina (virtually anhydrous form)

and proposed the following general scheme.

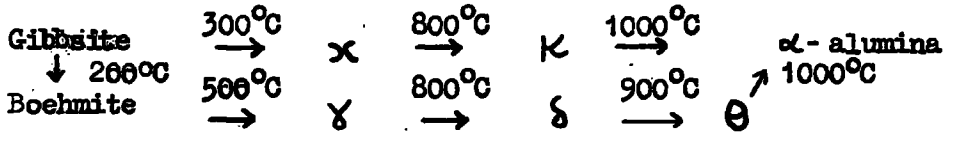

Day and Hill[75] proposed that the various intermediate forms were a result of dehydration and rehydration processes occurring according to the following scheme

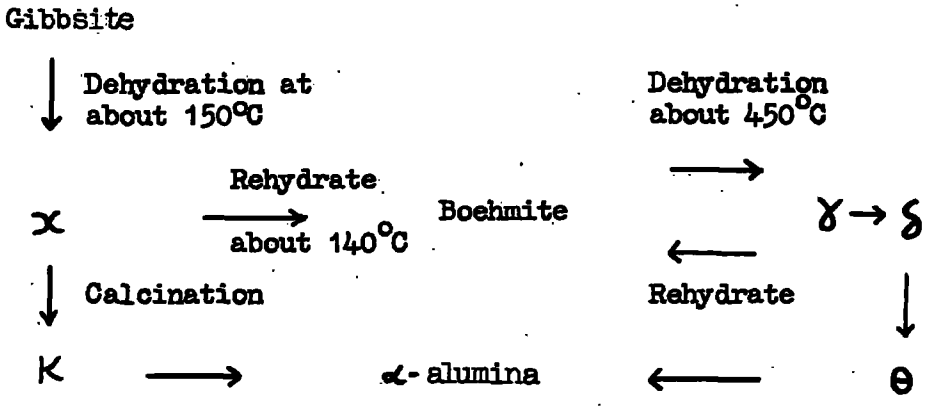

Thus in a closed system, where the water vapour remained in contact with the alumina, complete conversion to boehmite occurs and the subsequent decomposition of the boehmite at high temperatures would proceed via the series $\gamma \rightarrow \delta \rightarrow \theta \rightarrow \alpha$-alumina . With an open system, only some of the water vapour remains in close contact with the alumina and partial rehydration occurs producing a mixture of anhydrous aluminas characteristic of both series.

The manufacturers state that the sample of alumina used in this investigation has been produced by heating to 800°C and describe it as γ -alumina. A X-ray powder diffraction photograph of the alumina sample using copper filtered K_{α} radiation was obtained and compared with those given in the literature (Table (7)).

Table (7) X-ray Powder Diffraction Data.

Source	Sample		Brown	Day and Hill	Stumpf et.al.
Form of the Alumina		γ	χ	$\gamma + \chi$	χ
Wavelength Å	4.75w	4.50w	4.50w	4.50w	4.80vw
		2.77w		2.82w	
	2.44w	2.41m		2.39m	2.40mw
		2.28m		2.27m	2.29vw
	2.15w	2.20vw	2.13mw	2.11mw	2.13m
	2.00w	1.98ms		1.98ms	2.00vm
		1.95m		1.97w	
			1.87vw	1.22w	
		1.53mw	1.71vw	1.52w	1.54vw
		1.40m	1.40s	1.44w	
	1.39ms	1.39s		1.39s	1.40ms

s = strong
ms = moderately strong
m = moderate
mw = moderately weak
w = weak
vw = very weak

The X-ray photograph obtained was not well defined due to the presence of very fine particles. The presence of the highly characteristic line at 2.13Å seemed to indicate one of the components of the sample was x-alumina.

However, examination of the alumina by the British Petroleum Company Ltd., using X-ray photography indicated that the sample was γ - alumina admixed with α -monohydrate (Boehmite) to the extent of about 10%.

(ii) Constitution of the Alumina Surface.

The crystal of aluminium oxide is built up of layers of tightly-packed oxygen atoms with the smaller aluminium atoms situated interstitially. As the oxygen atoms outnumber the aluminium atoms, vacant sites, to the extent of one third of those possible, occur. Previously this cation deficiency has been invoked to explain strained oxide linkages and the resulting presence of active sites on the alumina surface. Thus transition aluminas were thought to possess defect spinel structures with various arrangements of the aluminium ions, and with different crystal planes, edges or corners exposed. However, X-ray diffraction evidence suggests that dehydration of boehmite yields γ -alumina in which a considerable part of the surface is formed by the 100 plane of a spinel lattice.(76) Arguments for the preferential exposure of the 111 plane based on the greater density of packing of oxide ions in this face(77) are thought to be unconvincing as actual exposure may still reflect the relative stabilities of hydrated faces rather than those of dehydrated faces.

It is reasonable to suppose that the extent of chemisorption of water should be closely related to the spacing of the oxide ions

on the exposed faces of a cubic, close-packed oxide lattice. Each oxide ion in a 111 plane occupies 6.74$\AA^2$ whereas in a 100 plane, the area per oxide ion is 7.9$\AA^2$ (Fig. 41)

Peri[78] heated alumina to 800°C and then slowly resorbed water onto the surface at 100°C. The water was irreversibly adsorbed and the monolayer value obtained from the 100°C adsorption isotherm corresponded to 6.25 molecules of water adsorbed per 100$\AA^2$ of the alumina surface. This value suggests one molecule of water is adsorbed per two oxide sites, the 100 plane being preferentially exposed. Thus, after adsorption, the surface is probably covered with a monolayer of hydroxyl ions; one molecule of water forming two surface hydroxyl ions as shown in Fig. 42. A total of 12.5 molecules per 100$\AA^2$ of surface was found to be adsorbed when the surface was exposed to a water vapour atmosphere at room temperature, implying physical adsorption of water molecules onto the surface layer of hydroxyl ions to the extent of one molecule per two ion sites. On evacuation at 100°C, the alumina was found to still retain 8.3 molecules of water per 100$\AA^2$ of surface, corresponding to one water molecule physically adsorbed per six ion sites.

Infra-red[78][79] studies provide evidence that the active sites on the alumina surface are hydroxyl groups rather than strained oxide linkages and also enable a distinction to be made between hydroxyl groups and physically adsorbed water molecules.

FIG 41

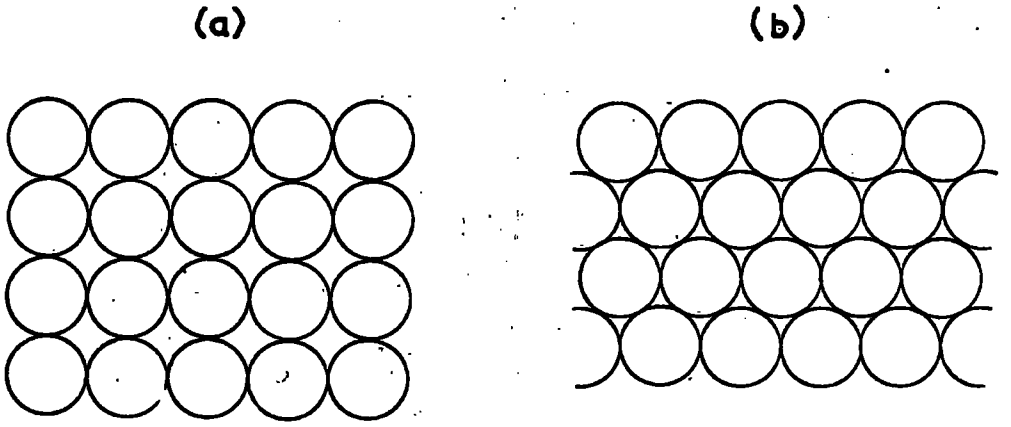

ARRANGEMENTS OF OXIDE IONS IN (a) 100 PLANE (b) 111 PLANE OF ALUMINA

FIG 42

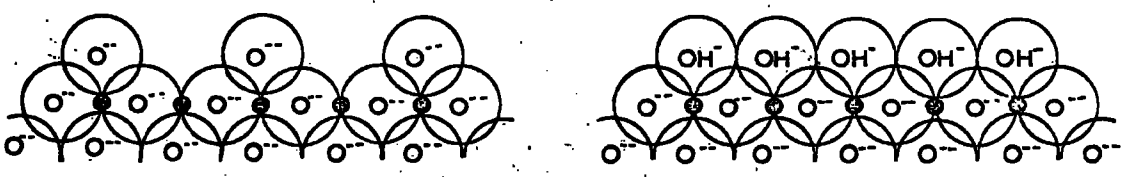

ADSORPTION OF WATER ON AN IDEAL ALUMINA SURFACE TO FORM HYDROXYL IONS

Liquid water gives rise to an infra-red adsorption band in the region 1650-1600 cm^{-1}, this band being due to a deformation vibration of the hydrogen atoms in the plane of the molecule. Undried alumina exhibits bands near 1650 and 3300 cm^{-1}, the latter being a consequence of O-H bond stretching and showing evidence of considerable hydrogen bonding. After evacuation at 650-700°C, the band at 1650 cm^{-1} disappears and bands are found at 3700, 3733, 3744, 3780 and 3800 cm^{-1}. Exposure of the alumina to deuterium oxide vapour and re-evacuation at 700°C removes these bands and produces new ones at frequencies which are each related to the original frequencies by the factor 0.738 indicating that all these bands are due to hydroxyl stretching vibrations. The extent of hydroxyl groups on the surface can be assessed by deuterium exchange. After drying at 400°C, the hydroxyl groups are found to cover 40% of the surface, at 800°C approximately 2% and above 900°C less than 1%.

By assuming a model for the fully hydroxylated alumina surface, Peri[80] was able to speculate on the nature of the hydroxyl groups present on the surface after evacuation at 650-700°C. Peri showed that removal of hydroxyl groups from the hydroxylated surface as water, i.e.

$$OH^- + OH^- = O^{--} + H_2O$$

such that neither two (or more) oxide ions were left on immediately adjacent sites nor two (or more) immediately adjacent sites were left vacant, resulted in 67% of the hydroxyl layer being removed.

If the condition of local order in the residual oxide layer was then relaxed, further removal of water was possible until only 9.6% of the original hydroxyl layer remained when any further loss of water necessitated surface migration of the hydroxyl groups. Experimentally, Peri found that a sample of alumina when evacuated at 650-700°C left approximately 10% of the surface covered by hydroxyl groups and in this state the alumina surface was assumed to resemble that of the model. The remaining hydroxyl groups on the surface were found to be in five possible environments having 0, 1, 2, 3 and 4 nearest oxide neighbours. The five types of hydroxyl ion sites differ in local charge density because of the nearest neighbour configuration and the frequencies of the corresponding infra-red bands can be expected to decrease with decreasing electron density. Further dehydration of the alumina assuming surface migration of the remaining hydroxyl groups showed that the various types of isolated groups were removed at different rates so enabling Peri to assign an adsorption band to each particular type.

(iii) Surface Area Determination by Adsorption from Solution

De Boer et al.[77] recognised specific site adsorption in their determination of the surface areas of aluminium oxides and hydroxides from adsorption data of long-chain polar organic molecules in solution in non-polar solvents. The polar group of

the organic molecule is firmly bound to the adsorbent surface and the hydrocarbon chain orientated perpendicularly to the surface. Lauric acid was considered to be the best-suited adsorbate, since the lower fatty acids were known to undergo chemical reaction with some of the aluminas and the higher acids had limited solubilities in non-polar solvents. As both solute and solvent are capable of being adsorbed by the adsorbent, a solvent was required whose affinity for the adsorbent surface is very small compared to that of the solute. The saturated aliphatic hydrocarbons were found to be the only suitable solvents and of these, n-pentane was found to be the best.

The adsorption isotherm of lauric acid from n-pentane on alumina (Fig.43) showed a pronounced saturation character. A monolayer of lauric acid is formed on the surface at low equilibrium concentrations owing to strong dipole forces. After the formation of this monolayer, the surface is deprived of its polarity and further adsorption is impossible.

For a series of alumina samples (prepared from the hydrates by heating in air), the specific lauric acid adsorption 'f' (expressed as mmoles acid per $100m^2$ of surface area) was seen to be dependent on the temperature of pre-treatment and nature of the sample. The lowest and most diverging values of 'f' were found for aluminas obtained from crystalline hydrates heated just above the decomposition temperature at which the internal surface is formed. De Boer concluded that steric effects were responsible for these low values

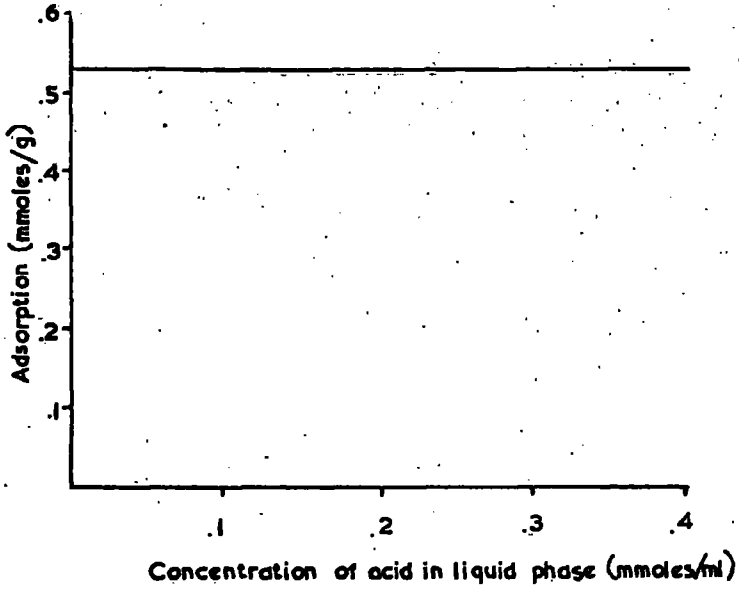

FIG 43

ADSORPTION OF LAURIC ACID FROM n-PENTANE SOLUTION BY ALUMINA

FIG 44

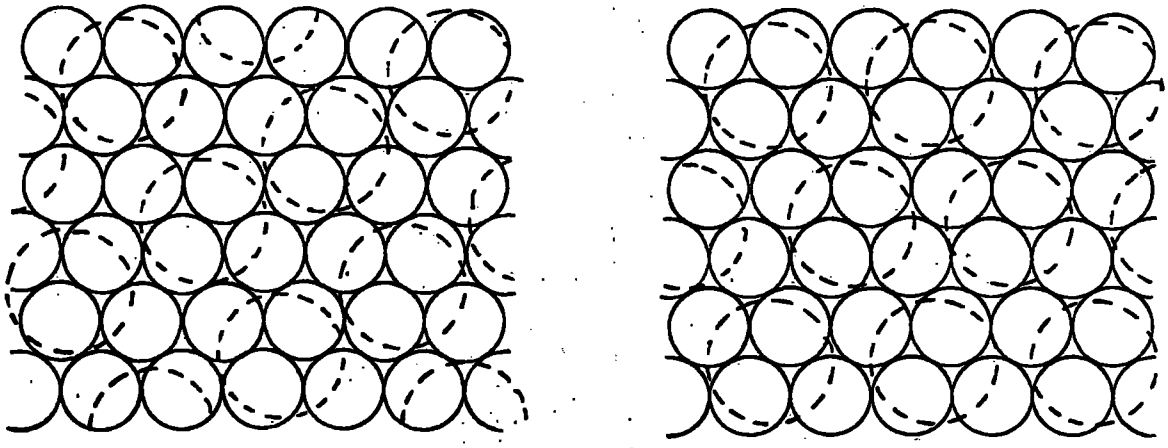

ARRANGEMENT OF LAURIC ACID MOLECULES (DOTTED OUTLINE) ON THE ALUMINA SURFACE (111 PLANE)

as the mean pore width was found to be very low (10Å), as compared to the length of the hydrocarbon chain of lauric acid (18Å). At increasing temperatures of pretreatment of increased and converged to a constant value (independent of the nature of the hydrate) of 0.617 mmoles per 100 m^2 after preheating above 800°C.

For adsorption on the original hydrates, dried at 120°C, the mean value for the specific lauric acid adsorption was 0.43 mmoles per 100m^2. This low figure could not be attributed to steric effects occurring in narrow pores as a determination of the geometrical surface areas of three samples of microcrystalline boehmite from electron micrographs showed good agreement with those obtained from the B.E.T. method, thus indicating the hydroxides to be of a non-porous nature.

In order to determine the surface area of the adsorbent from the lauric acid adsorption isotherm, the packing arrangement of the acid on the surface must be known. De Boer considered that preferential exposure of the 111 plane of the oxygen sub-lattice of the alumina crystal occurred on heating the hydrates to high temperatures. One oxygen atom in this plane will occupy a surface area of 6.74$Å^2$ and using a minimum surface area value of 20.5$Å^2$ (obtained from the study of monolayer films of fatty acids on water) for the lauric acid molecules, two possible stacking arrangements were found as shown in Fig. 44. In both cases, the lauric acid molecule is seen to cover a surface area corresponding to four oxygen atoms i.e. 26.96$Å^2$. The experimental value of the specific lauric acid

adsorption (0,617 mmoles per 100 m^2) was found to be equivalent to a molecular surface area requirement of lauric acid of 26.9$\mathring{A}^2$, in good agreement with calculation.

Thus, if steric hindrance in narrow pores is known to be absent, the adsorption isotherm of lauric acid from n-pentane can be used for the determination of the specific surface area of aluminium oxide and hydroxide samples. The surface area (m^2g^{-1}) is the lauric acid limiting adsorption value (mmoles g^{-1}) multiplied by a factor of 162 for an alumina sample and by a factor of 232 for an aluminium hydroxide sample. Comparison of the surface area obtained with the B.E.T. surface area will indicate whether narrow pores are present or not in the sample under investigation.

(iv) Adsorption of the Solvents Cyclohexane and Tetrahydrofuran

In the adsorption of solids from solution, it is necessary to consider the extent of adsorption of the solvent. This involves a knowledge of the arrangement of the solvent molecules on the adsorbent surface and in certain cases specific site adsorption is to be expected. By determining the area requirement of the solvent molecules on the alumina surface by vapour phase adsorption, the occurrence of specific site adsorption can be deduced by comparison with the cross-sectional area of the molecule (calculated from known bond lengths and bond angles assuming a

probable orientation). Specific site adsorption is to be expected in the case of tetrahydrofuran, the molecule bonding to the alumina surface via its oxygen atom. The cyclohexane molecules, however, would be expected to form a close-packed adsorbed layer independent of specific sites on the alumina surface.

(b) Experimental Adsorption of Lauric Acid from n-Pentane Solution onto Alumina.

(i) Materials

n-Pentane was treated with concentrated sulphuric acid, washed with water, dried and then fractionally distilled under anhydrous conditions (Boiling point 36.0°C).

0.1001 M Lauric acid solution was prepared by dissolving 10.0257 gms. lauric acid in 500 ml. n-pentane solution.

Alumina of the same grade as used in Part B was dried at 120°C for 48 hours.

Approximately 0.05 M ethanolic potassium hydroxide solution was used as titrant in determining equilibrium concentration after adsorption.

(ii) Method of Adsorption

50 ml. of lauric acid solution were pipetted into four 100 ml. volumetric flasks which had previously been cleaned with chromic acid. Two grams of alumina were transferred directly from the drying oven to each solution and the flasks immediately sealed

with a quick drying solution of cellulose acetate in acetone. The solutions were then left to reach equilibrium for a period of 24 hours with occasional shaking. After allowing the alumina to settle, 10 ml. of the supernatant clear liquid were pipetted into 50 ml. of ethanol and titrated against the alcoholic potassium hydroxide solution using thymol blue as indicator. The titration blank was determined by omitting the lauric acid solution.

(iii) Calculation of Results

Molarity of KOH solution = 0.04360

Mean titre of lauric acid solutions after adsorption = 17.85 ml. alcoholic KOH

Concentration of equilibrium solution = 0.07661 M

Number of moles of acid adsorbed per gram of alumina = 0.587×10^{-3}

Surface Area of alumina per gram

$= 0.587 \times 10^{-3} \times 6.023 \times 10^{23} \times 26.96 \times 10^{-20} m^2$

$= 95.3\ m^2$

(c) Vapour Phase Adsorption of Cyclohexane and Tetrahydrofuran

(1) The Adsorption Experiment

The apparatus was the same as that used for the nitrogen adsorption experiment and is shown schematically in Fig. 33.

The experimental procedure was as follows:-

One gram of alumina previously dried for 48 hours at 120°C, was placed in the adsorption bulb D and outgassed for several hours. Two ml. of the organic solvent were placed in the adsorption bulb F

and outgassed for approximately one minute. With taps b, d, h and i closed, tap f was momentarily opened and a small volume of vapour admitted into the doser volume. After recording the pressure, tap h was opened and the system allowed to reach equilibrium when the pressure was again recorded. The procedure was repeated by admitting further small volumes of vapour and the volume adsorbed at increasing equilibrium pressures calculated. The saturation vapour pressure of the solvent was determined by opening tap f fully with tap h closed, and allowing the system to reach equilibrium.

(ii) Calculation of Results

Adsorption of Cyclohexane

The experimental results are recorded in Table (8) and the plot of 'v_a' against 'P/P_o' shown in Fig. 45.

Table (8)

Adsorption of Cyclohexane on Alumina

Vapour Phase

Doser Pressure cm.	Mercury Meniscus (e) cm.	Temp. °C	Equilibrium Pressure cm.	Mercury Meniscus (e) cm.	Temp °C	P/P_o	Volume of vapour adsorbed (at N.T.P.) v_a ml.
1.68	22.15	22.6	0.44	20.91	22.8	0.050	1.90
2.39	22.85	22.8	1.05	21.52	22.9	0.119	4.29
2.78	23.23	22.8	1.65	22.10	22.9	0.188	6.31
3.88	24.31	22.9	2.25	22.70	22.4	0.256	9.26
4.75	25.17	22.3	2.83	23.27	21.8	0.322	12.78
5.30	25.69	22.0	3.22	23.64	21.8	0.366	16.64
5.74	26.12	21.8	3.39	23.82	20.6	0.385	21.45
6.41	26.77	20.9	3.99	24.40	22.5	0.453	26.00

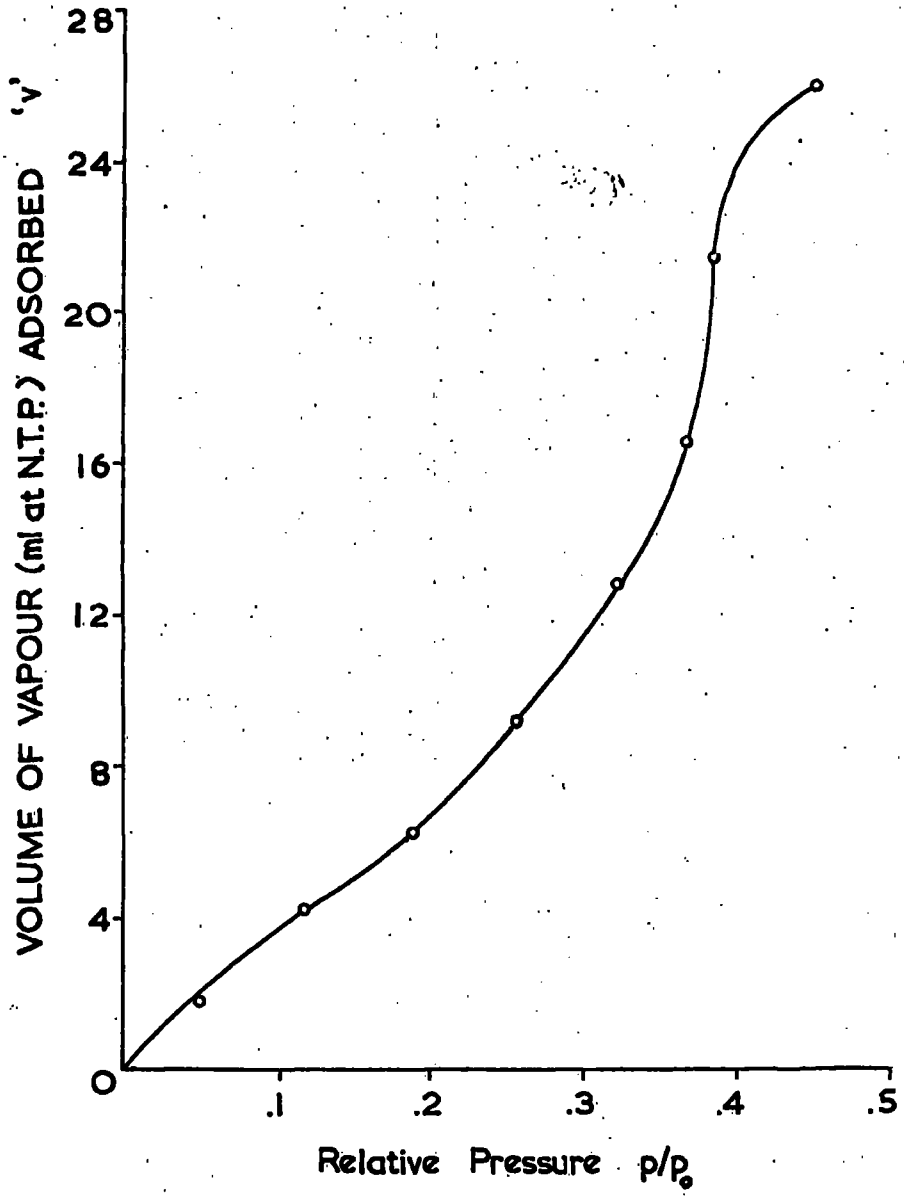

VAPOUR PHASE ADSORPTION OF CYCLOHEXANE ON ALUMINA

FIG 45

As the adsorption isotherm possesses no distinct 'knee' and hence a low 'c' value, the B.E.T. equation cannot be used for the determination of the monolayer value.

Adsorption of Tetrahydrofuran

The experimental results are recorded in Table (9) and the plot of v_a against P/P_o shown in Fig. 46.

Table (9) Adsorption of Tetrahydrofuran on Alumina

Vapour Phase

Doser Pressure cm.	Mercury Meniscus (e) cm.	Temp. °C	Equilibrium Pressure cm.	Mercury Meniscus (e) cm.	Temp °C	P/P_o	Volume of vapour adsorbed (at N.T.P.) v ml.
1.45	21.75	23.4	0.05	20.35	23.5	0.004	2.61
2.20	22.50	23.4	0.60	20.91	23.3	0.048	5.50
2.39	22.71	23.2	1.41	21.71	23.7	0.113	7.20
2.79	23.09	23.9	2.10	22.40	23.8	0.168	8.37
3.57	23.76	23.8	2.85	23.15	23.7	0.227	9.58
4.28	24.43	23.7	3.51	23.80	23.7	0.280	10.91
5.06	25.30	23.1	4.26	24.56	23.5	0.340	12.30
6.08	26.20	23.6	5.15	25.42	23.8	0.411	13.90

Calculated values of $\frac{P}{v(p_o-p)}$ and P/P_o are recorded in Table (10) and the linear plot of these quantities shown in Fig. 47.

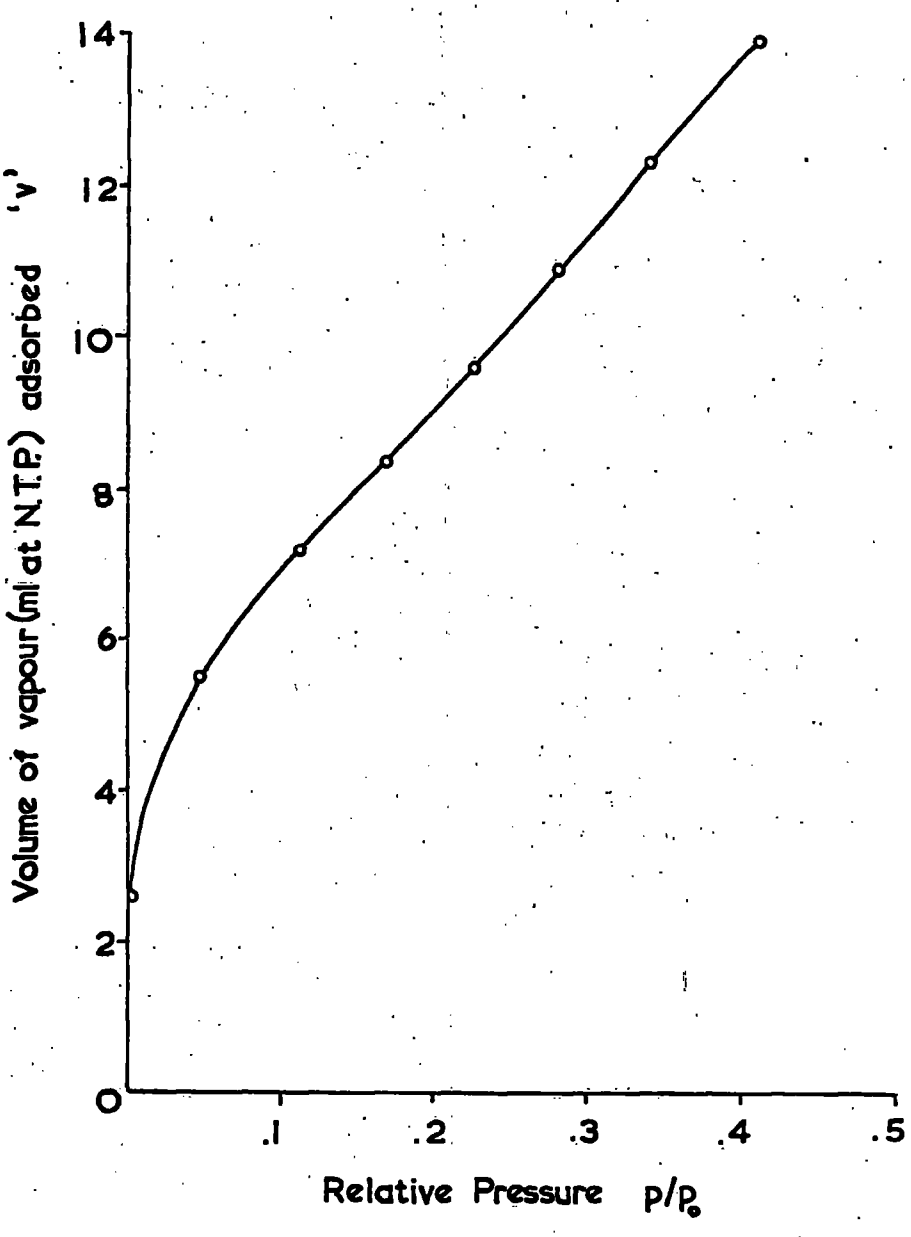

VAPOUR PHASE ADSORPTION OF TETRAHYDROFURAN ON ALUMINA

FIG 46

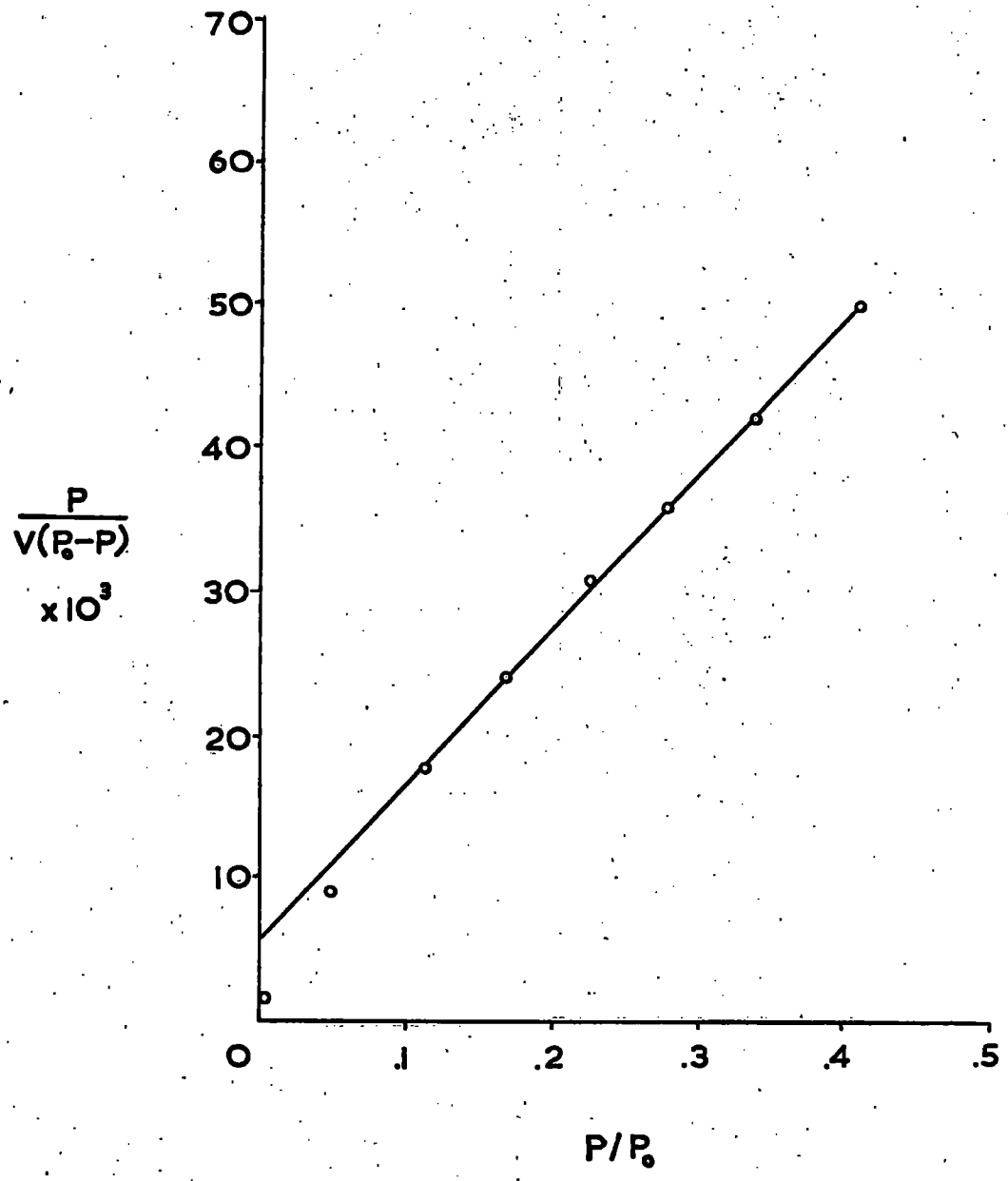

FIG 47

Table (10)

Vapour Phase Adsorption of Tetrahydrofuran on Alumina

Relative Pressure P/P_o	Volume of vapour (at N.T.P.) v (c.c.)	$\frac{P}{v(P_o-P)} \times 10^3$
0.004	2.61	1.54
0.048	5.50	9.14
0.113	7.20	17.62
0.168	8.37	24.07
0.227	9.58	30.73
0.280	10.91	35.66
0.340	12.30	41.88
0.411	13.90	49.80

The slope of the graph (Fig.47) is found to be 0.1058 and the intercept has a value of 6.1×10^{-3}

From equation (21)

$$\frac{(c-1)}{Vm.c} = 0.1058 \qquad \frac{1}{Vm.c} = 6.1 \times 10^{-3}$$

Eliminating 'c' $V_m = 8.94$ mls.

Substituting V_m in equation (23)

$$S = 2.40\ Am.$$

where Am = the cross sectional area of the tetrahydrofuran molecule on the alumina surface (A^{o2})

If the accessible surface area of the alumina sample is taken as $\underline{95.3}\,m^2 g^{-1}$, then the area requirement of the tetrahydrofuran molecule on the surface is $\underline{39.7}\,\text{Å}^2$.

5. Conclusions

(a) The surface area of the alumina under investigation, as assessed by low temperature nitrogen adsorption, is 131.1 $m^2 g^{-1}$

(b) The shape of the 't' curve (Fig.38) indicates the alumina to be of a porous nature, the surface area of the pores corresponding to 125.7 $m^2 g^{-1}$

(c) A pore size distribution analysis of the desorption branch of the nitrogen adsorption isotherm (Fig.34) assuming slit-shaped pores, indicates the virtual absence of pores of less than 20Å in width. The plot of cumulative surface area against pore size (Fig.40) shows that the majority of pores in the alumina have a wall separation in the region of 20-35Å.

(d) An X-ray powder diffraction photograph has shown the alumina to exist in the γ-form admixed with a small percentage of unconverted boehmite.

(e) The surface area of the alumina as assessed by adsorption of lauric acid from n-pentane is 95.3 $m^2 g^{-1}$ which gives a value of 39.7Å^2 for the area requirement of the tetrahydrofuran molecule on the surface.

B. Adsorption of a Series of Substituted Phenols onto Alumina

1. Materials and Apparatus

(a) The Adsorbent

Activated aluminium oxide, "Camag M.F.C." graded between 100-200 B.S.S. with a Brockman Activity of 1 was used as adsorbent. All experiments were carried out using alumina from one bulk supply in order to eliminate variations in degree of activation. Before use, the alumina was dried at 120°C for 42 hours; prolonged heating producing no further loss in weight.

(b) The Solvents

Cyclohexane and tetrahydrofuran were dried with sodium wire, refluxed over sodium for several hours and then fractionally distilled under anhydrous conditions. The tetrahydrofuran was distilled under nitrogen to prevent formation of peroxide. The cyclohexane fraction boiling at 80.8°C and the tetrahydrofuran fraction boiling at 64.1°C under 760 mm. pressure were collected and used as soon as possible.

(c) The Adsorptives

Phenol, p-cresol, p-chlorophenol and p-tertiary butyl phenol were fractionally distilled twice, recrystallised from dry 40°-60° petroleum ether and stored over phosphorus pentoxide.

p-Bromo-phenol was recrystallised twice from dry 40°-60° petroleum ether and stored over phosphorus pentoxide.

p-Nitro-phenol was recrystallised twice from distilled water and stored over phosphorus pentoxide.

Physical constants of the adsorptives are given in Table (11).

Table (11)

	Mol. Wt.	M pt.($^{\circ}$C)	B pt.($^{\circ}$C)
Phenol	94.11	41	182-183
p-Cresol	108.14	34	202-203
p-Chlorophenol	128.56	43	218-219
p-Bromophenol	173.03	64	---
p-Tertiary Butyl Phenol	150.21	99	236-238
p-Nitrophenol	139.11	114	---

(d) The Apparatus

The Unicam SP 500 Photoelectric Quartz Spectrophotometer was used throughout the adsorption studies for all measurements of phenol concentration in solution. This instrument provides a means of investigating the transmission characteristics of compounds in solution over a wavelength range of 200-1,000 mμ . A hydrogen discharge lamp, supplied with a stabilised current of 300mA provides radiations of wavelengths 200-320 mμ . For the wavelength range 320-1,000 mμ , a tungsten lamp, operated from two large capacity six volt accumulators, is used. These accumulators also operate

the photo-cells and amplifier circuit. The monochromator unit consists of a quartz prism and collimating mirror, with a slit aperture calibrated from 0.01 to 2.00 mm. Two photo-calls are employed, a red-sensitive cell for use above 625 mμ and an ultra-violet sensitive cell for use below 625 mμ. The photo-cell current is fed to a two-stage amplifier and passes to an indicating meter which is adjusted to zero by a potentiometer calibrated in both optical density and percentage transmission scales.

2. Adsorption Procedure

All glassware before use, was soaked in chromic acid, rinsed with water and acetone, and then blown dry.

A stock solution of the phenol was prepared by dissolving a weighed quantity in the appropriate solvent, and making up the volume in a volumetric flask at 20°C. The stock solution was then allowed to attain room temperature, the latter being recorded. Calculated volumes of the stock solution were measured from a burette into 100 ml. flasks and diluted to 50 ml. with the solvent, to give a range of dilute solutions of suitable concentration for the adsorption experiments. Solutions of each concentration were prepared in triplicate.

A 2 gram (wet-weight) quantity of alumina, dried at 120°C for 48 hours, was transferred directly from the drying oven to each solution and the flasks immediately sealed with a quick drying solution of cellulose acetate in acetone. The flasks were placed

in a thermostat bath at a temperature of 35.0°C for a period of one week, during which they were intermittently shaken.

After this time, the flasks were taken from the bath, the solutions decanted from the alumina and the optical densities determined at a suitable but arbitrary wavelength. It was found necessary to use two silica cells of different pathlengths and a calibration curve using each cell was constructed using solutions of known concentration prepared from the original stock solution. The calibration curves were found to be straight lines and their equations evaluated by the methods of least squares.

Equilibrium concentrations were obtained from the calibration curves and the amount of phenol adsorbed per gram of alumina calculated. The composite isotherm for each phenol was drawn by plotting ($n_o \Delta x_1^{1}/m$) against the equilibrium mole fraction (x_1^{1}) and the limiting value of adsorption calculated using the Jowett[81] equation (37).

$$n_o \Delta x_1^{1}/m = A - (A-a)e^{-Bx_1^{1}} \qquad (37)$$

where A, a and B are constants; A giving the value of the asymptote.

The form of this equation is entirely empirical and no theoretical significance is attributed to it.

A plot of ($x_1^{1} m/n_o \Delta x_1^{1}$) against x_1^{1} was also made for each phenol to assess the applicability of the Everett equation to the systems studied.

3. Experimental Results

(a) Adsorption of Phenol from Cyclohexane

Table (12) : Calibration Curves

1 mm. cell Equation of the line: y = 20.654x-0.019

Concentration (moles.litre^{-1} x 10^2)	3.5939	2.6954	1.7970	.8985	.4492
Optical Density	.727	.528	.358	.166	.073

1 cm. cell Equation of the line: y = 149.59x-0.001

Concentration (moles.litre^{-1} x 10^3)	3.5939	2.6954	2.2462	1.7970	.8985
Optical Density	.540	.401	.332	.267	.137

The calibration curves are shown in Fig. 48.

Table (13) : Adsorption Data

Before Adsorption

Stock Solution (ml)	Concentration (moles.litre^{-1} x 10^2)	Moles of Phenol in 50ml.solution x 10^3	Mole Fraction of Phenol (x_1^o) x 10^3
36	4.6213	2.3107	4.9904
32	4.1079	2.0540	4.4385
27	3.4660	1.7330	3.7474
23	2.9514	1.4757	3.1928
16.5	2.1181	1.0591	2.2935
12	1.5405	.7703	1.6692

Density of cyclohexane at 23°C = 0.7755 g. cm^{-3}

Moles of cyclohexane in 50 ml. = 0.46072

After Adsorption

Mean Optical Density	Concentration (moles.litre^{-1} x 10^2)	Moles of Phenol in 50 ml.solution x 10^4	Mole Fraction of Phenol (x_1^1) x 10^3
.378	1.9222	9.611	2.0817
.274	1.4186	7.093	1.5372
.173	.9296	4.648	1.0078
.102	.5858	2.929	.6353
.245	.1644	0.822	.1784
.067	.0455	0.228	.0495

$\Delta x_1^1 \times 10^3$	2.9087	2.9013	2.7396	2.5575	2.1151	1.6197
$n_o \Delta x_1^1 / m \times 10^4$	6.7337	6.7134	6.3346	5.9104	4.8836	3.7375
$x_1^1 m / n_o \Delta x_1^1$	3.0914	2.2987	1.5909	1.0749	0.3653	0.1324

Limiting Adsorption Value, A = 6.782×10^{-4} moles per gram of alumina

The adsorption isotherm (Fig. 49) was constructed from the data in Table (13) and the plot of $x_1^1 m / n_o \Delta x_1^1$ against x_1^1 is shown in Fig. 50.

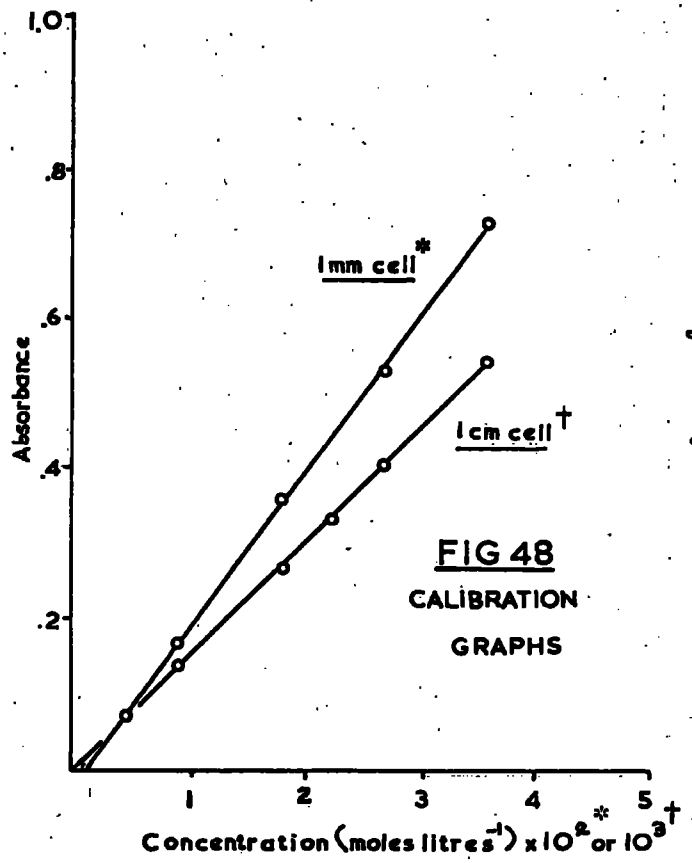

FIG 48

CALIBRATION GRAPHS

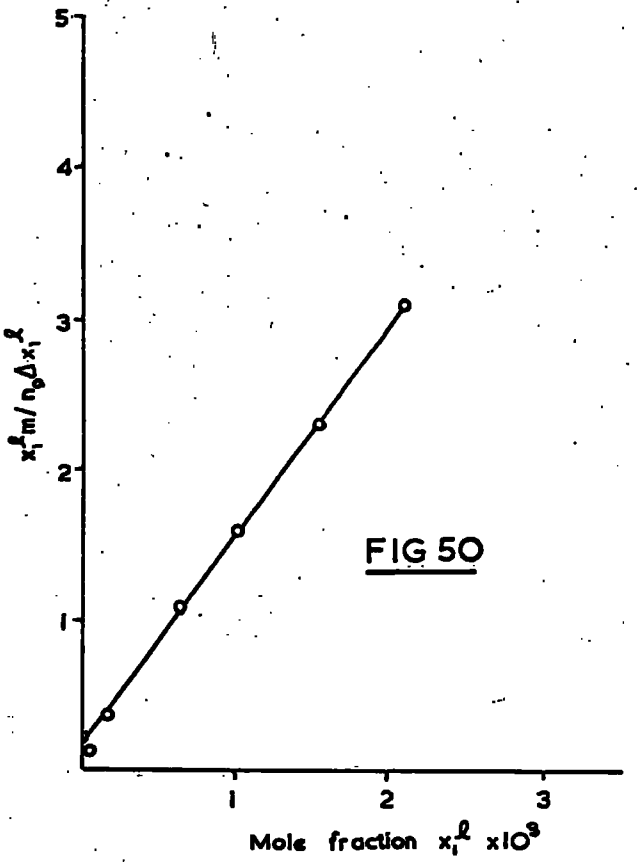

FIG 50

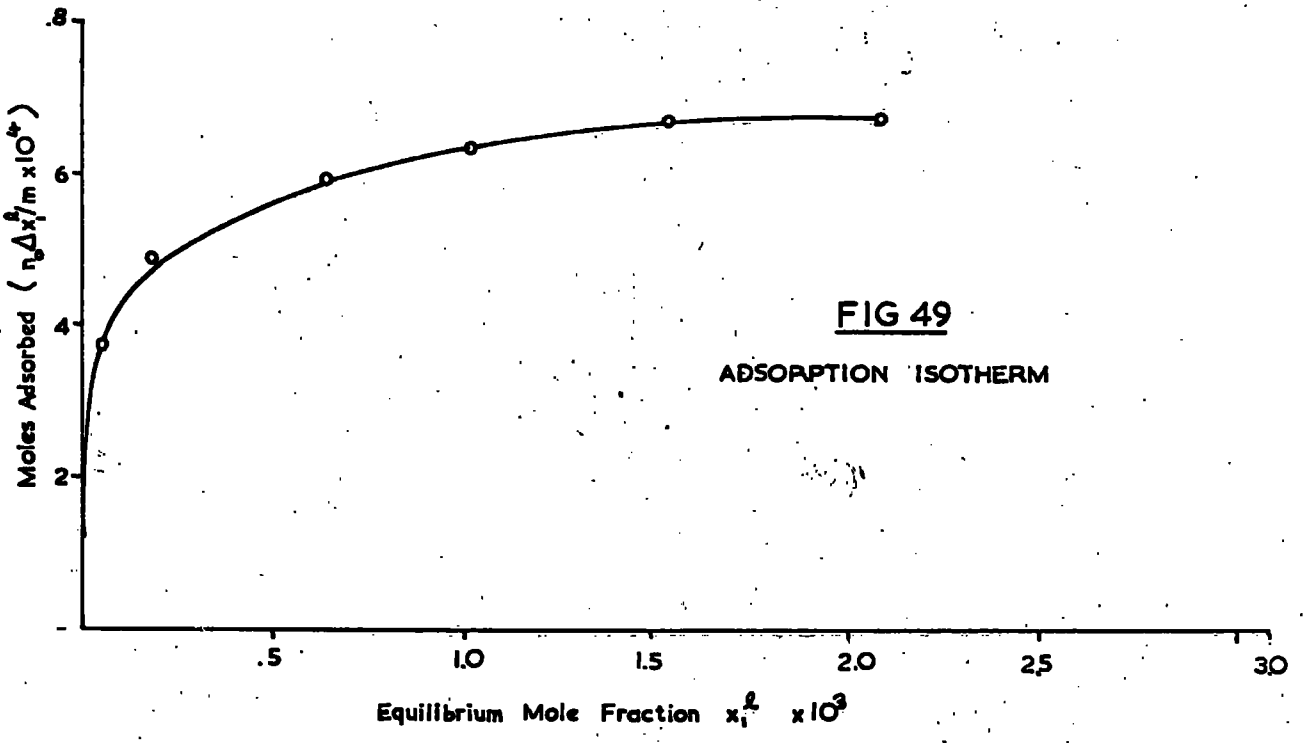

FIG 49

ADSORPTION ISOTHERM

(b) Adsorption of p-Cresol from Cyclohexane

Table (14) : Calibration Curves

1 mm. cell Equation of the line : $y = 19.950x + 0.029$

Concentration (moles.litre^{-1} x 10^{2})	4.2391	3.5326	2.8260	2.1195	1.4130
Optical Density	.873	.733	.598	.450	.310

1 cm. cell Equation of the line : $y = 178.22x + 0.034$

Concentration (moles.litre^{-1} x 10^{3})	4.9456	4.2391	3.5326	2.8260	1.4130
Optical Density	.910	.794	.665	.540	.283

The calibration curves are shown in Fig. 51.

Table (15) : Adsorption Data

Before Adsorption

Stock Solution (ml)	Concentration (moles.litre^{-1} x 10^2)	Moles of Phenol in 50 ml.solution x 10^3	Mole Fraction of Phenol (x_1^o) x 10^3
35	4.9456	2.4728	5.3314
30	4.2391	2.1196	4.5733
25	3.5326	1.7663	3.8139
20	2.8260	1.4130	3.0534
15	2.1195	1.0598	2.2919
10	1.5543	.7772	1.6818

Density of cyclohexane at 22°C = 0.7765 g.cm^{-3}

Moles of cyclohexane in 50 ml. = 0.46135

After Adsorption

Mean Optical Density	Concentration (moles.litre^{-1} x 10^2)	Moles of Phenol in 50 ml.solution x 10^4	Mole Fraction of Phenol (x_1^1) x 10^3
.477	2.2456	11.228	2.4278
.336	1.5388	7.694	1.6649
.224	0.9774	4.887	1.0582
.131	0.5112	2.556	0.5537
.335	0.1689	0.845	0.1831
.111	0.0432	0.216	0.0468

$\Delta x_1^1 \times 10^3$	2.9036	2.9084	2.7557	2.4997	2.1088	1.6350
$n_o \Delta x_1^1/m \times 10^4$	6.7337	6.7398	6.3811	5.7851	4.8757	3.7790
$x_1^1 m/n_o \Delta x_1^1$	3.6054	2.4703	1.6583	0.9573	0.3755	0.1238

Limiting Adsorption Value, A = 6.761×10^{-4} moles per gram of alumina.

The adsorption isotherm (Fig.52) was constructed from the data in Table (15) and the plot of $x_1^1 m/n_o \Delta x_1^1$ against x_1^1 is shown in Fig. 53.

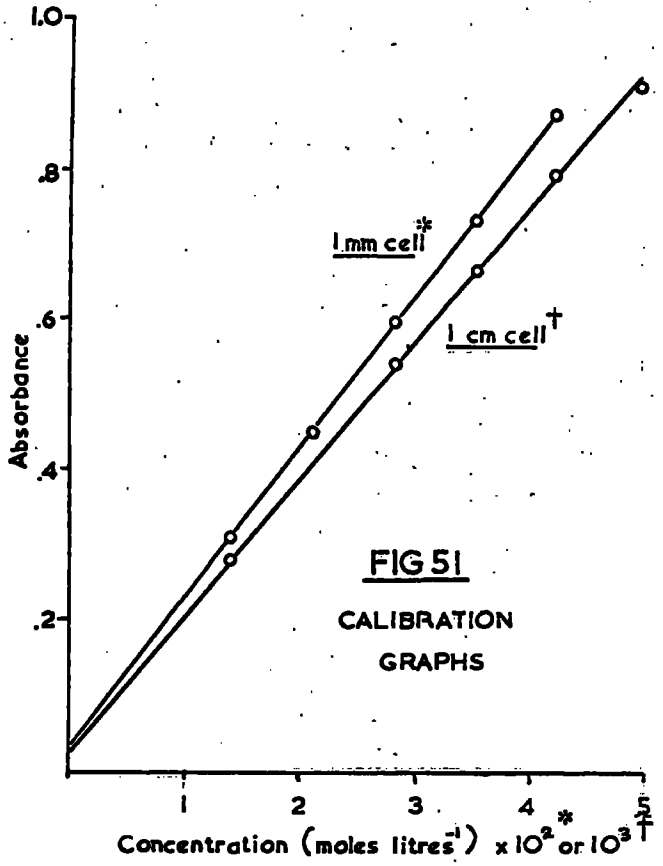

FIG 51

CALIBRATION GRAPHS

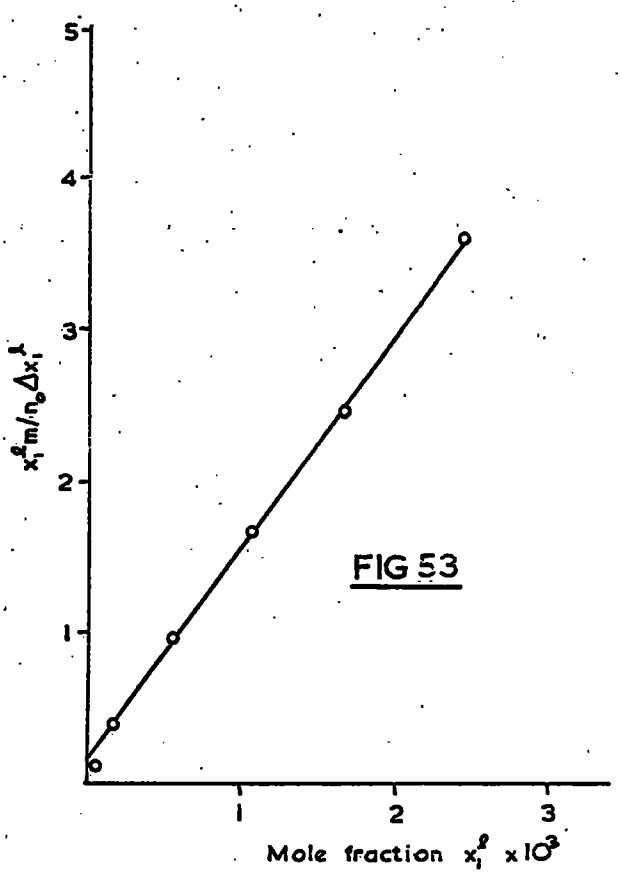

FIG 53

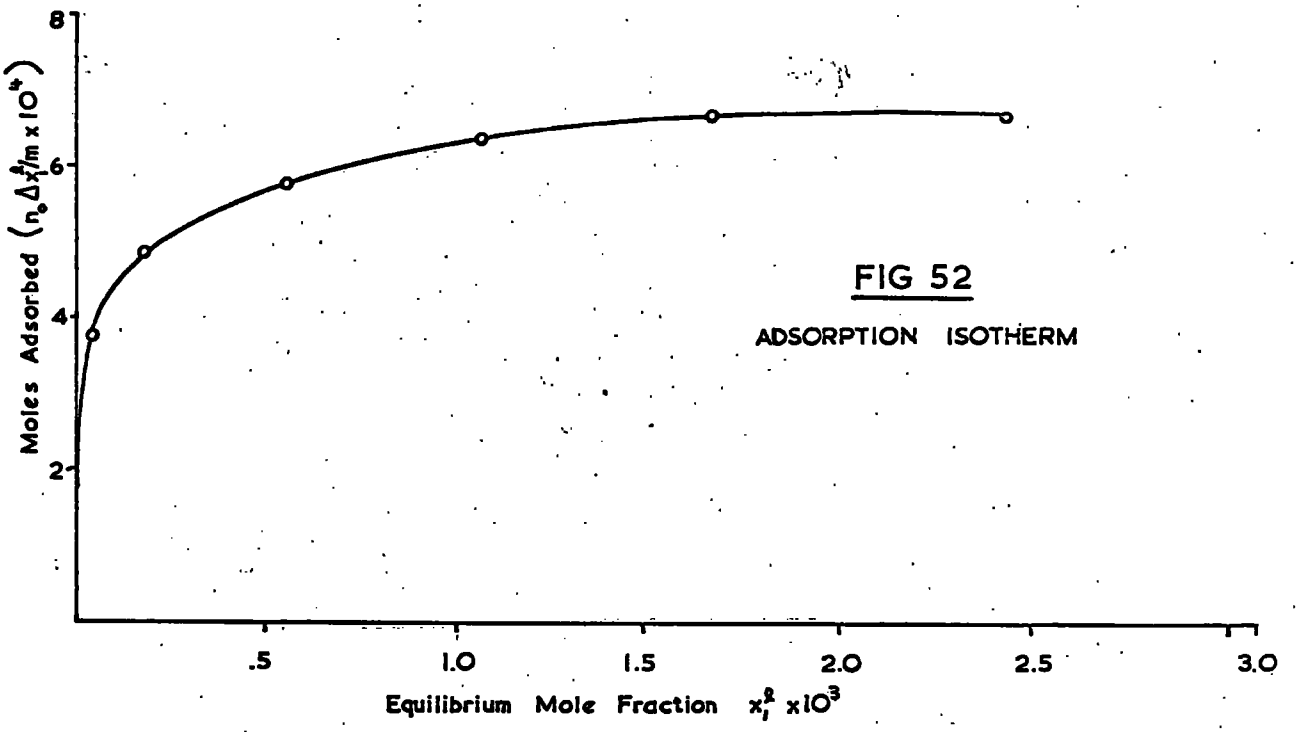

FIG 52

ADSORPTION ISOTHERM

(c) Adsorption of p-Chlorophenol from Cyclohexane

Table (16) : Calibration Curves

1 mm. cell Equation of the line : $y = 18.058x + 0.023$

Concentration (moles.litre^{-1} x 10^2)	4.9472	4.2404	3.5337	2.8270	1.4135
Optical Density	.916	.788	.661	.536	.277

1 cm. cell Equation of the line : $y = 173.72x - 0.002$

Concentration (moles.litre^{-1} x 10^3)	4.9472	4.2404	3.5337	2.8270	1.4135
Optical Density	.859	.726	.609	.491	.242

The calibration curves are shown in Fig. 54.

Table (17) : Adsorption Data

Before Adsorption

Stock Solution (ml)	Concentration (moles.litre^{-1} x 10^2)	Moles of Phenol in 50 ml.solution x 10^3	Mole Fraction of Phenol (x_1^o) x 10^3
35	4.9472	2.4736	5.3404
30	4.2404	2.1202	4.5808
25	3.5337	1.7669	3.8204
20	2.8270	1.4135	3.0587
16	2.2616	1.1308	2.4484
12	1.5548	0.7774	1.6845

Density of cyclohexane at 23°C = .7755g. cm^{-3}

Moles of cyclohexane in 50 ml. = 0.46072

After Adsorption

Mean Optical Density	Concentration (moles.litre^{-1} x 10^2)	Moles of Phenol in 50 ml.solution x 10^4	Mole Fraction of Phenol, (x_1^1 x 10^3)
.429	2.2483	11.242	2.4342
.303	1.5506	7.753	1.6800
.188	.9137	4.569	0.9907
.106	.4596	2.298	0.4985
.389	.2251	1.126	0.2443
.065	.0386	0.193	0.0419

$\Delta x_1^1 \times 10^3$	2.9062	2.9008	2.8297	2.5602	2.2041	1.6426
$n_o \Delta x_1^1 / m_x \times 10^4$	6.7306	6.7130	6.5437	5.9157	5.0899	3.7903
$x_1^1 m / n_o \Delta x_1^1$	3.6166	2.5026	1.5140	0.8427	0.4800	0.1105

Limiting Adsorption Value, A = 6.733×10^{-4} moles per gram of alumina.

The adsorption isotherm (Fig.55) was constructed from the data in Table (17) and the plot of $x_1^1 m / n_o \Delta x_1^1$ against x_1^1 is shown in Fig. 56.

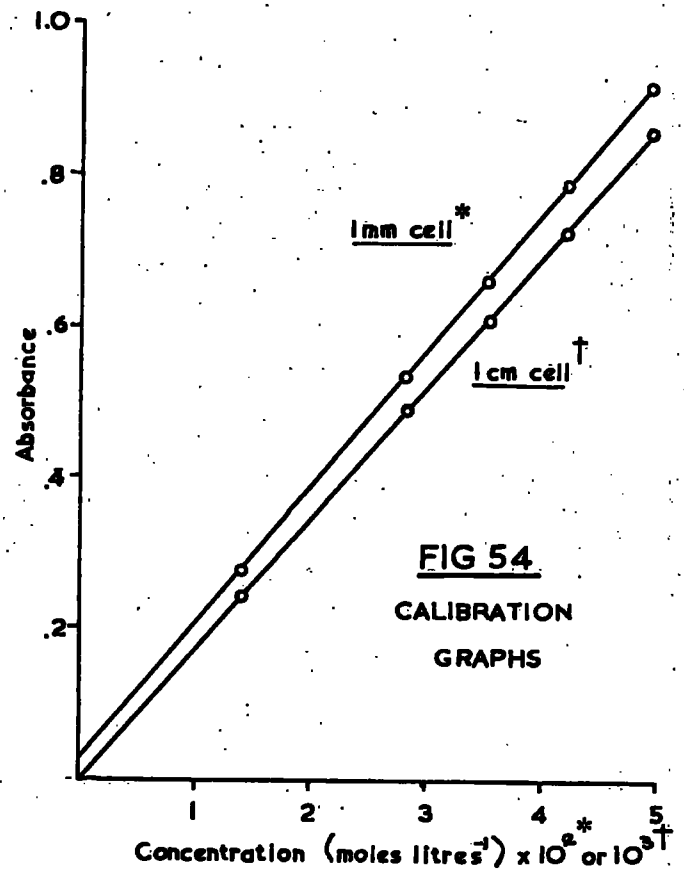

FIG 54

CALIBRATION GRAPHS

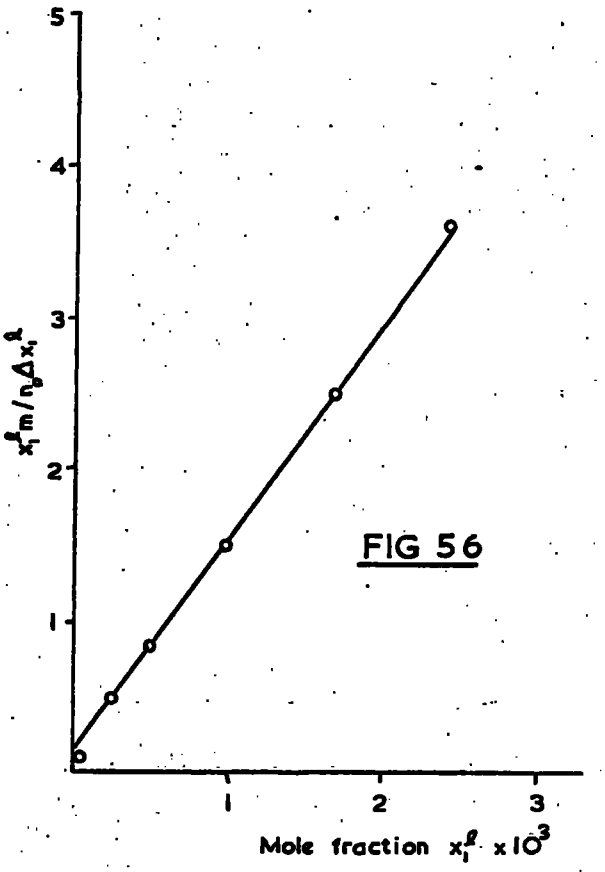

FIG 56

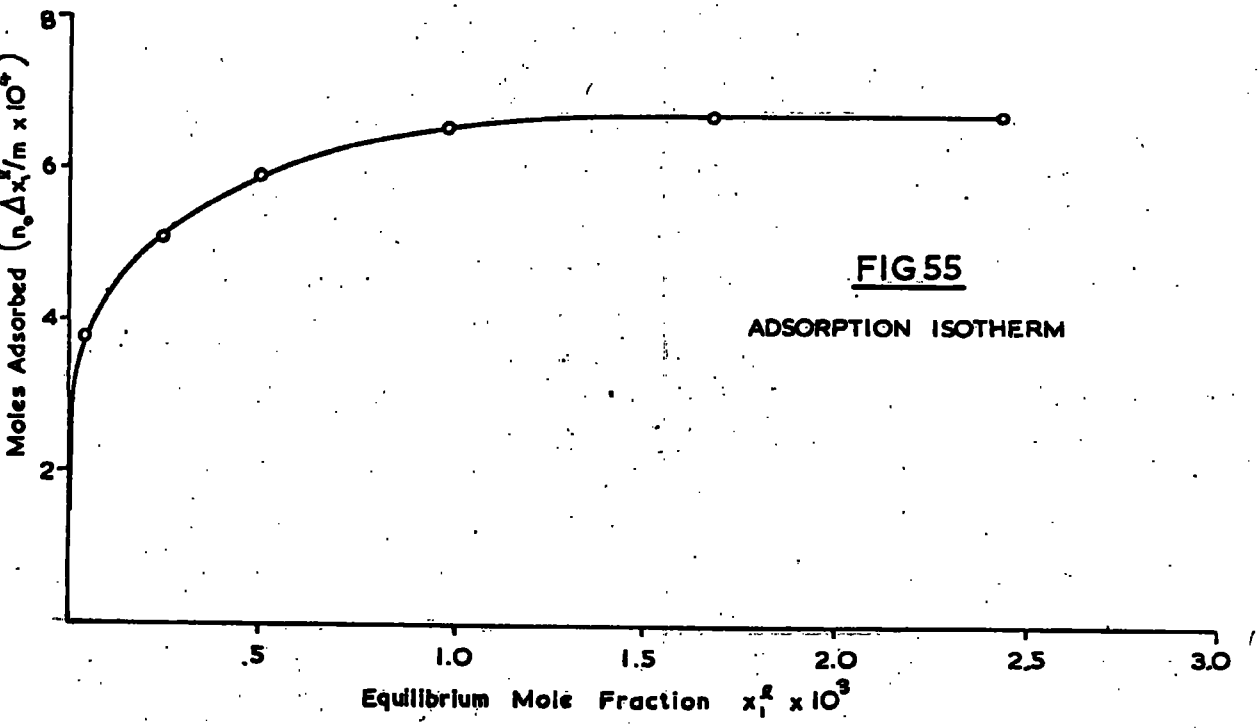

FIG 55

ADSORPTION ISOTHERM

(d) Adsorption of p-Bromophenol from Cyclohexane

Table (18) : Calibration Curves

1 mm. cell Equation of the line : $y = 22.237x - 0.022$

Concentration (moles.litre^{-1} x 10^2)	3.9933	3.3278	2.6622	1.9967	1.3311
Optical Density	.872	.712	.568	.420	.278

1 cm. cell Equation of the line : $y = 201.59 - 0.040$

Concentration (moles.litre^{-1} x 10^3)	4.6588	3.9933	3.3278	2.6622	1.3311
Optical Density	.903	.764	.627	.496	.231

The calibration curves are shown in Fig. 57.

Table (19) : Adsorption Data

Before Adsorption

Stock Solution (ml)	Concentration (moles.litre^{-1} x 10^2)	Moles of Phenol in 50 ml. of solution x 10^3	Mole Fraction of Phenol (x_1^o) x 10^3
38	5.0522	2.5291	5.4521
33	4.3926	2.1963	4.7402
26	3.4609	1.7305	3.7369
20	2.6622	1.3311	2.8769
15	1.9967	.9984	2.1594
12	1.5973	.7987	1.7282

Density of cyclohexane at 22°C = .7765 g. cm^{-3}

Moles of cyclohexane in 50 ml. = 0.46135

After Adsorption

Mean Optical Density	Concentration (moles.litre^{-1} x 10^2)	Moles of Phenol in 50 ml. of solution x 10^4	Mole Fraction of Phenol (x_1^1) x 10^3
.503	2.3609	11.805	2.5523
.367	1.7493	8.747	1.8924
.201	1.0028	5.014	1.0856
.085	0.4812	2.406	0.5212
.338	0.1875	0.938	0.2033
.118	0.0784	0.392	0.0850

$\Delta x_1^1 \times 10^3$	2.8998	2.8478	2.6513	2.3557	1.9561	1.6432
$n_o \Delta x_1^1 / m \times 10^4$	6.7258	6.5974	6.1388	5.4497	4.5220	3.7970
$x_1^1 m / n_o \Delta x_1^1$	3.7948	2.8684	1.7684	0.9564	0.4496	0.2239

Limiting Adsorption Value, A = 6.780×10^{-4} moles per gram of alumina.

The adsorption isotherm (Fig.58) was constructed from the data in Table (19) and the plot of $x_1^1 m / n_o \Delta x_1^1$ against x_1^1 is shown in Fig. 59.

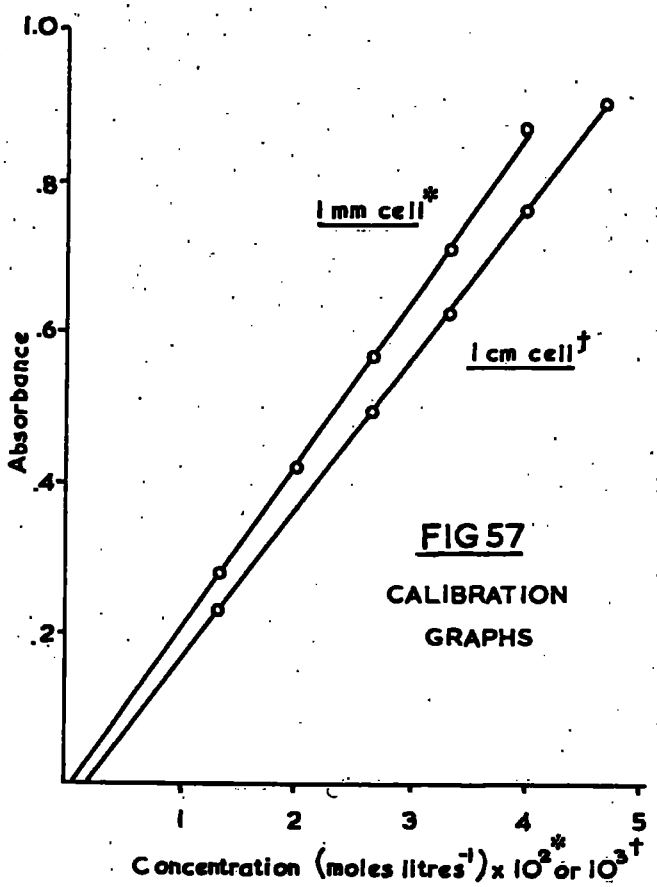

FIG 57

CALIBRATION GRAPHS

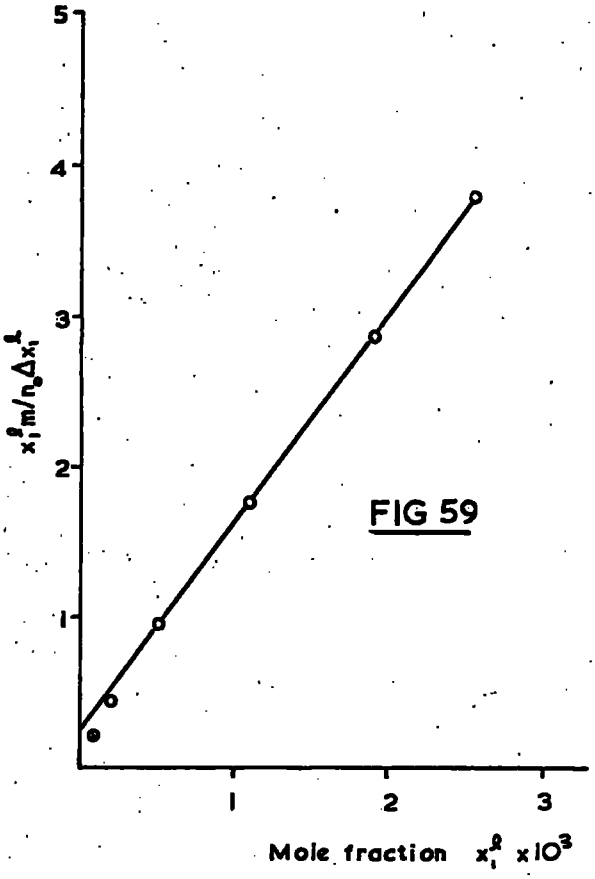

FIG 59

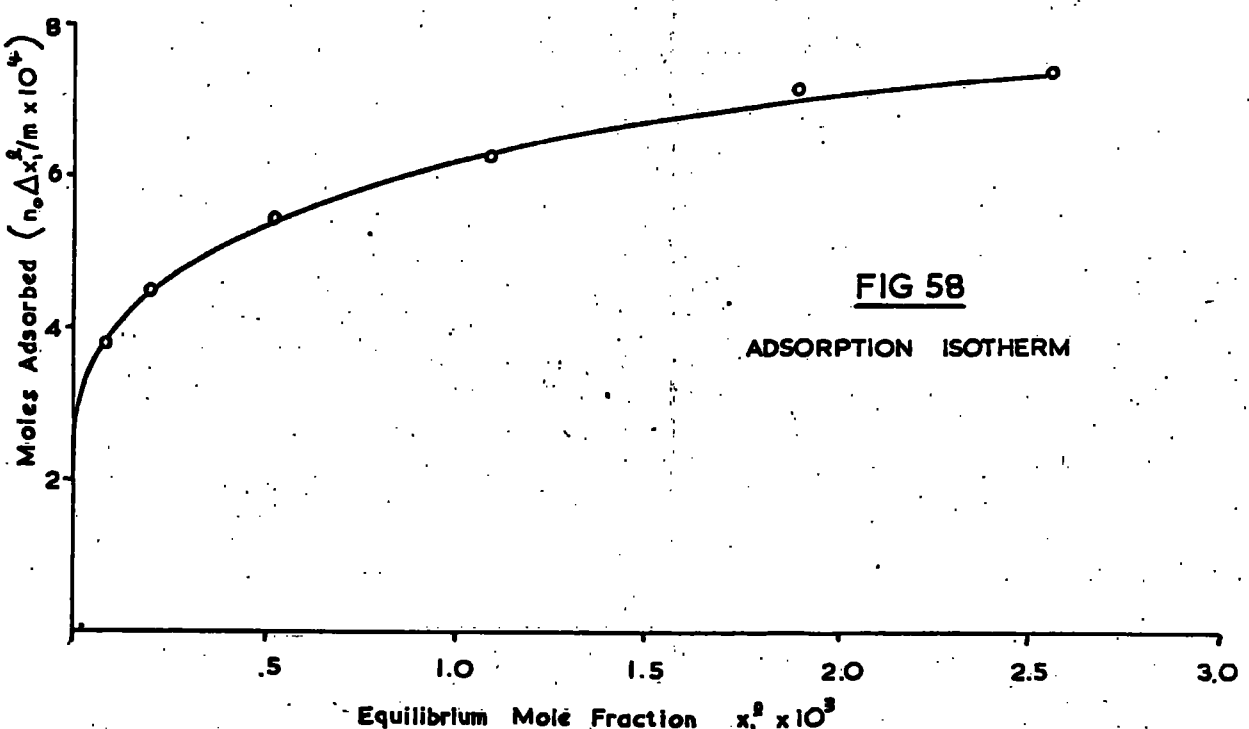

FIG 58

ADSORPTION ISOTHERM

(e) Adsorption of p-Tertiary Butylphenol from Cyclohexane

Table (20) : Calibration Curves

1 mm. cell Equation of the line : $y = 24.761x + 0.033$

Concentration (moles.litre^{-1} x 10^{2})	3.6032	3.0027	2.4021	1.8016	1.2011
Optical Density	.927	.776	.625	.478	.333

1 cm. cell Equation of the line : $y = 236.66x + 0.013$

Concentration (moles.litre^{-1} x 10^{3})	4.2037	3.6032	3.0027	2.4021	1.2011
Optical Density	.955	.839	.717	.600	.365

The calibration curves are shown in Fig. 60.

Table (21) : Adsorption Data

Before Adsorption

Stock Solution (ml.)	Concentration (moles.litre^{-1} x 10^2)	Moles of Phenol in 50 ml. solution x 10^3	Mole Fraction of Phenol (x_1^0) x 10^3
35	4.2037	2.1019	4.5353
30	3.6032	1.8016	3.8899
25	3.0027	1.5014	3.2438
20	2.4021	1.2011	2.5967
15	1.8016	.9008	1.9487
10	1.2011	.6006	1.3001

Density of cyclohexane at 22°C = .7765 g. cm^{-3}

Moles of cyclohexane in 50 ml. = 0.46135

After Adsorption

Mean Optical Density	Concentration (moles.litre^{-1} x 10^2)	Moles of Phenol in 50 ml. solution x 10^4	Mole Fraction of Phenol (x_1^1) x 10^3
.625	2.3909	11.955	2.5835
.491	1.8497	9.249	2.0008
.350	1.2802	6.401	1.3855
.211	0.7189	3.595	0.7786
.703	0.2916	1.458	0.3159
.189	0.0744	0.372	0.0806

$\Delta x_1^1 \times 10^3$	1.9518	1.8891	1.8593	1.8181	1.6328	1.2195
$n_o \Delta x_1^1 / m \times 10^4$	4.5228	4.3737	4.3006	4.2048	3.7728	2.8167
$x_1^1 m / n_o \Delta x_1^1$	5.7122	4.5746	3.2216	1.8517	0.8371	0.2862

Limiting Adsorption Value, A = 4.377×10^{-4} moles per gram of alumina

The adsorption isotherm (Fig.61) was constructed from the data in Table (21) and the plot of $x_1^1 m / n_o \Delta x_1^1$ against x_1^1 is shown in Fig. 62.

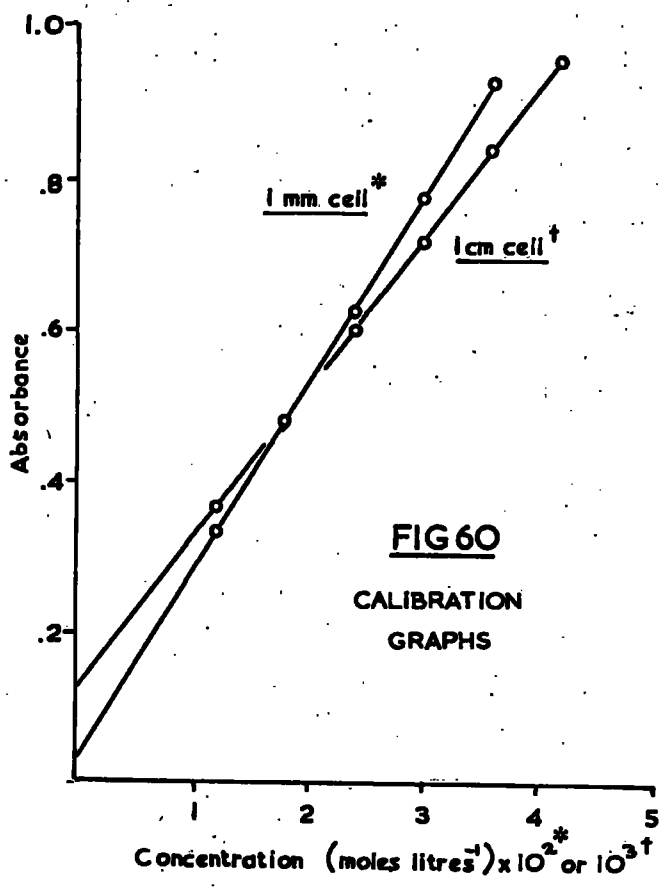

FIG 60

CALIBRATION GRAPHS

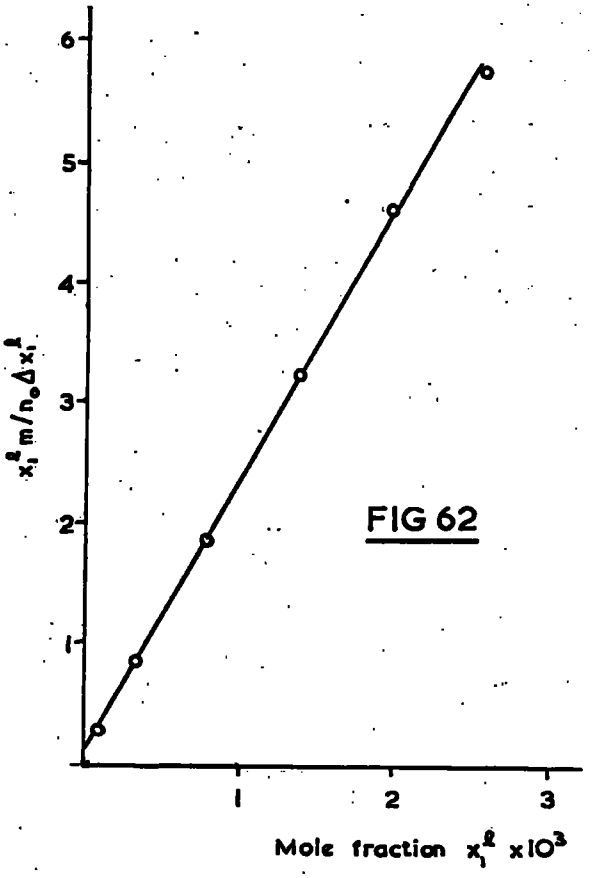

FIG 62

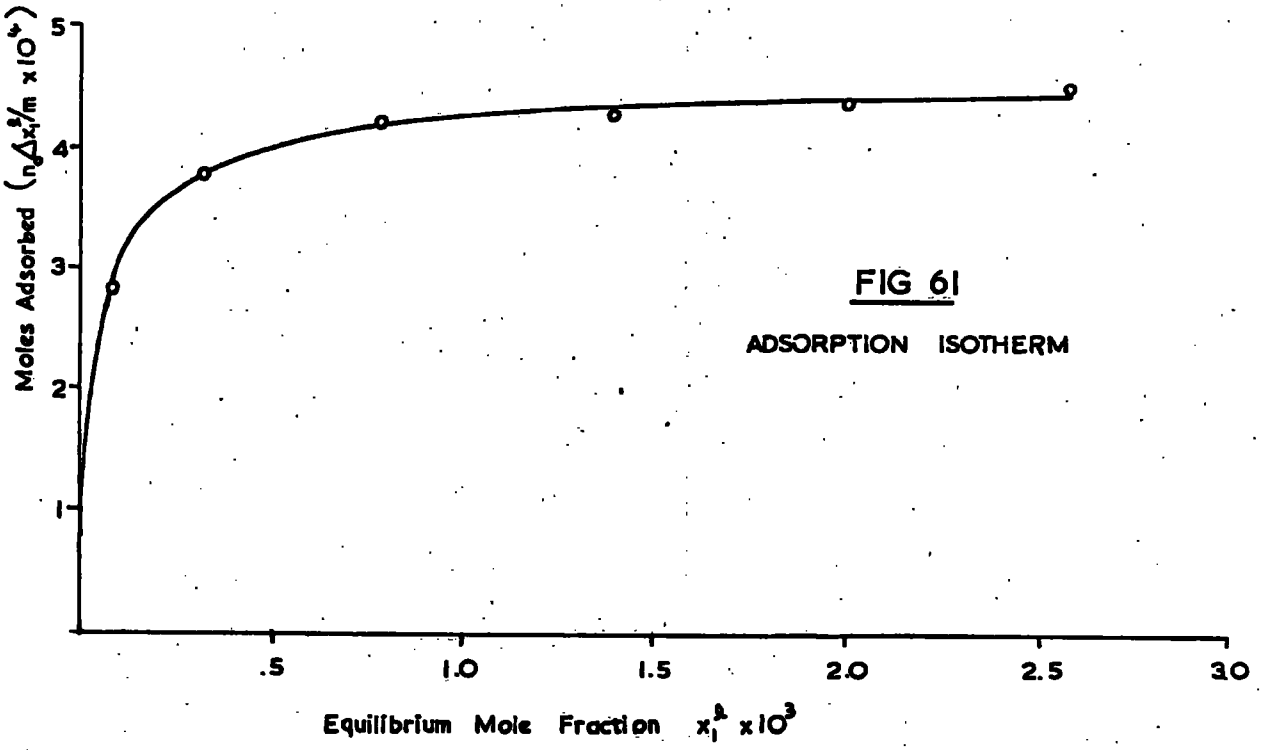

FIG 61

ADSORPTION ISOTHERM

(f) Adsorption of Phenol from Tetrahydrofuran

Table (22) : Calibration Curves

1 mm. cell Equation of the line : $y = 7.9969x - 0.001$

Concentration (moles.litre^{-1} x 10^{2})	8.7116	6.9693	5.2270	3.4846	1.7423
Optical Density	.696	.557	.414	.278	.139

1 cm. cell Equation of the line : $y = 72.455x - 0.004$

Concentration (moles.litre^{-1} x 10^{3})	6.9693	5.2270	4.3558	3.4846	1.7423
Optical Density	.501	.376	.309	.248	.123

The calibration curves are shown in Fig. 63.

Table (23) : Adsorption Data

Before Adsorption

Stock Solution (ml)	Concentration (moles.litre^{-1} x 10^2)	Moles of Phenol in 50 ml.solution x 10^3	Mole Fraction of Phenol (x_1^o) x 10^3
45	7.8404	3.9202	6.3441
37	6.4466	3.2233	5.2222
28	4.8785	2.4393	3.9570
18	3.1362	1.5681	2.5474
10	1.7424	.8712	1.4169
5	.8712	.4356	.7089

Density of tetrahydrofuran at 22.5°C = .8855 g. cm^{-3}

Moles of tetrahydrofuran in 50 ml. = 0.61401

After Adsorption

Mean Optical Density	Concentration (moles.litre^{-1} x 10^2)	Moles of Phenol in 50 ml.solution x 10^3	Mole Fraction of Phenol (x_1) x 10^3
.550	6.8902	3.4451	5.5795
.440	5.5146	2.7573	4.4705
.318	3.9890	1.9945	3.2378
.185	2.3259	1.1629	1.8904
.084	1.0629	0.5315	0.8649
.264	0.3699	0.1850	0.3101

$\Delta x_1^1 \times 10^3$	.7646	.7517	.7192	.6570	.5520	.3988
$n_o \Delta x_1^1 / m \times 10^4$	2.3623	2.3199	2.2168	2.0222	1.6971	1.2252
$x_1^1 m / n_o \Delta x_1^1$	23.619	19.270	14.606	9.348	5.096	2.531

Limiting Adsorption Value, A = 2.414×10^{-4} moles per gram of alumina

The adsorption isotherm (Fig.64) was constructed from the data in Table (23) and the plot of $x_1^1 m / n_o \Delta x_1^1$ against x_1^1 and is shown in Fig. 65.

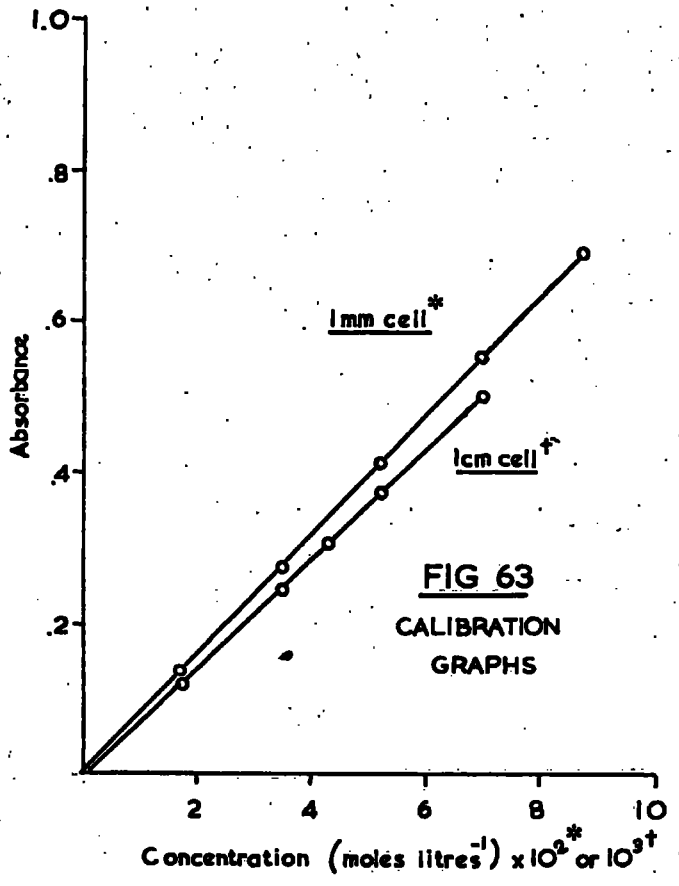

FIG 63

CALIBRATION GRAPHS

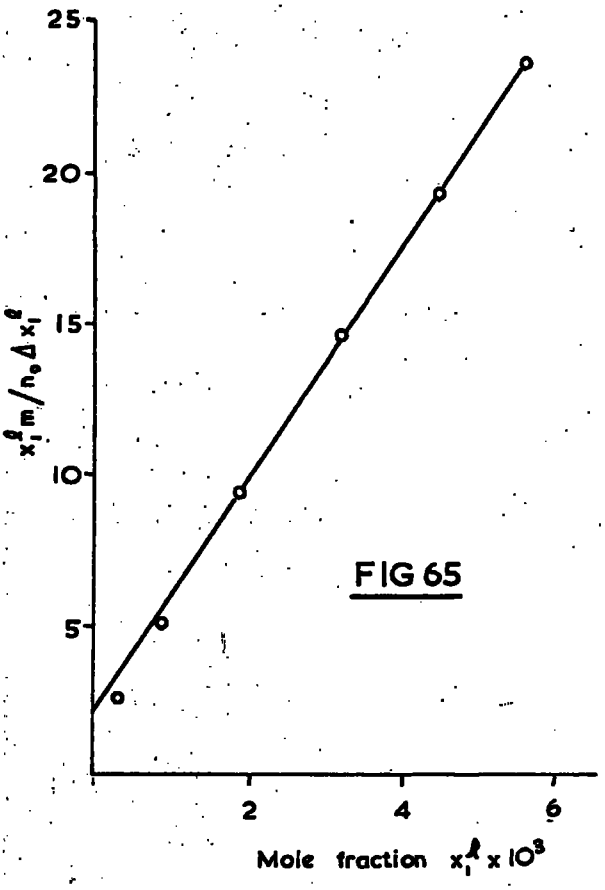

FIG 65

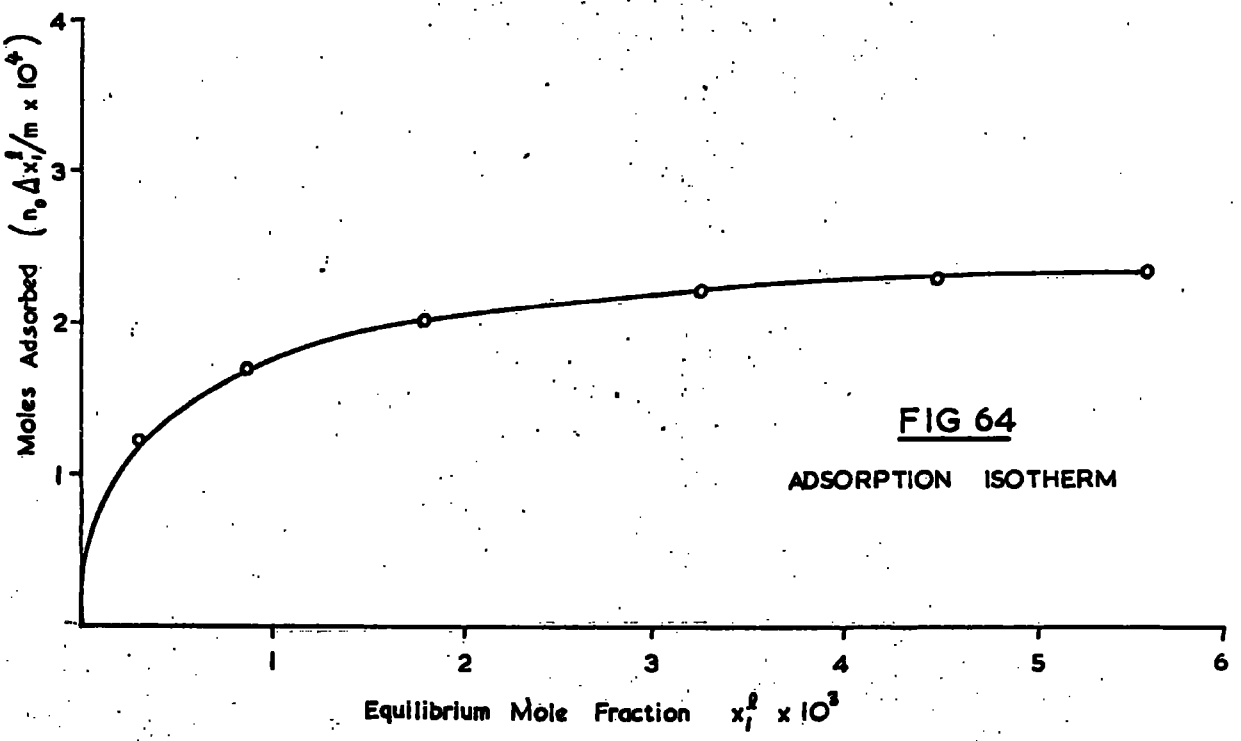

FIG 64

ADSORPTION ISOTHERM

(g) Adsorption of p-Cresol from Tetrahydrofuran

Table (24) : Calibration Curves

1 mm. cell Equation of the line : $y = 9.4830x + 0.006$

Concentration (moles.litre^{-1} x 10^{-2})	6.9581	5.2186	4.3488	3.4790	1.7395
Optical Density	.665	.500	.420	.335	.170

1 cm. cell Equation of the line : $y = 85.357x + 0.007$

Concentration (moles.litre^{-1} x 10^{-3})	6.9581	5.2186	4.3488	3.4790	1.7395
Optical Density	.604	.450	.376	.304	.158

The calibration curves are shown in Fig. 66.

Table (25) : Adsorption Data

Before Adsorption

Stock Solution (ml)	Concentration (moles.litre^{-1} x 10^2)	Moles of Phenol in 50 ml.solution x 10^3	Mole Fraction of Phenol (x_1^0) x 10^3
45	7.8278	3.9139	6.3340
37	6.4362	3.2181	5.2138
28	4.8707	2.4354	3.9507
18	3.1311	1.5656	2.5433
9	1.5656	.7828	1.2733
5	.8698	.4349	7078

Density of tetrahydrofuran at 22.5°C = .8855 g.cm^{-3}

Moles of tetrahydrofuran in 50 ml. = 0.61401

After Adsorption

Mean Optical Density	Concentration (moles.litres^{-1} x 10^2)	Moles of Phenol in 50 ml.solution x 10^3	Mole Fraction of Phenol (x_1^1) x 10^3
.658	6.8754	3.4377	5.5675
.527	5.4940	2.7470	4.4539
.382	3.9650	1.9825	3.2184
.225	2.3093	1.1547	1.8771
.093	0.9174	0.4587	0.7465
.339	0.3890	0.1945	0.3167

$\Delta x_1^1 \times 10^3$	.7664	.7599	.7323	.6662	.5278	.3911
$n_o \Delta x_1^1 / m \times 10^4$	2.3295	2.3072	2.2571	2.0504	1.5854	1.2015
$x_1^1 m / n_o \Delta x_1^1$	23.900	19.304	14.259	9.155	4.708	2.636

Limiting Adsorption Value, $A = 2.324 \times 10^{-4}$ moles per gram of alumina.

The adsorption isotherm (Fig.67) was constructed from the data in Table (25) and the plot of $x_1^1 m / n_o \Delta x_1^1$ against x_1^1 is shown in Fig. 68.

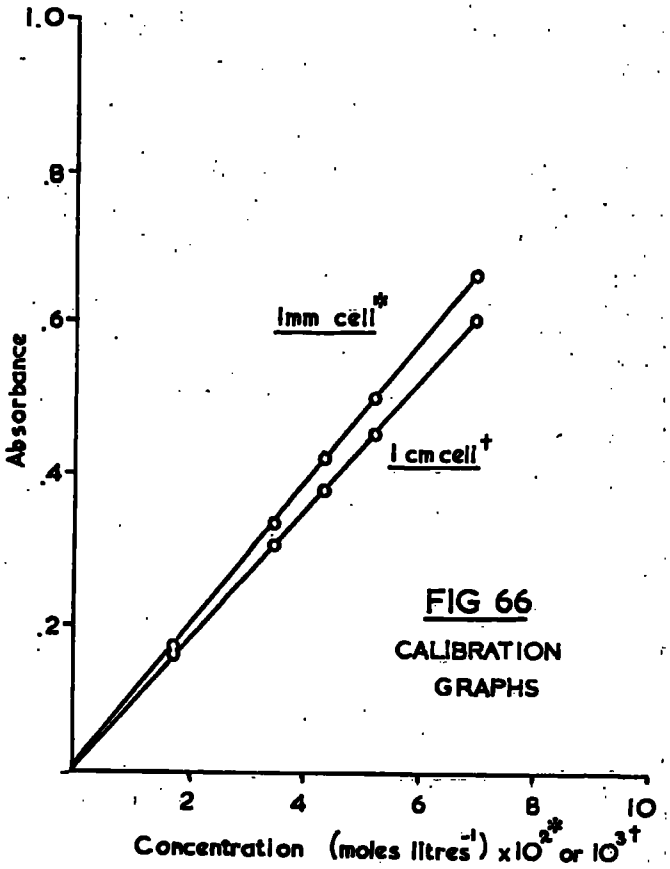

FIG 66
CALIBRATION GRAPHS

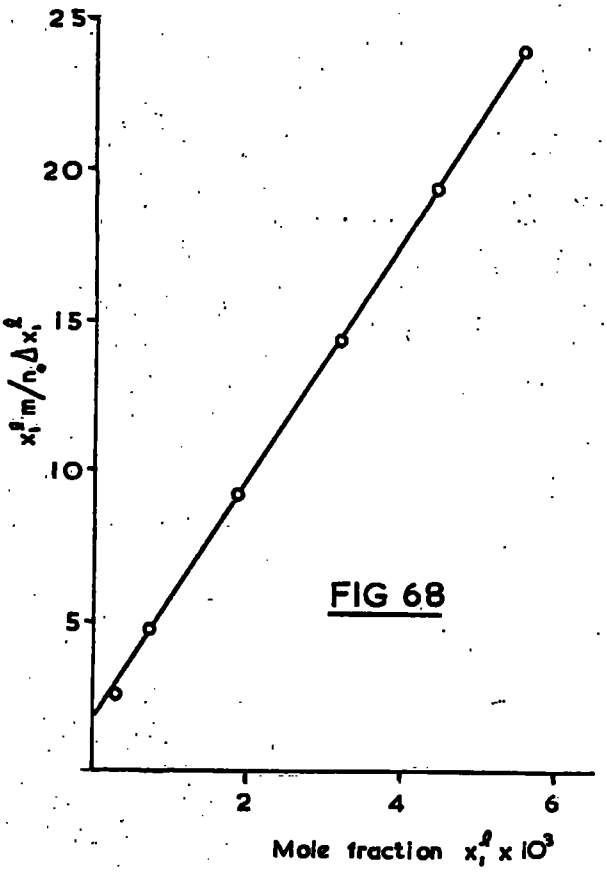

FIG 68

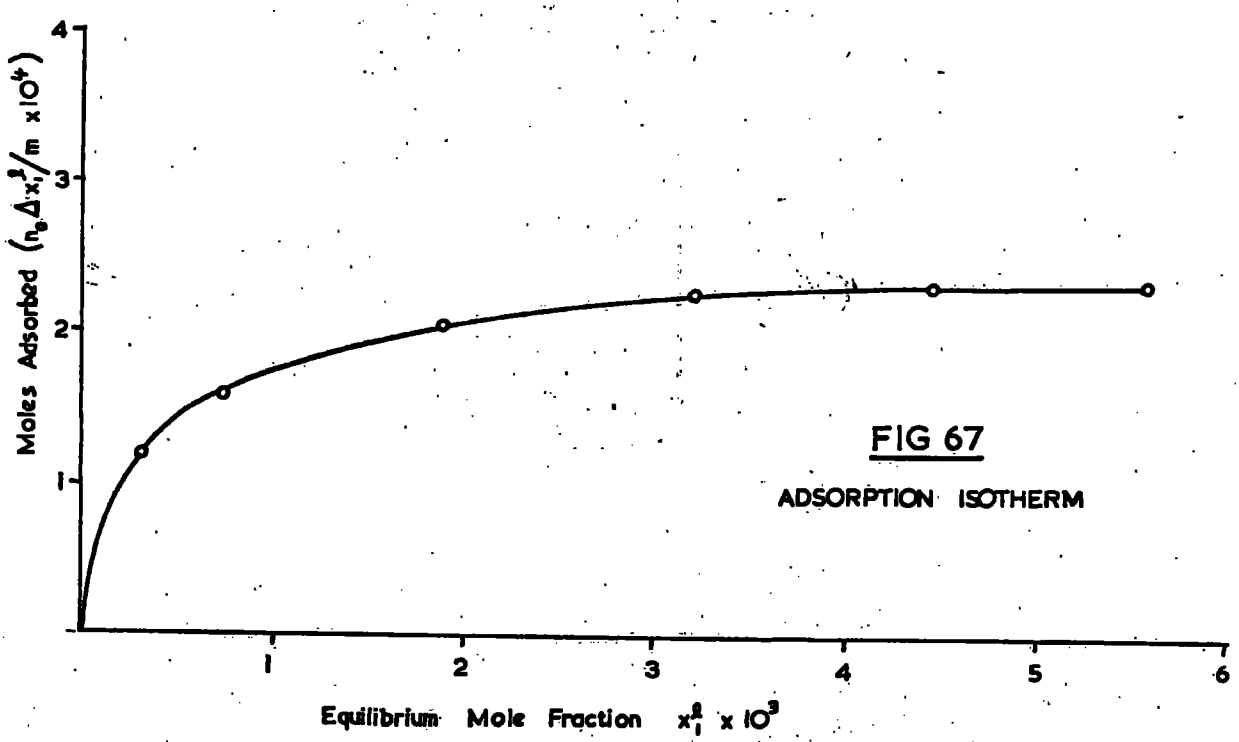

FIG 67
ADSORPTION ISOTHERM

(h) Adsorption of p-Chlorophenol from Tetrahydrofuran

Table (26) : Calibration Curves

1 mm. cell Equation of the line : $y = 9.3892x + 0.005$

Concentration (moles.litre^{-1} x 10^2)	8.6659	6.9327	5.1995	3.4664	1.7332
Optical Density	.819	.655	.492	.330	.168

1 cm. cell Equation of the line : $y = 87.607x + 0.016$

Concentration (moles.litre^{-1} x 10^3)	6.9327	5.1995	4.3330	3.4664	1.7332
Optical Density	.620	.474	.398	.320	.165

The calibration curves are shown in Fig. 69.

Table (27) : Adsorption Data

Before Adsorption

Stock Solution (ml)	Concentration (moles.litre^{-1} x 10^2)	Moles of Phenol in 50 ml.solution x 10^3	Mole Fraction of Phenol (x_1^o) x 10^3
45	7.7993	3.8997	6.3048
37	6.4128	3.2064	5.1897
28	4.8529	2.4265	3.9324
18	3.1197	1.5599	2.5315
9	1.5599	0.7799	1.2673
5	0.8666	0.4333	.7045

Density of tetrahydrofuran at 22°C = .8864 g. cm^{-3}

Moles of tetrahydrofuran in 50 ml. = 0.61463

After Adsorption

Mean Optical Density	Concentration (moles.litres^{-1} x 10^2)	Moles of Phenol in 50 ml.solution x 10^3	Mole Fraction of Phenol (x_1^1) x 10^3
.650	6.8696	3.4348	5.5574
.520	5.4850	2.7425	4.4422
.375	3.9407	1.9704	3.1956
.219	2.2792	1.1396	1.8507
.086	0.8627	0.4314	0.7014
.309	0.3344	0.1672	0.2720

$\Delta x_1^1 \times 10^3$	.7474	.7475	.7368	.6808	.5659	.4325
$n_g \Delta x_1^1/m \times 10^4$	2.3114	2.3092	2.2732	2.0975	1.7413	1.3301
$x_1^1 m/n_o \Delta x_1^1$	24.043	19.237	14.058	8.823	4.028	2.045

Limiting Adsorption Value, A = 2.333×10^{-4} moles per gram of alumina.

The adsorption isotherm (Fig.70) was constructed from the data in Table (27) and the plot of $x_1^1 m/n_o \Delta x_1^1$ against x_1^1 is shown in Fig. 71.

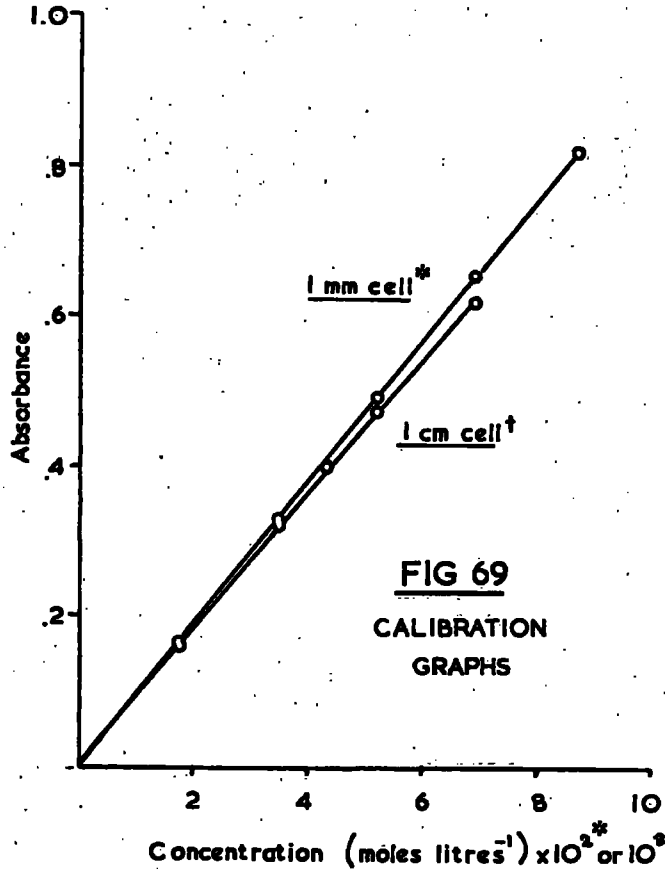

FIG 69

CALIBRATION GRAPHS

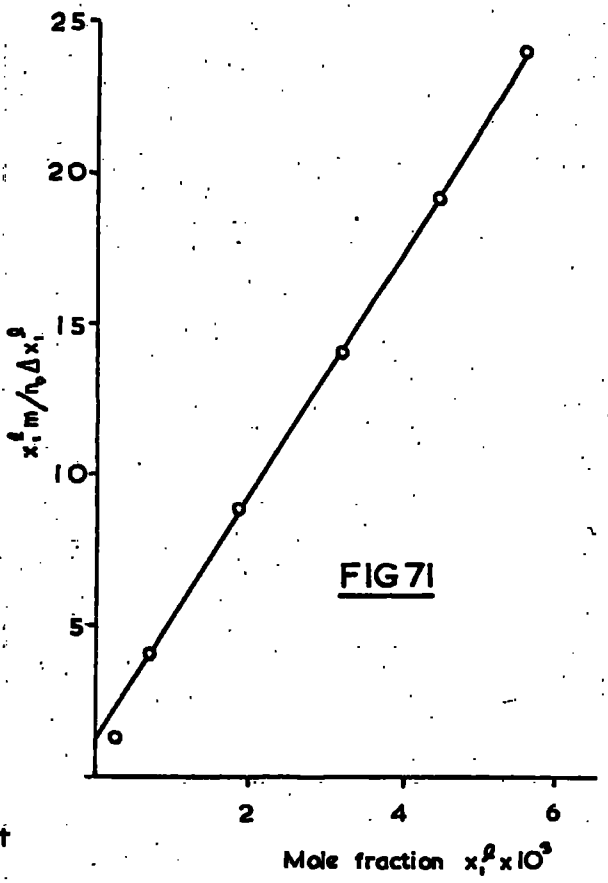

FIG 71

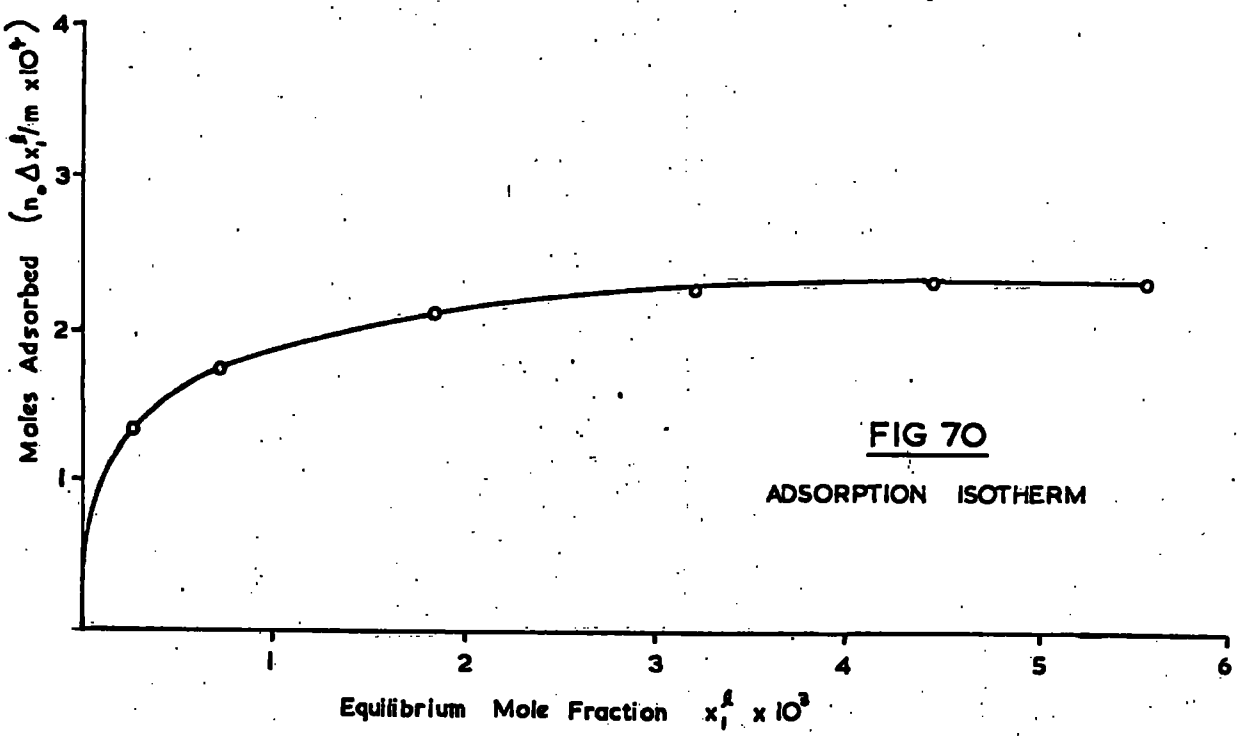

FIG 70

ADSORPTION ISOTHERM

(i) Adsorption of p-Tertiary Butylphenol from Tetrahydrofuran

Table (28) : Calibration Curves

1 mm. cell Equation of the line : $y = 8.3057x + 0.006$

Concentration (moles.litre^{-1} x 10^{2})	6.9542	5.2156	4.3464	3.4771	1.7385
Optical Density	.583	.440	.365	.295	.150

1 cm. cell Equation of the line : $y = 75.695x - 0.022$

Concentration (moles.litre^{-1} x 10^{3})	6.9542	5.2156	4.3464	3.4771	1.7385
Optical Density	.503	.375	.306	.245	.108

The calibration curves are shown in Fig. 72.

Table (29) : Adsorption Data

Before Adsorption

Stock Solution (ml)	Concentration (moles.litre^{-1} x 10^2)	Moles of Phenol in 50 ml.solution x 10^3	Mole Fraction of Phenol (x_1^o) x 10^3
45	7.8234	3.9117	6.3241
37	6.4326	3.2163	5.2056
28	4.8679	2.4340	3.9445
18	3.1294	1.5647	2.5393
9	1.5647	0.7824	1.2713
5	0.8693	0.4346	.7066

Density of tetrahydrofuran at 22°C = .8864 g. cm^{-3}

Moles of tetrahydrofuran in 50 ml. = 0.61463

After Adsorption

Mean Optical Density	Concentration (moles.litres^{-1} x 10^2)	Moles of Phenol in 50 mls.solution x 10^3	Mole Fraction of Phenol (x_1^1) x 10^3
.580	6.9109	3.4555	5.5906
.465	5.5263	2.7632	4.4756
.336	3.9732	1.9866	3.2218
.194	2.2635	1.1318	1.8381
.077	0.8548	0.4274	0.6947
.238	0.3435	0.1717	0.2793

$\Delta x_1^1 \times 10^3$	.7335	.7300	.7227	.7012	.5766	.4273
$n_o \Delta x_1^1/m \times 10^4$	2.2685	2.2552	2.2297	2.1604	1.7742	1.3140
$x_1^1 m/n_o \Delta x_1^1$	24.644	19.846	14.449	8.508	3.916	2.126

Limiting Adsorption Value, A = 2.280×10^{-4} moles per gram of alumina

The adsorption isotherm (Fig.73) was constructed from the data in Table (29) and the plot of $x_1^1 m/n_o \Delta x_1^1$ against x_1^1 is shown in Fig. 74.

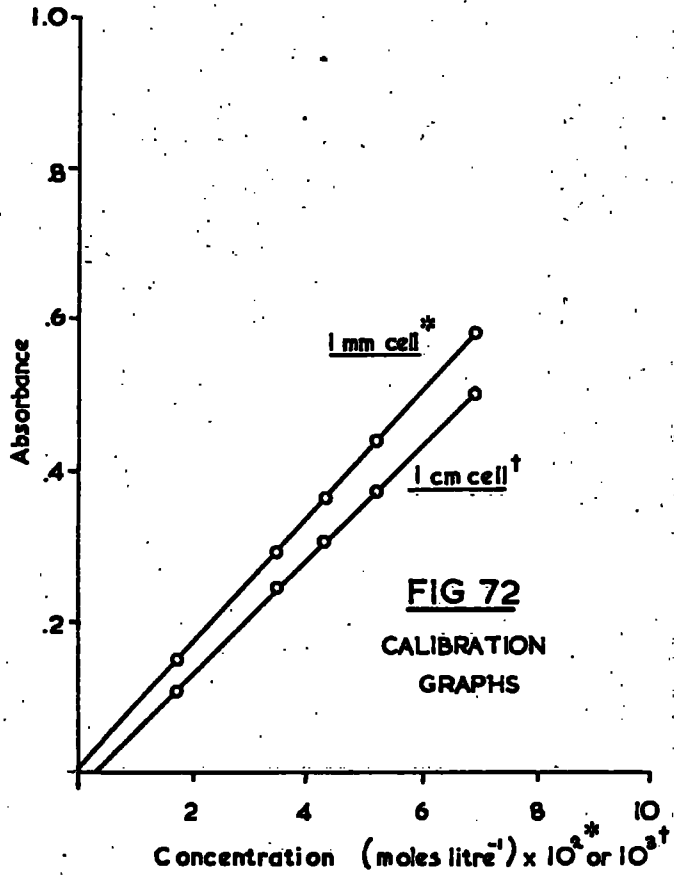

FIG 72

CALIBRATION GRAPHS

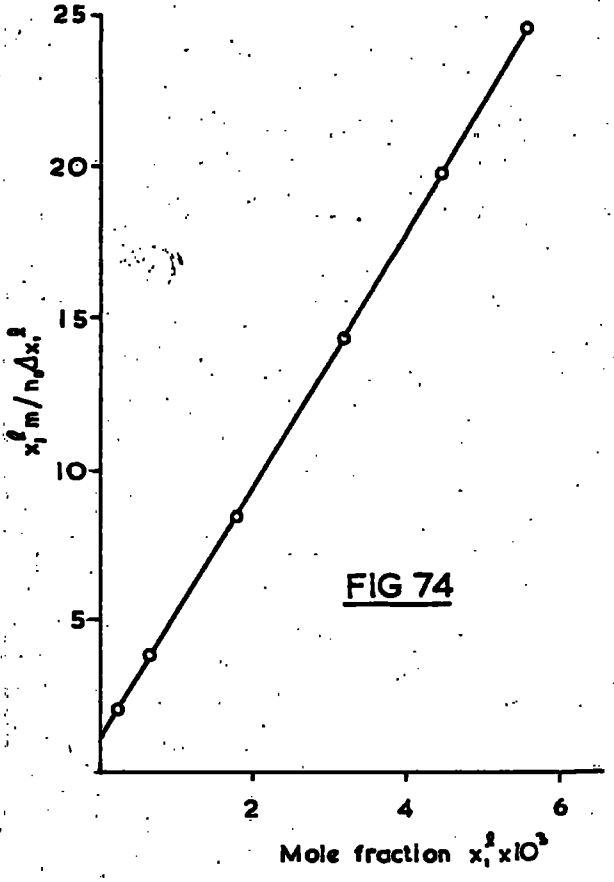

FIG 74

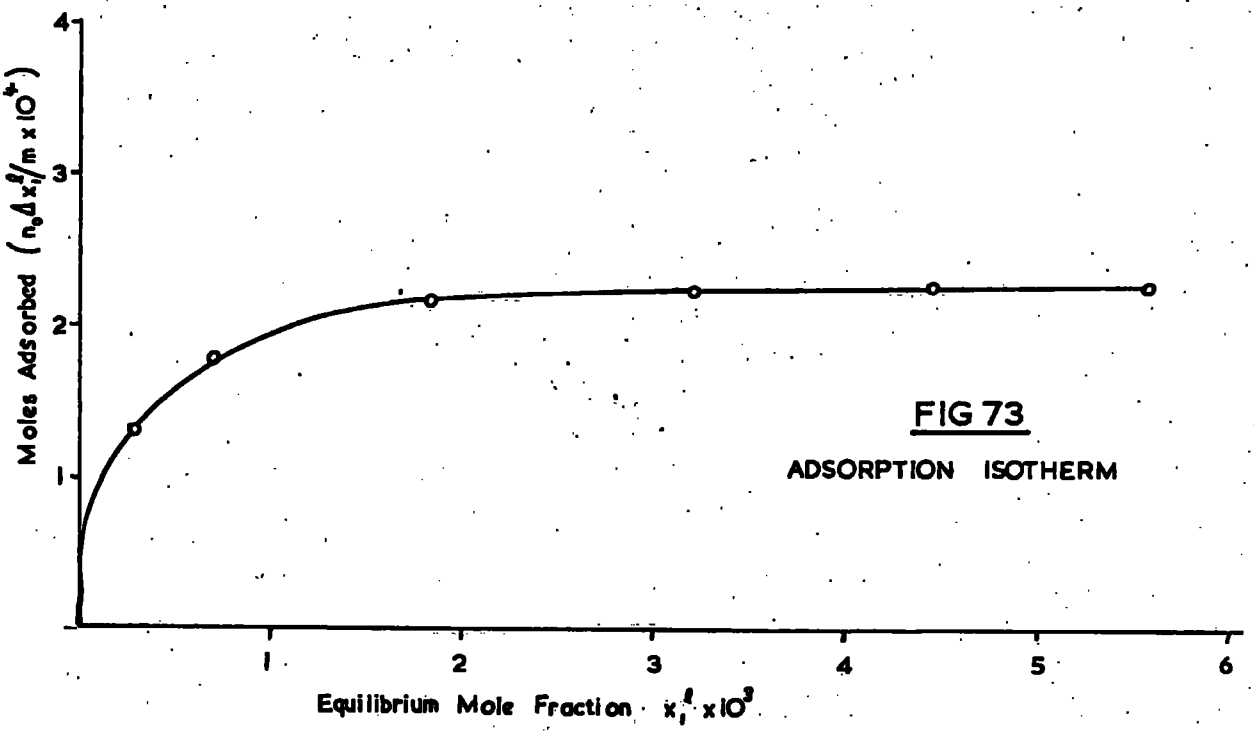

FIG 73

ADSORPTION ISOTHERM

(j) Adsorption of p-Nitrophenol from Tetrahydrofuran

Table (30) : Calibration Curves

1 mm. cell Equation of the line : $y = 9.4701x + 0.001$

Concentration (moles.litre^{-1} x 10^{2})	6.9745	5.2309	4.3591	3.4872	1.7436
Optical Density	.660	.500	.415	.328	.167

1 cm. cell Equation of the line : $y = 86.901x - 0.005$

Concentration (moles.litre^{-1} x 10^{3})	6.9745	5.2309	4.3591	3.4872	1.7436
Optical Density	.601	.447	.375	.300	.145

The calibration curves are shown in Fig. 75.

Table (31) : Adsorption Data

Before Adsorption

Stock Solution (ml)	Concentration (moles.litre^{-1} x 10^2)	Moles of Phenol in 50 ml. solution x 10^3	Mole Fraction of Phenol (x_1^o) x 10^3
45	7.8463	3.9232	6.3426
37	6.4514	3.2257	5.2208
28	4.8821	2.4411	3.9560
18	3.1385	1.5693	2.5467
9	1.5693	.7847	1.2751
5	0.8718	.4359	.7087

Density of tetrahydrofuran at 22°C = .8864 g. cm^{-3}

Moles of tetrahydrofuran in 50 ml. = 0.61463

After Adsorption

Mean Optical Density	Concentration (moles.litres^{-1} x 10^2)	Moles of Phenol in 50 ml. solution x 10^3	Mole Fraction of Phenol (x_1^1) x 10^3
.651	6.8637	3.4319	5.5527
.520	5.4804	2.7402	4.4385
.372	3.9176	1.9588	3.1768
.214	2.2492	1.1246	1.8264
.081	0.8448	0.4224	0.6866
.283	0.3314	0.1657	0.2695

$\Delta x_1^1 \times 10^3$	.7899	.7823	.7792	.7203	.5885	.4392
$n_o \Delta x_1^1 / m \times 10^4$	2.4430	2.4167	2.4041	2.2192	1.8110	1.3511
$x_1^1 m / n_o \Delta x_1^1$	22.729	18.366	13.214	8.230	3.791	1.995

Limiting Adsorption Value, A = 2.456×10^{-4} moles per gram of alumina

The adsorption isotherm (Fig.76) was constructed from the data in Table (31) and the plot of $x_1^1 m / n_o \Delta x_1^1$ against x_1^1 is shown in Fig. 77.

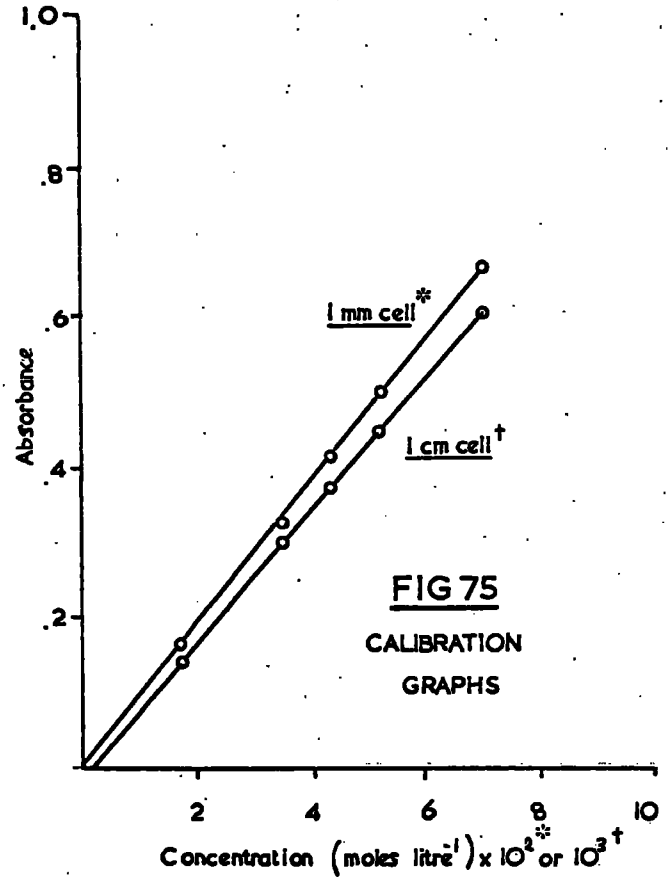

FIG 75

CALIBRATION GRAPHS

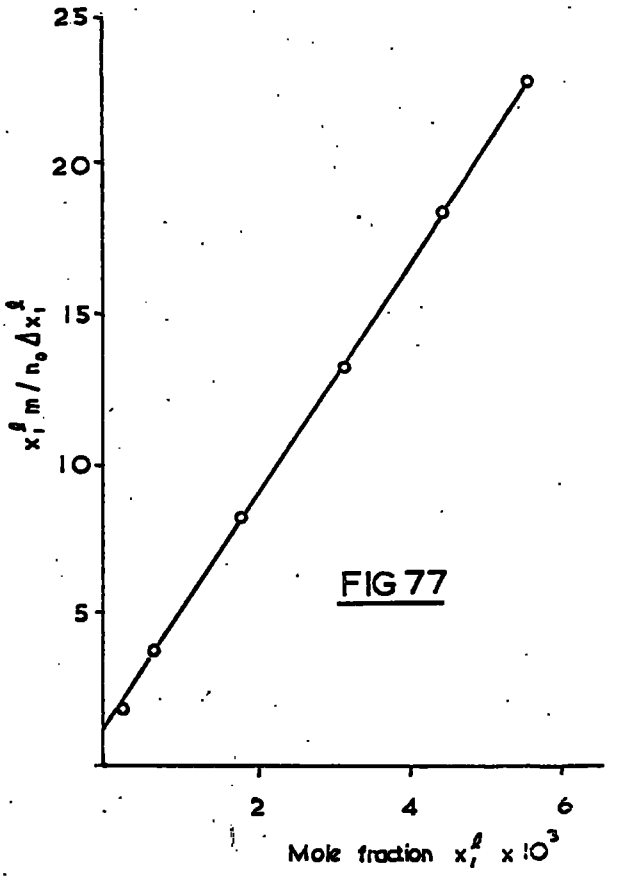

FIG 77

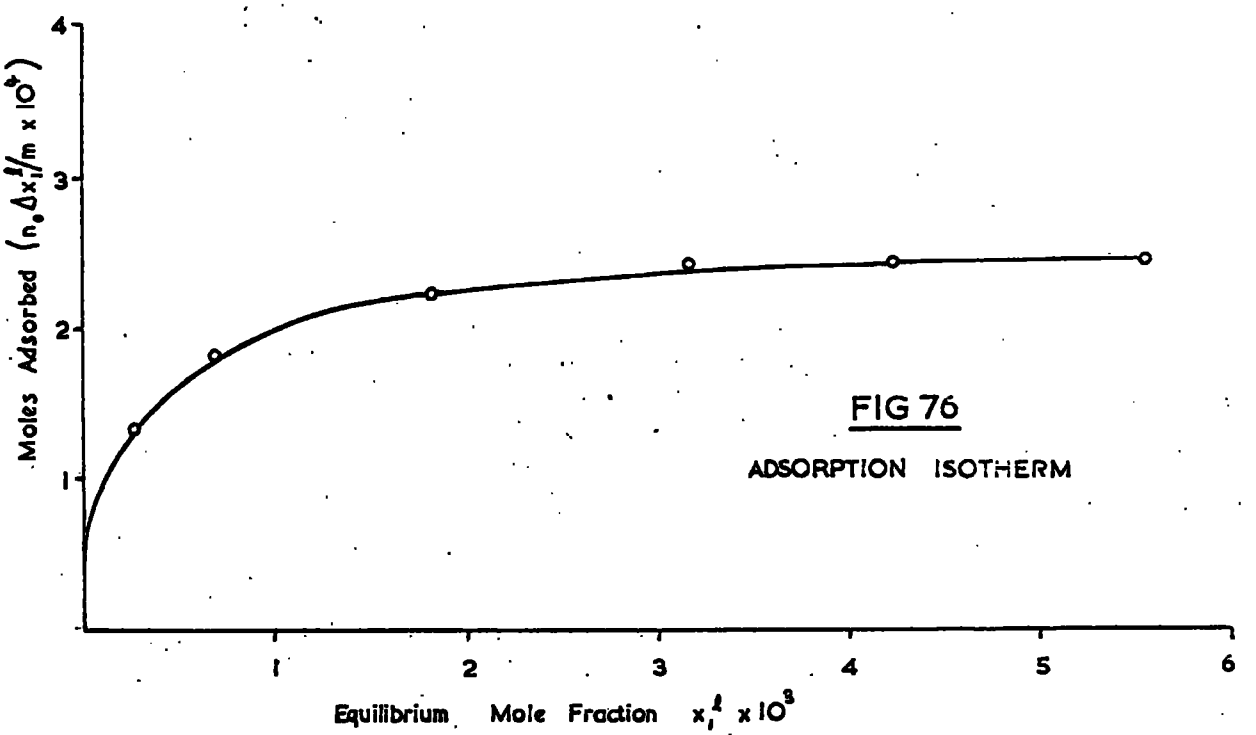

FIG 76

ADSORPTION ISOTHERM

DISCUSSION

In the discussion to this thesis, attention is concentrated on:-

(1) elucidating the mechanism of adsorption of the p-substituted phenols at the alumina-solution interface and predicting the orientation of the adsorbed molecules.

(2) assessing the influence of the solvent on adsorptive capacity.

(3) ascertaining any correlation which may exist between adsorptive affinity and structure of the adsorptive.

1. Mechanism of Adsorption and Orientation at the Interface

In order to elucidate the adsorption mechanism at the interface, it is important to characterise the alumina surface by determining its surface area and pore size distribution and to be reasonably certain of its chemical constitution. In this latter connection, results of dehydration experiments have proved useful.

(a) The Alumina Surface

(i) Surface Area Measurements

Characterisation of the alumina surface has been attempted by carrying out low temperature nitrogen adsorption experiments. Application of the B.E.T. equation to the adsorption isotherm gives a value of 131(1) $m^2 g^{-1}$ for the surface area of the alumina sample. From the relationship between the thickness of the adsorbed nitrogen layer and the volume of gas adsorbed at increasing relative pressures (t-curves P76) the existence of pores in the alumina is confirmed.

From the initial slope of the t-curve, it is estimated that the pore surface area is approximately 125.7 m^2g^{-1}. This value is very close to the surface area calculated from the B.E.T. equation. A pore size distribution analysis of the desorption branch of the isotherm shows that the diameter of the majority of the pores are in the range 20-35Å. This analysis is based on the assumption that the pores are predominantly slit-shaped[70], evidence for this assumption being provided by electron microscopy (P 156) and the conclusions of other workers.

As the adsorption experiments in this investigation have been carried out from the solution phase, the surface area of the alumina was determined by a solution adsorption method. Adsorption of lauric acid from n-pentane solution[77] gives a value of 95.3 m^2g^{-1} for the surface area of the alumina sample. This is lower than the B.E.T. surface area and could be explained if the alumina had a surface similar to that of an aluminium hydroxide. In this case, the surface area of the alumina as assessed by lauric acid adsorption would be 136.5 m^2g^{-1} (using the factor of 232 determined by De Boer P.98) and this value is reasonably close to the B.E.T. surface area. Alternatively the difference between the two surface area values of 131.1 m^2g^{-1} and 95.3 m^2g^{-1} could be explained by the difference in size of the adsorptive molecules used in their determination. Thus a narrowing of some of the pores at their lower extremities (e.g. as in wedge-shaped pores) would tend to exclude the lauric acid molecule

(a)

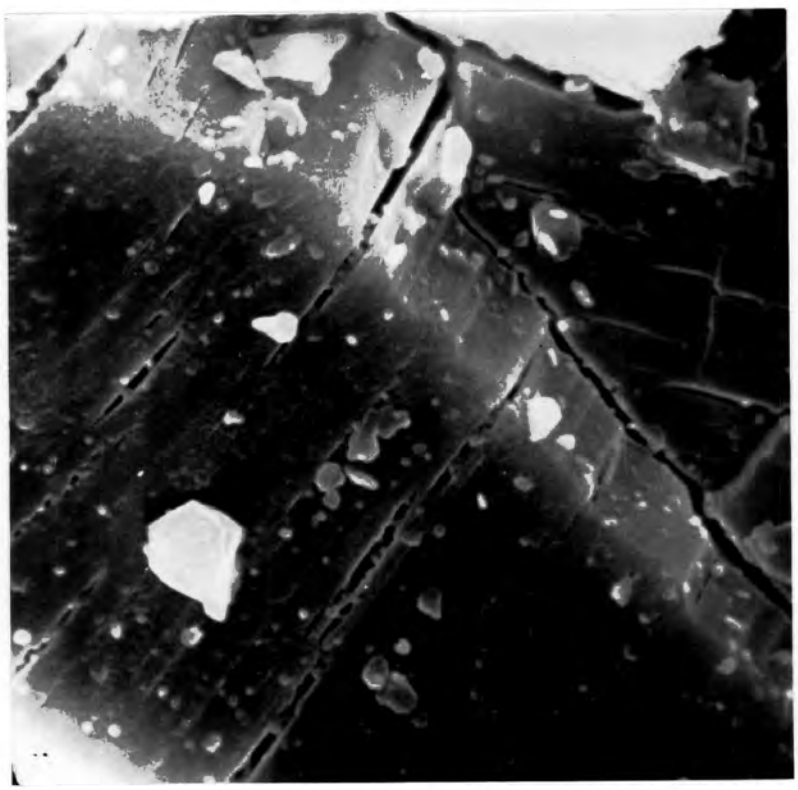

(b)

ELECTRON MICROGRAPHS OF ALUMINA UNDER INVESTIGATION

MAGNIFICATION (a) 2100X (b) 5250X

from part of the surface accessible to the smaller nitrogen molecule. This effect would also explain the surface area value of 104.7 m^2g^{-1} [82] obtained from vapour phase adsorption of benzene and calculated on the assumption of an area requirement of 41$Å^2$ [83] for the benzene molecule adsorbed parallel to the surface.

It is concluded that the surface area of the alumina sample accessible to single-ring aromatic compounds is in the region of 100 m^2g^{-1}.

(ii) Nature of the Surface

X-ray powder diffraction has shown that the alumina is mainly of the γ-form. All aluminas obtained between the decomposition temperature of the hydroxides and 1000°C have structures based on a nearly close-packed cubic oxygen sub-lattice and are closely related to that of spinel-type γ-alumina. It can therefore be assumed that the surface of the alumina is formed by planes with more or less simple indices of this oxygen sub-lattice. The evidence in the literature for preferential exposure of a particular crystal face is contradicting and unconvincing. Peri,[78] from water vapour adsorption studies, favours preferential exposure of the 100 planes of the crystal lattice. De Boer[77] considers that at higher temperatures where appreciable sintering has occurred, the most stable plane (i.e. the octahedral plane of the cubic oxygen lattice) will be the most abundant plane in the surface. Whether or not preferential exposure of a particular

crystal plane occurs, a completely dehydrated alumina surface consists mainly of oxide ions.

Infra-red[79] and gravimetric studies[78] show that water is rapidly chemisorbed on the surface of alumina to form hydroxide groups. Thus the surface of an alumina sample left exposed to the atmosphere will consist basically of hydroxyl groups rather than oxide ions. V. Vallance[82] has determined the percentage loss on ignition of the alumina under investigation at various temperatures for 48 hours. The results are recorded in Table (32).

Table (32)

Percentage Loss on Ignition of the Alumina at Various Temperatures

Temperature °C	Percentage Loss on Ignition
120	3.0
300	4.2
380	5.2
500	5.3
>800	6.8

It can be seen from Table (32) that increasing the temperatures produces a gradual dehydration of the alumina. According to Peri, the hydrated surface of γ-alumina retains 13.0 molecules of water per 100Å^2 of surface after evacuation at 25°C for 100 hours and even after drying at 120°C, the surface may still retain 8.25 molecules per 100Å^2. Although much of the water is held as

hydroxyl groups on the surface, infra-red studies have shown that some of the water strongly adsorbed at 25°C, remains molecular.

Assuming the alumina sample under investigation contains 10% α-monohydrate, then 1.5% of the water content at room temperature will be waters of crystallisation. As the percentage loss of water remains approximately constant between 380 and 500°C and dehydration of α-monohydrate occurs in the region of 500°C, the subsequent loss on heating to 800°C can be attributed to loss of waters of crystallisation i.e. (6.8-5.3) = 1.5%. If the extent of dehydration on heating to a temperature in excess of 800°C is representative of the total water content of the alumina (i.e. 6.8%) then the adsorbed water content of the sample can be deduced at various temperatures and from the surface area value of 131.1 $m^2 g^{-1}$ for the alumina sample, the number of water molecules per 100$Å^2$ of surface can be calculated. The results are recorded in Table (33)

Table (33)

Number of Water Molecules Adsorbed per 100$Å^2$ of the Alumina Surface at Various Temperatures

Temperature °C	Adsorbed Water %	No. of Water Molecules per 100$Å^2$
Ambient	5.3	13.4
120	2.3	5.8
300	1.1	2.8
380	0.1	0.3
500	-	-
800	-	-

According to Peri,[78] a water molecule occupies 16$\mathring{A}^2$ on the surface of alumina so that monolayer coverage corresponds to 6.25 molecules of water per 100$\mathring{A}^2$. It can be seen from Table (33) that at 120°C the number of water molecules is close to the value for monolayer coverage and it may be concluded that at this temperature the surface of the alumina sample is fully hydroxylated.

(b) Adsorption Mechanism and Molecular Orientation at the Interface

Having established the nature of the alumina sample, its surface area accessible to single ring aromatic molecules and the pore size distribution, it now becomes possible to speculate on the mechanism of adsorption and the molecular orientation at the interface.

The experimental adsorption saturation values of a series of p-substituted phenols from cyclohexane are tabulated below. Assuming an available surface area of 100 $m^2 g^{-1}$, molecular area requirements can be calculated and are recorded in Table (34).

Table (34)

Limiting Adsorption and Molecular Area Requirements of the p-substituted Phenols on the Alumina Surface when Adsorbed from Cyclohexane Solution.

Adsorptive	Limiting Adsorption (mmoles. g^{-1})	Molecular Area Requirement $(\text{Å})^2$
Phenol	0.678	24.5
p-Cresol	0.676	24.6
p-Chlorophenol	0.673	24.7
p-Bromophenol	0.678	24.5
p-t-Butylphenol	0.438	37.8

Since cyclohexane is one of the least interacting solvents (as illustrated by the vapour phase adsorption experiment p. 101) it is considered that the solvent molecules are excluded from the adsorbed phase at limiting adsorption. The molecular area requirements quoted therefore enable a prediction to be made as to the orientation of the molecules in the adsorbed phase.

The calculated area requirement of phenol indicates that the molecule adopts a perpendicular orientation on the alumina surface. Comparison with Adam's[84] value of 24 Å^2 for the cross-sectional area of an aromatic molecule in a thin film on water also suggests that the phenol covers the adsorbent surface with an almost complete monolayer. Variation in size of the p-substituent does not affect the area requirement until the large t-butyl group is

present when the area requirement per molecule shows an appreciable increase.

Various workers[25][26][85][86] have concluded that many non-ionic solutes are predominantly adsorbed onto the alumina surface by hydrogen-bonding. As evidence of this investigation points to perpendicular orientation of the phenols on an alumina surface saturated with hydroxyl groups, it is reasonable to conclude that the mechanism of adsorption is predominantly hydrogen-bonding.

2. The Influence of the Solvent on Adsorptive Capacity

The experimentally determined adsorption values and molecular area requirements for the p-substituted phenols when adsorbed from cyclohexane, tetrahydrofuran, and dioxan[87] are given in Table (35)

Table (35)

Limiting Adsorption and Molecular Area Requirements of $4\text{-}XC_6H_4OH$ on Alumina from Solution in Cyclohexane, Tetrahydrofuran and Dioxan

Adsorptive X =	-H	-Cl	$-CH_3$	-Br	$-C(CH_3)_3$	$-NO_2$
1. Limiting Adsorption ($mmoles.g^{-1}$)						
(i) Cyclohexane	.678	.673	.676	.678	.438	-
(ii) Tetrahydrofuran	.241	.233	.233	-	.228	.246
(iii) Dioxan	.168	.164	.157	-	.145	.213
2. Molecular Area Requirement ($\AA^2$)						
(i) Cyclohexane	24.5	24.7	24.6	24.5	37.8	-
(ii) Tetrahydrofuran	68.8	71.2	71.2	-	72.8	67.5
(iii) Dioxan	98.9	101.2	105.8	-	114.6	78.4

The adsorptive capacity of the alumina surface for the phenol molecules is seen to vary according to the solvent used. This can be attributed to the ability of the solvent molecules to effectively compete with the phenol molecules for the surface.

The importance of solvent adsorption by the alumina surface is illustrated on resolving the composite isotherms for the phenol-cyclohexane (Fig.78), - tetrahydrofuran (Fig.79), - dioxan (Fig.80) systems into their individual isotherms using equations (1) and (3) discussed in the 'Introduction'.

The values of $(n_1^s)_m$ and $(n_2^s)_m$ used for resolving the composite isotherms are listed below:-

$(n_1^s)_m$ for phenol (0.678×10^{-3}) is the adsorption saturation value for adsorption from cyclohexane solution, it being assumed that solvent molecules are excluded from the monomolecular layer.

$(n_2^s)_m$ for cyclohexane (0.426×10^{-3}) is calculated from an area requirement of 39 $Å^2$ (83) for a molecule of cyclohexane assuming an available surface area of $100 m^2 g^{-1}$.

$(n_2^s)_m$ for tetrahydrofuran (0.400×10^{-3}) is calculated from a molecular area requirement of 41.6 $Å^2$, determined by vapour phase adsorption, assuming an available surface area of $100 m^2 g^{-1}$.

$(n_2^s)_m$ for dioxan (0.400×10^{-3}) is calculated from a molecular area requirement of 41.6 $Å^2$, (88) determined by vapour phase adsorption, assuming an available surface area of $100 m^2 g^{-1}$.

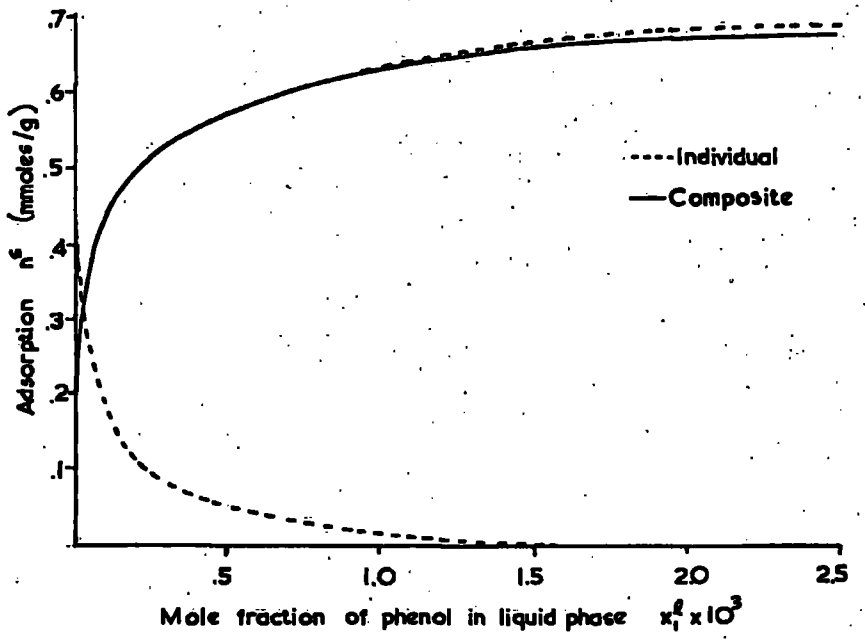

FIG 78

PHENOL–
CYCLOHEXANE

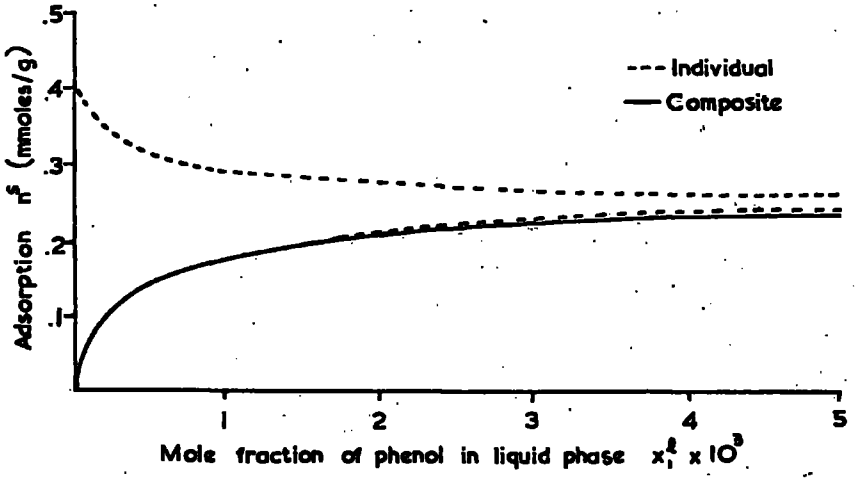

FIG 79

PHENOL –
TETRAHYDROFURAN

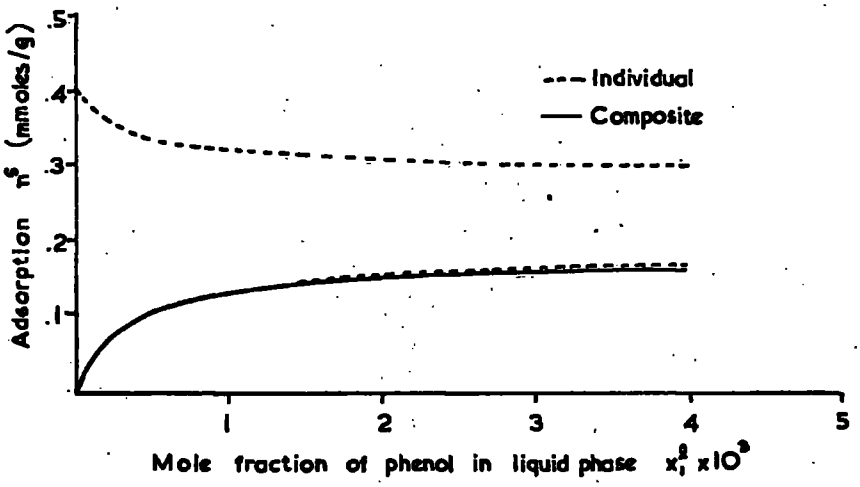

FIG 80

PHENOL–
DIOXAN

In the case of phenolic solutions of dioxan, B.J. Hawley[87] concluded that, at limiting adsorption, the adsorbed phase consisted of two dioxan molecules per phenol molecule; the molecules being bonded separately to the adsorbent surface. When adsorbed from tetrahydrofuran solution, the area requirement of phenol on the surface is 68.8 $\AA^2$ which is very close to the sum of the area requirements of a phenol molecule (24.5 $\AA^2$) and a tetrahydrofuran molecule (41.6 $\AA^2$). Thus, at limiting adsorption, the adsorbed phase would appear to consist of approximately equal numbers of phenol and tetrahydrofuran molecules.

The proportion of solvent to solute molecules present in the adsorbed phase indicates that dioxan is more strongly adsorbed by the alumina surface than tetrahydrofuran. The mechanism of adsorption of the solvent molecules may again be hydrogen-bonding as dioxan would be expected to form stronger bonds with the surface than tetrahydrofuran. (Association constant K_H phenol-dioxan at (25°C) 15.21; (35°C) 10.79[87] $l.mole^{-1}$; K_H phenol-tetrahydrofuran at (29°C) 10.4[89] $l.mole^{-1}$). Whereas parallel orientation of dioxan to the surface is likely because of its two polar end groups, the tetrahydrofuran molecule may be expected to have an orientation similar to phenol with its oxygen atom hydrogen-bonded to the alumina surface. Construction of the model of the tetrahydrofuran molecule illustrates that the surface area requirement of the molecule is almost the same whether perpendicular or parallel orientation at the adsorbent surface occurs.

In conclusion, the adsorptive capacity of the alumina surface for the solute molecules is seen to be dependent upon the nature of the solvent used. Solvents capable of competing with the solute molecules for the adsorbent surface will reduce the adsorptive capacity by an amount which reflects the degree of interaction of the solvent with the surface.

3. Adsorptive Affinity and Structure of the Adsorptive

(a) Introduction

One of the most widely used relationships in attempting to correlate structure and reactivity is the Hammett equation (38).[90][91]

$$\log \left\{ \frac{K}{K_o} \right\} = \sigma . \rho \qquad (38)$$

where K, K_o are equilibrium or rate constants of substituted and unsubstituted benzene derivatives, respectively.

σ is a substituent constant varying with the nature and position of the substituent.

ρ is a reaction constant varying with the type of reaction, the physical conditions under which it takes place and the nature of the side-chain.

As far as hydrogen-bonding interactions in solution are concerned, a number of workers[92][93] have shown the existence of a Hammett-type relationship between σ and the association constant K.

Hawley[87] considered the process:-

Substituted Phenol + Dioxan $\rightleftharpoons$ Complex

and evaluated the association constants for a series of p-substituted phenols (Table (36)).

Table (36)

Association Constants K_H for a Series of p-substituted Phenols in Dioxan Solution

Adsorptive	Association Constant K_H (litre.mole^{-1}) at 25°C	Association Constant K_H (litre.mole^{-1}) at 35°C	pK_H 25°C	pK_H 35°C	Substituent Constant[94] σ (normal)
Phenol	15.21	10.79	-1.182	-1.033	0
p-Cresol	10.94	8.81	-1.039	-0.945	-0.170
p-Chlorophenol	24.43	18.28	-1.388	-1.262	+0.227
p-t-Butylphenol	10.42	8.50	-1.018	-0.929	-0.197
p-Nitrophenol	66.83	49.00	-1.825	-1.690	+0.778

[87]

At both temperatures, the values of K_H are seen to reflect the effect of the p-substituent on the hydrogen-bonding tendency of the hydroxyl group of the phenol Fig.(81).

If the adsorption process at the alumina surface is considered analogous to hydrogen-bonding association in solution, then it becomes of interest to attemp correlation of the Hammett substituent constant 'σ' with some defined 'index of adsorption'.

(b) An Index of Adsorption

In theory, the process of adsorption from solution onto a solid is essentially one of phase change as the accessible surface is at all times completely covered by solute and solvent molecules.

Describing adsorption equilibrium at the solid-solution interface as:-

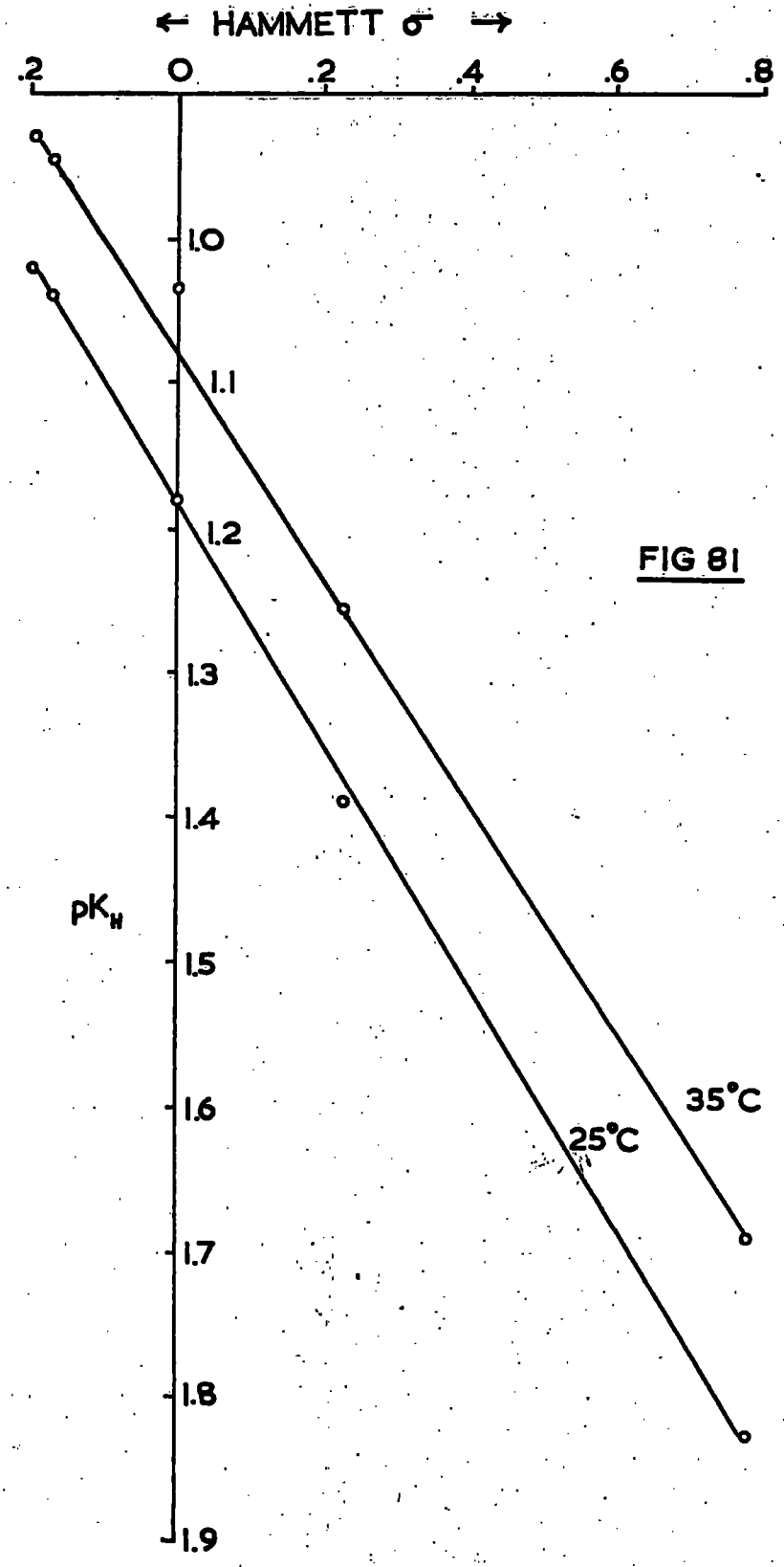

FIG 81

$$(1)^s + (2)^1 \rightleftharpoons (1)^1 + (2)^s$$

where the superscripts 1, s refer to the liquid and adsorbed phases respectively.

Everett,[8] on the basis of an ideal adsorption model, derived, from thermodynamic arguments, the equation for dilute solution as

$$\frac{mx_1^1}{(n_o \Delta x_1^1)} = \frac{1}{Kn^s} + \frac{x_1^1}{n^s} \qquad \text{(P.13)}$$

where $(n_o \Delta x_1^1/m)$ represents 'adsorption' as measured experimentally

x_1^1, x_2^1 are the mole fractions of components 1 and 2 respectively in the liquid phase at equilibrium.

n^s is the total number of moles which can be accommodated in the adsorbed phase by unit weight of solid adsorbent

and $K = \frac{x_1^s x_2^1}{x_1^1 x_2^s}$ where x_1^s, x_2^s; x_1^1, x_2^1 are the mole fractions of components 1 and 2 on the solid and in solution, respectively.

Although it is noted that good straight lines are obtained if the experimental adsorption data ~~is~~ are plotted as above (P.116, 120, 124, 128, 132, 136, 140, 144, 148, 152), the adsorption systems cannot be considered to conform to Everett's perfect model and the author considers that it is unjustifiable to attribute the same significance to the slope and intercept as proposed by Everett.

In the adsorption systems studied by the author, deviations from ideality arise, in consequence of:-

(i) strong hydrogen-bonding between solute and solvent molecules in the solution.

(ii) interaction between solute and solvent molecules in the adsorbed phase.

(iii) differing area requirements of adsorptive molecules so that the number of moles in the adsorbed phase will not remain constant.

Defining an arbitrary "index of adsorption" K_A as the "number of moles of adsorptive present in the adsorbed phase at constant equilibrium mole fraction in the mobile phase", and plotting K_A against the Hammett substituent parameter σ, for a series of a constant values of x_1^1, relationships obtained are as shown in Figs. 82 and 83.

At low equilibrium mole fractions, the fluctuations which occur are attributed to experimental uncertainty and/or to the alumina surface possessing some degree of heterogeneity. The relationship is seen to deviate from linearity again at higher equilibrium mole fractions where the adsorbed phase approaches monolayer formation. This can be attributed to such close packing of the molecules in the adsorbed layer that lateral interactions between the adsorbed molecules become significant.

It is not unreasonable, therefore, to select for overall comparison, a value for the constant equilibrium mole fraction in

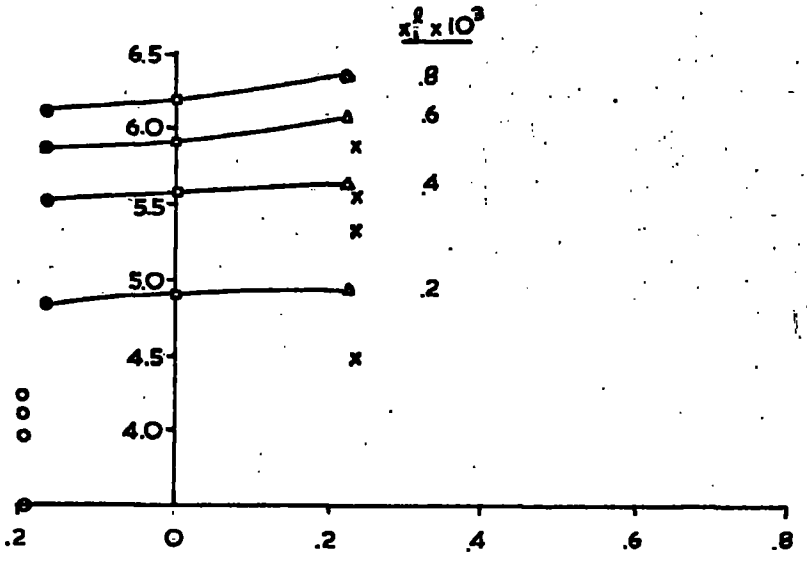

FIG 82

p-SUBSTITUTED PHENOLS — CYCLOHEXANE

o – $C(CH_3)_3$
● – CH_3
□ – H
△ – Cl
× – Br

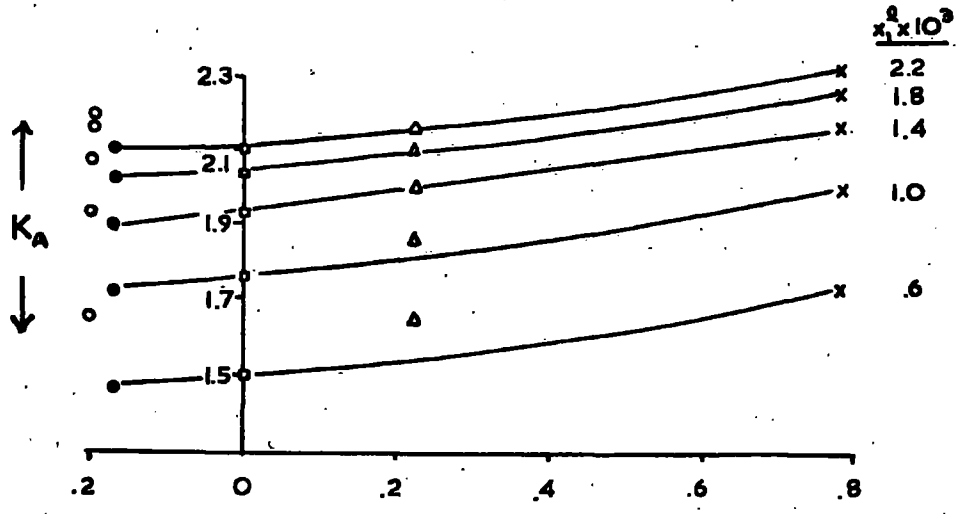

FIG 83

p-SUBSTITUTED PHENOLS — TETRAHYDROFURAN

o – $C(CH_3)_3$
● – CH_3
□ – H
△ – Cl
× – NO_2

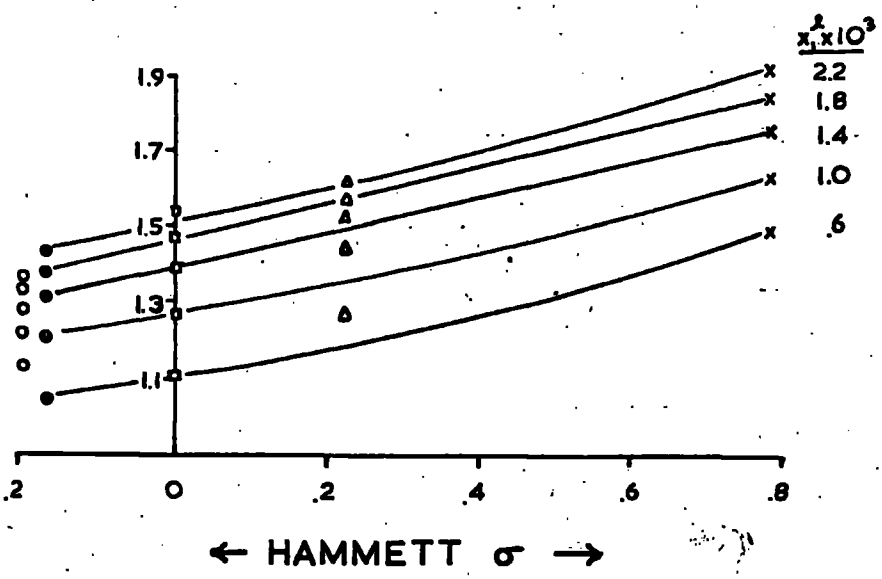

FIG 84

p-SUBSTITUTED PHENOLS — DIOXAN

o – $C(CH_3)_3$
● – CH_3
□ – H
△ – Cl
× – NO_2

the liquid phase which lies intermediate between the two extremes discussed above. Consideration of Figs. 82 and 83 shows that a suitable value for the phenol-cyclohexane system is $x_1^1 = 0.4 \times 10^{-3}$, and for the phenol-tetrahydrofuran system $x_1^1 = 1.4 \times 10^{-3}$. The results obtained by B.J. Hawley[87] for the phenol-dioxan system can also be expressed as above, (Fig.84), from which a value of $x_1^1 = 1.8 \times 10^{-3}$ is an appropriate selection.

The K_A values of the adsorptives for the alumina surface when adsorbed from cyclohexane, tetrahydrofuran, and dioxan are given in Table (38). As the Hammett substituent constant is a parameter in a logarithmic relationship, it is thought more suitable to express the relationship between the substituent constant and pK_A.

Table (38)

Correlation of Hammett, Sigma and an 'Index of Adsorption' K_A

	Adsorptive	Phenol	p-Cresol	p-Chloro-	p-Bromo-	p-t-Butyl-	p-Nitro-
1.	Hammett (σ) (normal)	0	-0.170	+0.227	+0.232	-0.197	+0.778
2.	Cyclohexane						
	$K_A \times 10^4$	5.58	5.53	5.64	5.33	3.91	-
	pK_A	3.253	3.257	3.249	3.273	3.408	-
3.	Tetrahydrofuran						
	$K_A \times 10^4$	1.93	1.90	2.00	-	2.07	2.16
	pK_A	3.714	3.721	3.699	-	3.684	3.666
4.	Dioxan						
	$K_A \times 10^4$	1.47	1.38	1.58	-	1.33	1.85
	pK_A	3.833	3.860	3.801	-	3.876	3.733

On plotting pK_A against the Hammett parameter σ, a linear relationship is obtained for the three systems considered Figs. 85, 86, 87, the adsorptives p-t-butylphenol and p-bromophenol proving exceptions.

When considering the adsorption of these two compounds from cyclohexane, the size of the substituent group may be predominantly responsible for the low values of K_A, since cyclohexane is not so strongly adsorbed (see Fig. 78). In the case of solutions of tetrahydrofuran and dioxan, the solvent is appreciably adsorbed at the highest equilibrium concentrations of phenol (see Figs. 79, 80) and hence the size of the p-substituent is unlikely to be so important

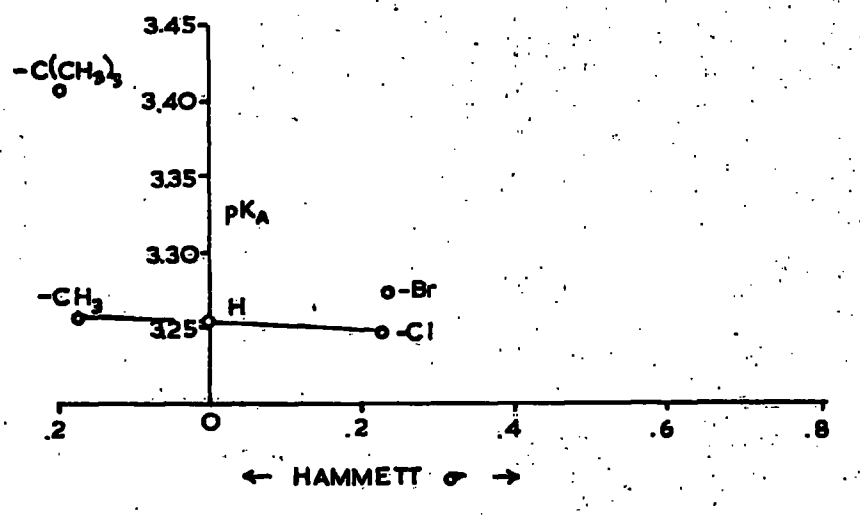

FIG 85

CYCLOHEXANE

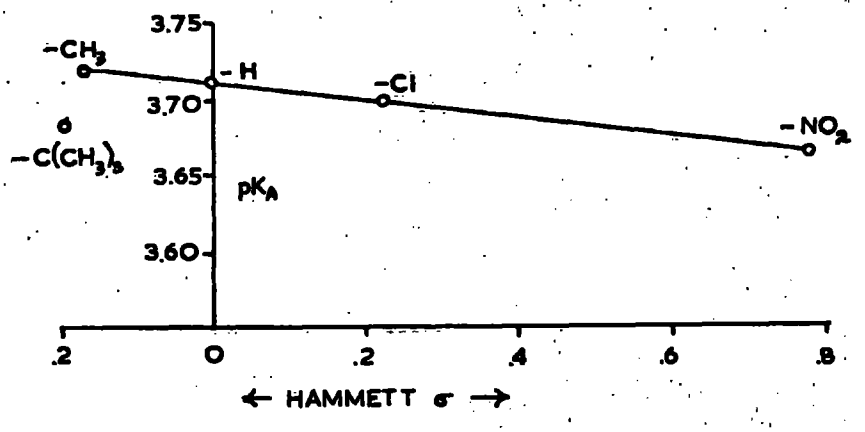

FIG 86

TETRAHYDROFURAN

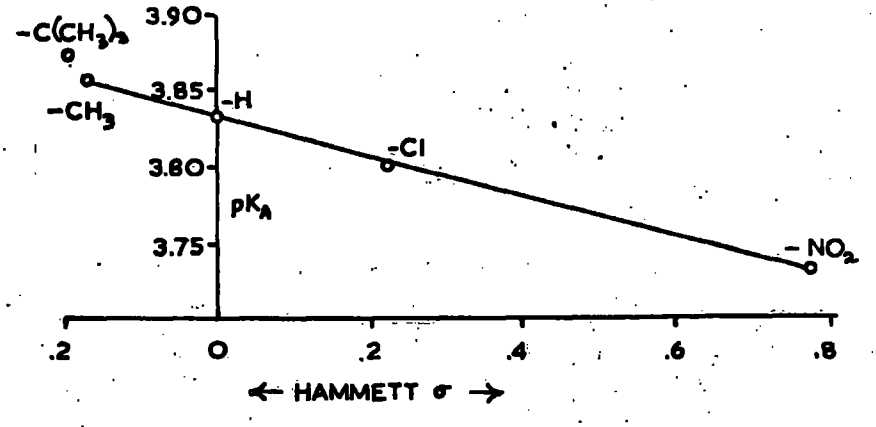

FIG 87

DIOXAN

in determining extent of adsorption. Electrical effect of the p-substituent could be determinative in these systems.

The values of K_A for the substituted phenols are seen to reflect the changes occurring in the electrical character of the hydroxyl group of the adsorptive due to the presence of the p-substituent, and are in accord with the relationship observed between hydrogen-bonding association in solution and p-substituent character. It is noted that the slopes of the plots shown in Figs. 85, 86 and 87 increase in the order cyclohexane, tetrahydrofuran, dioxan and it is interesting to speculate to what extent this effect is a consequence of change in solute-solvent interactions in solution. The experimental error involved in determining the 'index of adsorption' K_A is of the order of 1% and thus whereas the slope of Fig. 85 is zero within the limits of this experimental error, the slopes of Figs. 86 and 87 are meaningful.

REFERENCES

References

1.	Kipling	Quart. Rev.	1951, 5, 60
2.	Freundlich	'Colloid and Capillary Chemistry'	Methuen, London 1926
3.	Swan and Urquhart	J. Phys. Chem.	1927, 31, 251
4.	Ostwald and De Izagguirel	Koilloid. Z	1922, 279, 30
5.	Elton	J. Chem. Soc.	1951, 2958
6.	Kipling and Tester	J. Chem. Soc.	1952, 4123
7.	Day and Parfitt	J. Phys. Chem.	1967, 71, 3073
8.	Everett	Trans. Fara. Soc.	1964, 60, 1803
9.	Langmiur	J. Amer. Chem. Soc.	1916, 38, 2219
10.	Langmuir	J. Amer. Chem. Soc.	1918, 40, 1361
11.	Blackburn and Kipling	J. Chem. Soc.	1954, 3819
12.	Kipling and Peakall	J. Chem. Soc.	1956, 4828
13.	Giles, Mc.Ewan, Nakhua, and Smith	J. Chem. Soc.	1960, 3973
14.	Kipling and Wright	J. Chem. Soc.	1962, 855
15.	Kipling, Cornford and Wright	Trans. Fara. Soc.	1962, 58, 74
16.	Smith, Geiger and Pierce	J. Phys. Chem.	1953, 57, 382
17.	Hansen and Hansen	J. Phys. Chem	1955, 59, 496
18.	Wheeler and Levy	Canad. J. Chem	1959, 37, 1235
19.	Davidson and Kipling	unpublished results	
20.	Claesson	Rec.Trav. Chim.	1946, 65, 571
21.	Ganichenko, Kiselev and Krasilnikov	U.S.S.R. Proc.Acad.Sci.	1959, 125, 1277

22.	Kipling and Wright	J. Chem. Soc.	1964, 3535
23.	Russel and Cochran	Ind. Eng. Chem.	1950, 42, 1332
24.	De Boer, Hermans, Vleeskens	Proc. K. ned. Akad. Wetenschop	1957, 1960, 54
25.	Eric, Goode and Ibbitson	J. Chem. Soc.	1960, 55.
26.	Cummings, Garven, Giles Rahman, Sneddon and Stewart	J. Chem. Soc.	1959, 535
27.	Giles and McKay	J. Chem. Soc.	1961, 58.
28.	Daniel	Trans. Fara. Soc.	1951, 47, 1345
29.	Smith and McGill	J. Phys. Chem.	1957, 61, 1025
30.	Smith and Fort	J. Phys. Chem.	1958, 62, 519
31.	Smith and Fuzek	J.Amer.Chem.Soc.	1946, 68, 229
32.	Cook and Hackerman	J. Phys. Chem.	1951, 55, 549.
33.	Kipling, Sherwood and Shooter	Trans. Fara. Soc.	1964, 60, 401.
34.	Rao	J. Phys. Chem.	1932, 36, 616.
35.	Kipling	'Proceedings of the Second International Congress of Surface Activity'	Butterworth, London 1957,Vol.3.P.463
36.	Smith	Quart. Rev.	1959, 13, 287
37.	Smith and Schaeffer	'Proceedings of the Second Rubber Technology Conference'	London, 1948
38.	Gasser and Kipling	'Proceedings of the Fourth Conference on Carbon'	Pergammon Press London 1960,P.55
39.	Abram and Parfitt	'Proceedings of the Fifth Conference on Carbon'	Pergammon Press London 1962,P.97
40.	Hildebrand and Scott	'The Solubility of Non Electrolytes'	Reinhold, N.York 1950, 3rd Edition

41.	Bartell, Scheffer and Sloan	J.Amer.Chem.Soc.	1931, 53, 2510
42.	Jones and Outridge	J. Chem. Soc.	1930, 1574
43.	Bartell and Scheffer	J.Amer.Chem.Soc.	1931, 53, 2507
44.	Schroeder	J.Amer.Chem.Soc.	1951, 73, 1122
45.	Elder and Springer	J. Phys. Chem.	1940, 44, 943
46.	Dublinin and Zaverina	Acta. Physicochim U.R.S.S.	1936, 4, 647
47.	Kipling	Quart. Rev.	1956, 10, 1.
48.	Goodman and Gregg	J. Chem. Soc.	1959, 694.
49.	Hansen, Hansen and Craig	J. Phys. Chem.	1953, 57, 215
50.	Morrison and Miller	Canad. J. Chem.	1955, 33, 330
51.	Hansen and Hansen	J. Colloid, Chem.	1954, 9, 1.
52.	Kiselev and Shcherbakova	Acta. Physicochim U.R.S.S.	1946, 21, 539.
53.	Kipling and Wright	J. Chem. Soc.	1963, 3382
54.	Linner and Williams	J. Phys. Chem.	1950, 54, 605
55.	Kipling and Wilson	J. Appl. Chem.	1960, 10, 109
56.	Jones and Mill	J. Chem. Soc.	1957, 213.
57.	Kipling and Peakall	J. Chem. Soc.	1957, 4054
58.	Kipling and Peakall	J. Chem. Soc.	1957, 834
59.	Linner and Gortner	J. Phys. Chem.	1935, 39, 35.
60.	Kolthoff and van der Groot	Rec. Trav. Chim.	1929, 48, 265.
61.	Gupta and De	J. Ind.Chem.Soc.	1946, 23, 353
62.	Brunaeur, Emmett and Teller	J. Amer. Chem. Soc.	1938, 60, 309
63.	Brunaeur, Deming, Deming and Teller	J. Amer. Chem. Soc.	1940, 62, 1723

64.	Emmett and Brunaeur	J. Amer.Chem.Soc.	1937, 59, 1553
65.	Brunaeur, Emmett and Teller	J. Amer.Chem.Soc.	1937, 59, 2682
66.	Harkins and Jura	J. Amer.Chem.Soc.	1944, 66, 1362
67.	Livingstone	J. Colloid Sci.	1949, 4, 447
68.	Lippens, Linsen and De Boer	J. Catalysis	1964, 3, 32
69.	De Boer, Linsen and Osinga	J. Catalysis	1965, 4, 643
70.	De Boer, Steggerda and Zwietering	P. Koninkl Ned.Akad, Wetenschap Proc.	B59, 435, 1956
71.	Cohan	J.Amer.Chem.Soc.	1938, 60, 433
72.	De Boer	'The Shape of Capillaries' The Structure and Properties of Porous Materials	Butterworth, London 1958
73.	Stumpf, Russel, Newsome and Tucker	Ing. Eng. Chem.	1950, 42, 1398
74.	Brown, Clark, and Elliot	J. Chem. Soc.	1953, 84
75.	Day and Hill	J. Phys. Chem.	1953, 57, 946
76.	Lippens	'Structure and Texture of Aluminas'	Thesis Technische Hogeshool of Delft. The Netherlands, 1961
77.	De Boer, Houben,Lippens, Meijs and Walrave	J. Catalysis	1962, 1, 1.
78.	Peri	J. Phys. Chem.	1965, 69, 211
79.	Peri and Hannan	J. Phys. Chem.	1960, 64, 1526
80.	Peri	J. Phys. Chem.	1965, 69, 220
81.	Frangiskos, Harris and Jowett	'Proceeding of the Third International Congress of Surface Activity'	Verlag der Unwersitats-druckerei Mainz 1961 Vol.4,P.404

82.	Vallance	Private Communication	
83.	Smith, Pierce and Cordes	J.Amer.Chem.Soc.	1950, 72, 5595
84.	Adam	'The Physics and Chemistry of Surfaces'	Oxford University Press, London 1941
85.	Giles, Mehta, Stewart and Subramanian	J. Chem. Soc.	1954, 4360
86.	Ibbitson, Jackson, Mc.Carthy and Stone	J. Chem. Soc.	1960, 5127
87.	Hawley	M.Sc.Thesis, University of Durham.	1968
88.	Hawley	Private Communication	
89.	Bellamy, Eglinton and Morman	J. Chem. Soc.	1961, 4762
90.	Hammett	J.Amer.Chem.Soc.	1937, 59, 96.
91.	Hammett	Trans. Fara. Soc.	1938, 34, 156
92.	Hibbert	M.Sc. Thesis, University of London	1966
93.	Ibbitson and Sandall	J. Chem. Soc.	1964, 4547
94.	Jaffe	Chem. Reviews	1953, 53, 191.